FABRICATION OF WATER- AND OIL/GREASE-RESISTANT PAPER COATING FOR PACKAGING APPLICATION

By

Zhao Li

A DISSERTATION

Submitted to
Michigan State University
in partial fulfillment of the requirement
for the degree of

Packaging—Doctor of Philosophy

2020

ABSTRACT

FABRICATION OF WATER- AND OIL/GREASE- RESISTANT PAPER COATING FOR PACKAGING APPLICATION

By

Zhao Li

Paper materials are highly desirable for a wide range of applications in packaging and nonpackaging sectors due to their advantages of low cost, light-weight, excellent mechanical
properties, biodegradability, and renewability. However, paper is a porous material with polar
groups that cause it to absorb water and oil. Lamination and coating are commonly used methods
to improve the water- and oil-resistance of paper. After use, the separation of laminates and
coatings from the paper fibers/pulp presents a significant challenge. In addition, persistent and
environmentally harmful fluorinated chemicals are also used to render paper water- and oilresistant. Thus, there is an urgent need to address the above challenges by developing closed-loop
approaches for water- and grease/oil-resistant paper. This research aims to develop facile,
economical, and closed-loop approached for fabricating fluorine- and plastic-free water- and
grease/oil- resistant paper coating.

To achieve PFAS- and plastic-free water-repellent coating for paper, paper substrates were first coated with melamine as a primer, an FDA approved material for food contact applications, to provide amine group sites on the cellulosic fibers. Polydimethylsiloxane-isocyanate (PDMS-NCO) was applied as a water-repellent outer layer, which was bonded to cellulosic fibers via biodegradable urea linkages formed between the NCO and amine groups. The obtained coated paper substrate showed excellent water-resistant properties with high water contact angles ($\sim 125^{\rm o}$) along with a significant reduction in water absorption. However, the coating paper was lacking oil resistance, which is evidently due to the porous textures of the coated paper.

To impart paper substrates both water- and oil-resistant properties, a two-step PFAS-free approach was developed using chitosan as a first layer, while PDMS-NCO as a second layer Chitosan was applied as a coating to mask paper's pores as well as create free amine groups on the paper substrate. A PDMS coating layer was then chemically grafted to the chitosan-coated-paper via urea linkages to render water and oil-resistant. The coated paper with a coating load of 8.6% of chitosan and 2.2% of PDMS showed excellent oil/grease resistance (kit rating value of 12/12) as well as excellent water contact angle (WCA 95.2°).

Next, a closed-loop approach for one-step water- and oil-resistant paper-based materials was developed. Chitosan-*graft*-PDMS copolymer was prepared by grafting PDMS onto the chitosan polymer, which was then applied as an aqueous coating solution on paper substrates in a single step. Remarkable water- and oil-resistant properties were obtained which is evident from high WCA of 120.53°, low Cobb 60 values of 9.89 g/m² and very high kit value of 11.7/12. In addition, the pulp of the coated paper was 100% recyclable by repulping and washing treatment. Furthermore, overall migration of siloxane into two food simulants (50% aqueous ethanol and Miglyol 812) was below 46.19 µg/mL (7.16 mg/dm²), which is well below the overall migration limit 60 mg/kg food (100 mg/dm²) by the Council of Europe's Resolution AP (2004).

Finally, sustainable and biobased chitosan-*graft*-castor oil (CHI-*g*-CO) copolymer was synthesized and applied for paper coating. The castor oil was grafted onto the chitosan polymer backbone via a urea linkage formed between –NCO and amine groups. The obtained waterborne solution of CHI-*g*-CO was coated onto paper, which showed good water- and oil-resistance with a Cobb60 value of 29.16 g/m² and a kit rating value of 9/12, respectively. Meanwhile, this fabrication strategy offers a sustainable and environmental-friendly approach toward grease- and water-resistant paper-based materials considering the biobased nature of chitosan and castor oil.

Copyright by ZHAO LI 2020 致我亲爱的父母。

ACKNOWLEDGEMENTS

Upon completion of Ph.D. degree, I would like to express my sincere and deepest gratitude to my supervisor and committee chair, Dr. Muhammad Rabnawaz, for his continuous guidance and support throughout my Ph.D. program, for his patience, immerse knowledge, enthusiasm, motivation and caring about his students. I always feel lucky and appreciated to work with him in my doctoral program. I am grateful to have Dr. Donatien Pascal Kamdem, Dr. Rafael Auras, and Dr. Mojgan Nejad as my committee members. I am greatly appreciated for their valuable suggestions and kind help. Their professional knowledge and rigorous altitude to research and academia will continuously influence me in work and life. I greatly appreciate Dr. Maria Rubino and Dr. Susan Selke for their kind help and support, especially at the beginning of my Ph.D. program. I would like to thank my middle school teachers Dan-Ping Peng and Ren-Xue Wu who encouraged me and had a great expectation on me at my young age.

I am very grateful to all the faculty and staff of the School of Packaging, Michigan State University; the Packaging Development Team of Biogen, Inc., Cambridge, MA, for all the great packaging experiences in classroom, lab and industry. I am thankful to Dr. Mohammed G. Sarwar for his assistance on NMR; Dr. Stanley Flegler, Amy Albin for their assistance on SEM; my group members Shamila, Nopphachai, Aditya, Burhan, etc. for great collaboration on paper-coating projects.

I would like to express my appreciation to all my friends in MSU, Jin Zhang, Xin-Yi Wang, Rui-Qiong Guo, Sui-Han Liu, Peng-Fei Yuan, Ke-Xin Zeng, Hao-Yang Wang, Wanwarang Limsukon and Sonal Karkhanis, for all the help and great memories. My appreciation also goes to Ying Zhu, Fan-Qi Kong, Bi-Yun Gao, Huan Liu, and Meng-Di Li, for their long-term friendship

though we are locating at different corners of the world. I would also like to acknowledge MI East

Lansing Hot Yoga Studio, where I spent tons of perspiration and energy in past three years

allowing me staying physically strong and mentally peaceful.

Last but most importantly, I would like to express my deepest love and gratitude to my

family: my beloved parents Yue-Xue Li and Chun-Ying Zhao for their endless love and

unconditional support, my cousin Shuang-Yi Zhu, my grandma Xiu-Qing Bi and my late grandpa

Xue-Mu Zhao for their love and encouragement, my dog Xi-Bei Dou for being a good company

with my parents while I am abroad.

Pursuing a Ph.D. degree is never easy, it is a long journey with difficulties and challenges.

What I can do is being mentally and physically strong, trying my best moving forward without

hesitation. I will always remember and appreciate those who have helped and supported me. I'll

move on with the love and hope from all of you.

Zhao Li

Lansing, MI

viii

TABLE OF CONTENTS

LIST O	F TABLES	xii
LIST O	F FIGURES	xiii
LIST O	F SCHEMES	xvii
KEY TO	O ABBREVIATION	xviii
СНАРТ	TER 1: INTRODUCTION	1
1.1	Background and Motivation	1
1.2	Goals and Objectives	4
REFER	ENCES	
СНАРТ	TER 2: LITERATURE REVIEW	12
2.1	Polysaccharide	
2.1.1	Structure and properties of saccharide	
2.1.2	Approaches to enhance water and oil properties of chitosan film/coating	
2.2	Polysiloxane	
2.2.1	Structure and properties	
2.2.2	Application of siloxane	
2.3	Fabrication of coating on paper-based materials	
2.3.1	Dip-coating	
2.3.2	Rod coating	
2.3.3	Spray coating	
2.4	Wettability	
2.4.1	Static contact angle	21
2.4.2	Sliding angle and contact angle hysteresis	23
2.5	Barrier Properties	25
2.5.1	Water absorption	25
2.5.2	Water vapor transmission rate	26
2.6	Mechanical properties	27
2.7	Recyclability	27
2.8	Migration study	28
2.9	Characterization	
2.9.1	Coating Load	29
2.9.2	Structure and morphology	29
REFER	ENCES	30
СНАРТ	TER 3: FABRICATION OF FOOD-SAFE WATER-RESISTANT PAPER	
	TINGS USING A MELAMINE PRIMER AND POLYSILOXANE OUTER LA	YER
		35
3.1	Abstract	36
3 2	Introduction	36

3.3	Experimental	39
3.3.1	Materials	
3.3.2	Methods and Characterization	
3.4	Results and Discussion	
3.5	Conclusions	
	ENCES	
KLI LK	LIVELO	
СНАРТ	TER 4: OIL- AND WATER-RESISTANT COATINGS FOR POROUS CELL	ULOSIC
	STRATES	
4.1	Abstract	
4.2	Introduction	
4.3	Experimental	
4.3.1	Materials.	
4.3.2	Methods and Characterization	
4.3.3	Statistical analysis	
4.4	Results and Discussion	
4.4	Conclusions	
	ENCES	
KEFEK	ENCES	89
СНАРТ	TER 5: A CLOSED-LOOP AND SUSTAINABLE APPROACH FOR THE	
	RICATION OF PLASTIC-FREE OIL- AND WATER-RESISTANT PAPER	02
	DUCTS	
5.1	Abstract	
5.2	Introduction	
5.3	Materials and Methods	
5.3.1	Materials.	
5.3.2	Methods and Characterization	
5.3.3	Characterization	
5.3.4	Recyclability	
5.3.5	Mechanical property tests	
5.3.6	Overall Migration Study	105
5.3.7	Quantitative analysis of migrated silicone	106
5.4	Results and Discussion	107
5.5	Conclusions	126
APPEN	DICES	128
APPEN	DIX A: ¹ H NMR spectra of Chitosan (recorded in D ₂ O at 2wt% CD ₃ COOD)	
	DIX B: ¹ H NMR spectra of Chitosan-g-PDMS, Chitosan and PDMS-NCO using	
	2wt% CD ₃ COOD	
APPEN	DIX C: ¹ H NMR spectra of Chitosan-g-PDMS (after extraction) using D2O with	2wt%
	COOD	
	DIX D: ¹ H NMR spectra of Chitosan-g-PDMS (after extraction) using D2O with	
	COOD.	
	ENCES	
TET EIG		133
СНАРТ	TER 6: RESPONSE SURFACE METHODOLOGY DESIGN FOR BIOBASE	D AND
	TAINABLE COATINGS FOR WATER- AND OIL-RESISTANT PAPER	
505	Delication of the state of the second	10/

6.1	Abstract	138
6.2	Introduction	138
6.3	Materials and Methods	142
6.3.1	Materials.	142
6.3.2	Methods	142
6.3.3	Characterization	145
6.4	Results and Discussion	147
6.5	Conclusions	160
APPEN	NDICES	162
APPEN	NDIX A: ¹ H NMR of isophorone diisocyanate recorded in CDCl ₃	163
APPEN	NDIX B: Central Composite Design of experimental and experimental responses	164
APPEN	NDIX C: Regression coefficients for the second-order polynomial model	165
	NDIX D: TGA and DTG of coating materials (CHI-g-CO and CHI) and coated and	
	pated samples	166
REFER	RENCES	167
CHAP	ΓER 7: GENERAL CONCLUSIONS AND FUTURE WORK	173
7.1		
7.2	Future Work	

LIST OF TABLES

Table 2.1 Literature data	18
Table 2.2 Mechanical properties, instruments and testing standards	27
Table 3. 1 Theoretical and experimental coating load and melamine load of cup paper and printing paper.	46
Table 4. 1 CCD experimental design and experimental responses	75
Table 4. 2 Regression coefficients of the second-order polynomial model	75
Table 4. 3 Basis weight of unmodified paper, chitosan-coated paper, and chitosan-PDMS-c paper	
Table 4. 4 Comparison of room temperature curing and heat-cured chitosan-PDMS coated	
Table 5. 1 Formulations and corresponding codes used in this article	100
Table 5. 2 Hydrodynamic diameters (<i>D</i> _h) of chitosan- <i>g</i> -PDMS micelles	112
Table 5. 3 Basis weight, thickness, and coating load of uncoated and coated paper	112
Table 5. 4 Analytical parameters of H1-NMR determination of PDMS	125
Table 6. 1 Levels and codes of the independent variables	144
Table 6. 2 Mechanical properties of CHI-g-CO-coated paper, CHI-coated paper, and uncoa paper.	
Table A- 1 Central Composite Design of experimental and experimental responses	164
Table A- 2 Regression coefficients for the second-order polynomial model	165

LIST OF FIGURES

Figure 2.1 Categories of biobased polymers based on origin and production ¹⁻²	13
Figure 2.2 Partial deacetylation of chitin to chitosan.	14
Figure 2.3 Chemical structure of PDMS.	19
Figure 2.4 Approaches of coating fabrication: dip coating (a), rod coating (b) and spray coating (c)	
Figure 2.5 Liquid droplet in Cassie state (a) and Wenzel state (b)	22
Figure 2.6 CAH measurement using a tilted plane method (a) and sessile drop method (b)	24
Figure 3.1 Illustration of the fabrication procedure for the water-resistant melamine-PDMS primed paper.	40
Figure 3.2 FTIR spectra of a) printing paper and b) cup paper.	44
Figure 3.3 TGA traces of unmodified paper and melamine-PDMS primed paper under nitrogen for a) printing paper, b) cup paper.	
Figure 3.4 Water uptake profile of a) printing paper and b) cup paper.	46
Figure 3.5 Static behavior of water droplets and water contact angles (WCAs) observed on a) printing paper and b) cup paper.	48
Figure 3.6 Plot showing the variation in the water contact angles with the concentration of the PDMS-NCO coating solution.	49
Figure 3. 7 SEM images of the cup paper at different stages of fabrications. a) unmodified, b) melamine coated, c) melamine-HDIT, and d) melamine-PDMS coated paper. The inset images are taken at 1000X magnification.	50
Figure 3. 8 SEM images of the printing paper at different stages of fabrications. a) unmodified, b) melamine coated, c) melamine-HDIT, and d) melamine-PDMS coated papers. The inse images are taken at 1000X magnification.	t
Figure 4. 1 Illustration of preparation procedure of water and oil/grease resistant chitosan-PDN coated paper	
Figure 4.2 Synthesis of PDMS-NCO.	69
Figure 4.3 1 H NMR spectrum of PDMS-NH ₂ (M_n = 2000 g/mol, CDCl ₃ , 500 MHz)	69
Figure 4.4 ¹ H NMR spectrum of hexamethylene diisocyanate trimer (HDIT)	70

Figure 4.5 Schematic illustration of the coated paper before and after PDMS-NCO application.70
Figure 4.6 ¹ H NMR spectrum the concentrated extract of the uncoated paper (CDCl ₃ , 500 MHz).
Figure 4.7 ¹ H NMR spectrum of the concentrated extract of the Chitosan-PDMS coated paper (CDCl ₃ , 500 MHz).
Figure 4.8 ¹ H NMR spectrum of the concentrated extract of the Chitosan-PDMS coated paper treated with NaHCO ₃ (CDCl ₃ , 500 MHz)
Figure 4. 9 Response surface plots of water-gain for water-resistance (a) and kit rating for oil-resistance (b). (Figure generated using JMP Statistical Software (SAS Institute Inc., NC, USA)
Figure 4.10 FTIR results of chitosan-coated and chitosan-PDMS-coated paper samples
Figure 4.11 TGA traces of unmodified paper, chitosan-coated paper, and chitosan-PDMS-coated paper
Figure 4.12 Contact angles of papers at different stages of fabrications. Water and castor oil droplets on uncoated paper (A), chitosan coated paper (B), PDMS coated paper (C), and chitosan-PDMS coated paper (D) and after 30 sec and 5-minute. Note: "PDMS coated" paper represents PDMS-HDIT coating applied on paper in the absence of chitosan
Figure 4.13 A and B depict the behavior of water droplet on chitosan-PDMS coated paper and chitosan coated paper, respectively. C and D show the behavior of castor oil droplet on chitosan-PDMS coated paper and chitosan coated paper, respectively. A1 to D1 represent images of the paper after water or oil droplets were removed after sitting for 5-min
Figure 4.14 SEM images (100×) with zoomed-in pictures (1000×) shown as insets in the upper right corners for unmodified paper (a), chitosan-coated paper (b) and chitosan-PDMS-coated paper (c)
Figure 4.15 Effect of hexane extraction on the water- (a) and oil- (b) resistance properties of non-and NaHCO ₃ -treated paper coatings ("*" indicates a significant difference at the 95% confidential level based on Student's t-test).
Figure 4.16 WVTR of unmodified paper (Un paper), PDMS coated paper (P paper), chitosan coated paper (C paper), chitosan-PDMS coated paper (C-P paper), 3Layer chitosan coated paper (3Lc paper), and 3Layer chitosan-PDMS coated paper (3Lc-P paper)
Figure 4.17 Contact angles of paperboards at different stages of fabrications. Water and castor oil droplets on uncoated paperboard and chitosan-PDMS coated paperboard and after 30 sec and 5-minute. Note: PDMS-coated paper without chitosan has poor water-resistance as reported by us previously. 87

Figure 4.18 A and B depict the behavior of water droplet on chitosan-PDMS coated paper and chitosan coated paperboard, respectively. C and D show the behavior of castor oil droplet on chitosan-PDMS coated paper and chitosan coated paperboard, respectively. A1-D1 represent images of the paperboard after water or oil droplets were removed after sitting for 5-min.
Figure 5. 1 ATR FTIR analysis of the model reactions between a) HDI and ethanolamine and b) HDI and ethanol. In "a", IR is recorded 1 min after the addition of HDI, in "b" IR was recorded after 25 min of the addition of HDI.
Figure 5. 2 ¹ H NMR (recorded in DMSO-d6) of the: A) HDI, B) ethanolamine, and C) product of the urea product of the ethanolamine and HDI
Figure 5. 3 ¹ H NMR spectra of PDMS-NH ₂ (A), HDI (B), and PDMS-NCO (C) (recorded in CDCl ₃).
Figure 5. 4 FT-IR spectra of U-p (bottom), C-p (middle), and P1C-p (top)
Figure 5. 5 WVTR (g/m²-day) and Cobb 60 values (g/m²) of uncoated paper and coated paper samples. U-p represents uncoated paper and C-p represents chitosan-coated paper. Notations PnC-p (where P denotes PDMS, n denotes the weight of the PDMS with respect to the weight of chitosan in the chitosan-g-PDMS, C represents chitosan, p denotes paper) represent paper coated with chitosan-g-PDMS at different PDMS content in the graft copolymer.
Figure 5. 6 Sliding angles and CAs (after 30 s and 5 min) of: a) water and b) castor oil. For the uncoated as well as the chitosan-coated paper, water slides on these surfaces but leaves a mark behind.
Figure 5. 7 Surface tensions and kit rating values of coated and uncoated paper samples. A kit-rating of 12 corresponds to the maximum oil-resistance.
Figure 5. 8 SEM images (200×) of unmodified paper U-p (a), chitosan-coated paper C-p (b), and chitosan-g-PDMS-coated paper, including P0.5C-p (c), P1C-p (d), and P2C-p (e) 120
Figure 5. 9 Tensile strength (a), ring crush test (b), bending stiffness (c), and internal tearing (d) of uncoated paper (U-p), and coated paper (C-p, P0.25C-p, and P0.5C-p)
Figure 5. 10 FT-IR spectra of paper samples prepared from unwashed U-p as well as P1C-p fibers and fibers that had been washed with DI water and acetic acid solutions
Figure 5. 11 Calibration curve for PDMS quantification
Figure 5. 12 Concertation of PDMS in food simulants after storing for 10 days under 4 °C 125
Figure A- 1 ¹ H NMR spectra of Chitosan (recorded in D ₂ O at 2wt% CD ₃ COOD)

Figure A- 2 ¹ H NMR spectra of Chitosan-g-PDMS, Chitosan and PDMS-NCO using D2O with 2wt% CD ₃ COOD
Figure A- 3 ¹ H NMR spectra of Chitosan-g-PDMS (after extraction) using D2O with 2wt% CD ₃ COOD
Figure A- 4 TGA (a) and DTG (b) plots of uncoated paper (U-p) and coated paper (C-p and P1C-p). Also shown are TGA (c) and DTG (d) plots of the chitosan coating (C), P1C coating (P1C), and unmodified paper (U-p)
Figure 6. 1 ¹ H NMR (recorded in CDCl ₃ at 500 MHz) spectra of: (top) CO and (bottom) CO-capped-NCO.
Figure 6. 2 ATR-FTIR spectra of: (a) CO-capped-NCO, (b) IPDI, and (c) Castor oil (CO) 150
Figure 6. 3 Surface profiles for the (a) kit rating, (b) Cobb60 value, (c) coating load, and (d) thickness
Figure 6. 4 FTIR spectra of: (a) CHI-g-CO-coated paper, (b) CHI-coated paper, and (c) uncoated paper.
Figure 6. 5 SEM images of: (a) uncoated paper, (b) CHI-coated paper, and (c) CHI-g-CO-coated paper
Figure 6. 6 WCAs on CHI-g-CO-coated, CHI-coated, and uncoated paper as a function of time. Images of the water droplet sitting on different paper samples were taken every 5 s until a duration of 1400 s was reached. A 5 μ L droplet size was used in these tests
Figure 6. 7 Top-down images of the castor oil on: (a) CHI-g-CO-coated paper, (b) CHI-coated paper, and (c) uncoated paper (several drops were placed on the same spot). The inset images represent the OCAs of castor oil droplets on: (a) CHI-g-CO-coated paper, (b) CHI-coated paper, and (c) uncoated paper. For the OCA measurements, the CO droplet volume was 5 μL
Figure 6. 8 WVTRs of uncoated-paper, CHI-coated paper, CHI-g-CO-coated paper, and paper coated by four layers of CHI-g-CO after these samples had been preconditioned at 50% RH and 0% RH for 72 h
Figure A- 5 ¹ H NMR of isophorone diisocyanate recorded in CDCl ₃
Figure A- 6 (a) TGA curves for coating materials (CHI-g-CO and CHI) as well as a paper substrate, (b) DTG curves for coating materials (CHI-g-CO and CHI) as well as the paper substrate, (c) TGA curves for coated paper (including uncoated paper) at various stages of fabrication, and (d) DTG curves for coated paper at various stages of fabrication

LIST OF SCHEMES

Scheme 5. 1	Homemade migration cell	106
Scheme 5. 2	Illustration of the pulp recycling process for the coated paper.	123
	The synthetic route followed for the preparation of the CHI-g-CO copolymer in t	

KEY TO ABBREVIATION

AFM Atomic Force Microscopy

ASTM American Society for Testing and Materials

CAH Contact Angle Hysteresis

CHI Chitosan

CHI-g-CO Chitosan-graft-Castor Oil

Chitosan-g-PDMS Chitosan-graft-Polydimethylsiloxane

CO Castor Oil

EDC 1-ethyl-3-(3-dimethylaminopropyl)carbodiimide

EPA Environmental Protection Agency

EVOH Ethylene Vinyl Alcohol

FTIR Fourier-transform Infrared

FDA Food and Drug Administration

HDIT Hexamethylene diisocyanate trimer

ISO International Organization for Standardization

NHS N-hydroxysuccinimide

NMR Nuclear magnetic resonance

OCA Oil contact angle

PDMS Poly(dimethylsiloxane)

PDMS-NCO Poly(dimethylsiloxane)-isocyanate

PDMS-NH₂ Monoaminopropyl-terminated Poly(dimethylsiloxane)

PE Polyethylene

PVDC Polyvinylidene Chloride

PVOH Polyvinyl Alcohol

RH Relative Humidity

RSM Response Surface Methodology

SA Sliding Angle

SEM Scanning Electron Microscopy

TAPPI Technical Association of the Pulp and Paper Industry

TGA Thermogravimetric Analysis

WCA Water Contact Angle

WVP Water Vapor Permeability

WVTR Water Vapor Transmission Rate

CHAPTER 1: INTRODUCTION

1.1 Background and Motivation

Paper is a highly desirable material in the packaging, printing and labeling industry due to the advantages of low cost, light-weight, good mechanical properties, biodegradability, and renewability. However, paper has poor water and oil resistance owing to the porous structure as well as the polar hydroxyl groups of lignocellulose. As a result, the paper has limited applications especially in the field of packaging where it encounters water or other liquids. Extensive research has been conducted to develop paper-based materials with good water-and oil-resistance. Approaches such as chemical modification (grafting approach, layer-by-layer, etc.), physicochemical modification (plasma etching, etc.) have been studied, most of which, however, commercially non-viable due to the complicated processing procedure, relative high-cost, safety-concern as well as harmful influence on the ecosystem.

On the other hand, paper sizing and pulp refining^{7-9,10,11}, coatings and laminations on paper substrates are common industrial practice for producing water- and oil- resistant paper products which account for most of the market share nowadays. Internal paper sizing has been systematically reviewed¹². Paper materials modified using paper sizing and pulp refining are usually deficient in barrier properties¹³. This thesis is focused on the use of paper coating for imparting water and oil-resistance, while the paper sizing and pulp refining are beyond the scope of this work.

Commercially, synthetic plastics liners such as low-density polyethylene (LDPE)¹⁴ and polyvinylidene chloride (PVDC) are laminated on paper substrates to impart good water and gas barrier as well as provide water- and oil-resistance¹⁵. While waxed-paper is also used for food packaging applications such as meat and burgers.¹⁶⁻¹⁷ Main challenges with the use of laminated-

1

and waxed-paper are the separation of laminates/coatings from the paper fibers or pulp due to which they are difficult to recycle; thus ends up in landfills. Recently, the EU parliament voted to ban single-use plastics from cutlery, plates, and straws and also urged reduced use of single-use cups and beverage containers.¹⁸

Polylactide (PLA), a biobased thermoplastic derived from renewable resources (corn starch, sugarcane, cassava roots), has been utilized as a liner for paper plates and cups. ^{15, 19-20} However, the recyclability of the PLA laminated paper is as challenging as LDPE laminated paper because solid plastic particles are trapped in the recycled pulp that makes it unsuitable for reuse. Also, PLA biodegrades only under industrial compost conditions, whereas paper could easily biodegrade under the natural environment, and that makes the natural biodegradation challenging for PLA laminated paper. Polyaleuriate, which is a biobased polymer, has also been applied used as a coating for cellulosic substrates, with subsequent addition of carnauba wax to enhance barrier properties against water vapor by up to ~80%. ²¹ However, the oil-resistance of coated substrates is insufficient due to relatively high surface energy. Although the use of biodegradable plastics for paper lamination helps to reduce the environmental footprint, however, they are less sustainable because the paper pulp is difficult to recycle.

Latex-based coatings have been used for paper coating for water- and grease- resistant purposes.²² The resistance against waterborne products of the obtained coated paper is weak especially under prolonged exposure due to the polar/ionic groups within the formulation. Besides, leaching of latex arouses safety concerns when these latex-based coatings applied as food packaging materials. ²³ Furthermore, disposal of latex into the environment during the paper recycling process imposes adverse effects on the ecosystem, such as microplastic pollution.

Another approach for fabricating water- and oil-resistant paper on a commercial scale is the use of per- and polyfluoroalkyl substances (PFAS). Due to low surface energies of the fluorochemicals, the fluorochemical coated paper substrates show excellent water- and oil-resistance, which make them useful for applications such as food wrappers, paper for baking, "to go" containers, and disposal plates. However, due to the environmental concerns and toxicity of fluorochemicals, there is a strong push to eliminate the use of fluorochemical from packaging²⁴⁻²⁵. In 2018, two towns in Michigan were declared under emergencies due to the elevated fluorinated materials in water up to 20 times higher than the permissible limits (70 ppt) ²⁶. Recently, EPA has called for strategies for analysis and separation of fluorochemicals from environment²⁷.

According to the U.S. Environmental Protection Agency (EPA), 68.05 million tons of paper and paperboard were generated in the United States in 2015, of which 66.6% were recycled, 6.5% were composted, and 26.9% were dumped in landfils²⁸. While the recycling numbers seem impressive, however, the recycling rates for different paper and paperboard products were varied dramatically. For example, in 2015, 92% of the corrugated boxes were recycled while the recycling rate for mixed paper containers/packaging was only 26.4%²⁷. Considering the above challenges associated with open-loop wasteful approaches as well as the use of toxic fluorine for paper coating, the development of environmentally friendly water- and oil-resistant paper-based materials is highly desirable.

Biopolymers such as protein²⁹⁻³², lipid³³⁻³⁵, and polysaccharides³⁶⁻³⁸ have attached attracted increasing attention for barrier coating as a replacement of synthetic polymers due to the advantage of good biodegradability, biocompatibility, renewability, and non-toxicity. For example, chitosan, a polysaccharide derived from the deacetylation of chitin, has attracted great interest in edible films and coating for packaging materials imparting great barrier (against grease, oxygen, and microbial,

etc.) to paper substrate³⁹⁻⁴¹. However, like most of the polysaccharides, chitosan film is naturally hydrophilic that absorbs water and moisture. Also, at high relative humidity, they have poor barrier properties because of an increase in the free volume of the films upon water absorption.⁴².

Polysiloxanes especially polydimethylsiloxane (PDMS) are receiving attractions as an alternative of fluorochemicals due to its advantage of low surface energy, low cost, and environmental friendliness. PDMS has a surface energy of ~20 mN/m at room temperature exhibiting good repellency to both hydrophilic and hydrophobic liquid⁴³. And it has been applied in improving water- and oil-resistant urethane and epoxy coating.⁴⁴ Therefore, we proposed PDMS could be applied to improve water- and oil- resistance of paper products.

Paper is comprised of cellulosic fibers with various pore sizes. The pore size depends on both the source of fiber as well as the manufacturing processes (calendaring, drying, pressure level, and coating). To render good water- and oil- resistance to paper materials, pores and voids as well as the hydrophilic hydroxyl groups need to be masked. Although chitosan coating has been applied to impart oil-resistance to paper materials by filling pores and voids of the paper substrate, however, the water-resistance remained low due to the hydrophilic structure of chitosan. To address the above problems, we initiated this study to explore the effect of masking paper's pores and lowering the surface energy to achieve both water and oil repellency without using fluorinated chemicals.

1.2 Goals and Objectives

The overall goal of this study is to develop plastic- and fluorine-free closed-loop approach toward water- and grease/oil-resistant paper, which will be accomplished using the following specific objectives:

- 1) PDMS coating on paper substrates without masking papers' pores: PDMS coating will be applied to paper substrates without masking papers' pores to test our hypothesis that PDMS alone can render paper substrates water resistance only. Melamine, a food-safe material, will be utilized as a linker to graft PDMS to paper substrates via hydrogen bonding. The obtained samples will be evaluated for their water- and oil-repellency properties.
- 2) Develop plastic- and fluorine-free water and grease resistant paper: Water- and grease-resistant paper will be fabricated by using chitosan and PDMS. Paper substrate will be first coated with chitosan to mask paper's pores as well as create free amine groups on the paper surface. Then, PDMS will be applied onto chitosan-coated paper to reduce the surface energy of the paper substrate.
- 3) Develop a closed-loop approach for one-step water- and grease-resistant paper products: Water- and grease- resistance paper substrate will be prepared by applying chitosan-*graft*-polydimethylsiloxane (Chitosan-g-PDMS) copolymers solution on paper substrate. Water- and oil-resistant properties as along with the mechanical properties of the coated paper substrates, will be evaluated. The closed-loop nature of this fabrication approach will be validated by testing the pulp recovery from the coated paper. Specific migration for Chitosan-g-PDMS paper coating: The Chitosan-g-PDMS coated paper will be subjected to extraction with food simulants at 40 °C for 10 days. The food simulant solution will be then analyzed using Nuclear magnetic resonance (NMR) for PDMS quantification using literature method.⁴⁵
- 4) Develop low-cost water- and grease-resistant paper products using chitosan and castor oil: Instead of chitosan-g-PDMS (see objective#3), castor oil and chitosan will be used for paper coating. The castor oil is selected because of its low cost, renewability, and food safety. In this study, first, castor oil will be modified to castor oil-isocyanate. The castor oil-isocyanate will then

be grafted onto chitosan to synthesize chitosan-*graft*-castor oil (CHI-*g*-CO). The chitosan-*g*-castor solution will be used for paper coating, and the performance of coated paper will be evaluated.

REFERENCES

REFERENCES

- 1. Kitaoka, T.; Isogai, A.; Onabe, F., Chemical modification of pulp fibers by TEMPO-mediated oxidation. *Nordic Pulp and Paper Research Journal* **1999**, *14* (4), 279-284.
- 2. Hon, D.-S., Chemical modification of lignocellulosic materials. Routledge: 2017.
- 3. Roy, D.; Semsarilar, M.; Guthrie, J. T.; Perrier, S., Cellulose modification by polymer grafting: a review. *Chemical Society Reviews* **2009**, *38* (7), 2046-2064.
- 4. Liu, C.-F.; Zhang, A.-P.; Li, W.-Y.; Yue, F.-X.; Sun, R.-C., Homogeneous modification of cellulose in ionic liquid with succinic anhydride using N-bromosuccinimide as a catalyst. *Journal of agricultural and food chemistry* **2009**, *57* (5), 1814-1820.
- 5. Yang, J.; Li, H.; Lan, T.; Peng, L.; Cui, R.; Yang, H., Preparation, characterization, and properties of fluorine-free superhydrophobic paper based on layer-by-layer assembly. *Carbohydrate polymers* **2017**, *178*, 228-237.
- 6. Dimitrakellis, P.; Travlos, A.; Psycharis, V. P.; Gogolides, E., Superhydrophobic paper by facile and fast atmospheric pressure plasma etching. *Plasma Processes and Polymers* **2017**, *14* (3).
- 7. Wurzburg, O. B., Paper sizing process using a reaction product of maleic anhydride with a vinylidene olefin. Google Patents: 1976.
- 8. Mazzarella, E. D.; Wood Jr, L. J.; Maliczyszyn, W., Method of sizing paper. Google Patents: 1977.
- 9. Guo, Y.-h.; Guo, J.-j.; Miao, H.; Teng, L.-j.; Huang, Z., Properties and paper sizing application of waterborne polyurethane emulsions synthesized with isophorone diisocyanate. *Progress in Organic Coatings* **2014**, *77* (5), 988-996.
- 10. Hubbe, M. A., Paper's resistance to wetting—A review of internal sizing chemicals and their effects. *BioResources* **2007**, *2* (1), 106-145.
- 11. Dang, C.; Xu, M.; Yin, Y.; Pu, J., Preparation and Characterization of Hydrophobic Non-Crystal Microporous Starch (NCMS) and its Application in Food Wrapper Paper as a Sizing Agent. *BioResources* **2017**, *12* (3), 5775-5789.
- 12. Hubbe, M. A., Paper's resistance to wetting- A review of internal sizing chemicals and their effects. *Bioresource* **2006**, *2* (1), 40.
- 13. Samyn, P., Wetting and hydrophobic modification of cellulose surfaces for paper applications. *Journal of Materials Science* **2013**, *48* (19), 6455-6498.

- 14. Martin Jr, L. L., Paper laminate and method for producing the laminate and paperboard containers. Google Patents: 1989.
- 15. Rastogi, V.; Samyn, P., Bio-Based Coatings for Paper Applications. *Coatings* **2015**, *5* (4), 887-930.
- 16. Oswald, R. G.; Harvey, W. T.; Johnson, H. L., Wax-coated paper. Google Patents: 1966.
- 17. Knights, E. F., Wax coated paper of improved water resistance. Google Patents: 1975.
- 18. Shoot, B., EU Parliament votes to ban single-use plastics, including plates, cutlery, and straws. http://fortune.com/2018/10/24/eu-ban-single-use-plastic-pollution/ (accessed on April 10, 2019).
- 19. Yamamatsu, T.; Uemura, M. Paper cup comprising a sheet of polylactic acid laminated paper. US20080176015A1, 2007.
- 20. Cleveland, C.; Reighard, T.; Marchman, J. Biodegradable paper-based laminate with oxygen and moisture barrier properties and method for making biodegradable paper-based laminate. AU2007212477B2, 2006-02-06, 2014.
- 21. Heredia-Guerrero, J. A.; Benítez, J. J.; Cataldi, P.; Paul, U. C.; Contardi, M.; Cingolani, R.; Bayer, I. S.; Heredia, A.; Athanassiou, A., All-Natural Sustainable Packaging Materials Inspired by Plant Cuticles. *Advanced Sustainable Systems* **2017**, *1* (1-2), 1600024.
- 22. Kotkamills Kotkamills' new plastic-free and easily recyclable consumer board AEGLE barrier light is now ready for world domination. <a href="https://www.google.com/url?sa=t&rct=j&q=&esrc=s&source=web&cd=1&cad=rja&uact=8&ved=2ahUKEwjSzfPT5bTcAhWJYJoKHWbXC44QFjAAegQIABAB&url=https%3A%2F%2Fwww.epressi.com%2Ftiedotteet%2Fpaperiteollisuus%2Fkotkamills-new-plastic-free-and-easily-recyclable-consumer-board-aegle-e2-84-a2-barrier-light-is-now-ready-for-world-domination.html&usg=AOvVaw0FUXLp9vfNaNJ7w I8nOiA (accessed August 3, 2019).
- 23. Du, Y.; Zang, Y.-H.; Du, J., Effects of starch on latex migration and on paper coating properties. *Industrial & Engineering Chemistry Research* **2011**, *50* (16), 9781-9786.
- 24. Rosenmai, A. K.; Taxvig, C.; Svingen, T.; Trier, X.; van Vugt-Lussenburg, B. M. A.; Pedersen, M.; Lesné, L.; Jégou, B.; Vinggaard, A. M., Fluorinated alkyl substances and technical mixtures used in food paper-packaging exhibit endocrine-related activity in vitro. *Andrology* **2016**, *4* (4), 662-672.
- 25. Zhang, X.; Wang, H.; Liu, Z.; Zhu, Y.; Wu, S.; Wang, C.; Zhu, Y., Fabrication of durable fluorine-free superhydrophobic polyethersulfone (PES) composite coating enhanced by assembled MMT-SiO 2 nanoparticles. *Applied Surface Science* **2017**, *396*, 1580-1588.
- 26. Hogue, C., Michigan Declares staetd of emergency in town with high PFOS, PFOA levels in drinking water. https://cen.acs.org/environment/pollution/Michigan-declares-state-emergency-town/96/i32. (accessed Feburary 10, 2019)

- 27. Paper and Paperboard: Material-Specific Data. https://www.epa.gov/facts-and-figures-about-materials-waste-and-recycling/paper-and-paperboard-material-specific-data-PaperTableandGraph (accessed January 7, 2019).
- 28. Advancing Sustainable Materials Management: 2015 Fact Sheet; United States Environmetal Protection Agency: 2018-6, 2018.
- 29. Guillaume, C.; Pinte, J.; Gontard, N.; Gastaldi, E., Wheat gluten-coated papers for biobased food packaging: Structure, surface and transfer properties. *Food Research International* **2010**, *43* (5), 1395-1401.
- 30. Han, J.; Salmieri, S.; Le Tien, C.; Lacroix, M., Improvement of water barrier property of paperboard by coating application with biodegradable polymers. *J Agric Food Chem* **2010**, *58* (5), 3125-31.
- 31. Khanzadi, M.; Jafari, S. M.; Mirzaei, H.; Chegini, F. K.; Maghsoudlou, Y.; Dehnad, D., Physical and mechanical properties in biodegradable films of whey protein concentrate-pullulan by application of beeswax. *Carbohydr Polym* **2015**, *118*, 24-9.
- 32. Rhim, J.-W.; Lee, J.-H.; Hong, S.-I., Water resistance and mechanical properties of biopolymer (alginate and soy protein) coated paperboards. *LWT Food Science and Technology* **2006**, *39* (7), 806-813.
- 33. Morillon, V.; Debeaufort, F.; Blond, G.; Capelle, M.; Voilley, A., Factors affecting the moisture permeability of lipid-based edible films: a review. *Crit Rev Food Sci Nutr* **2002**, *42* (1), 67-89.
- 34. Sothornvit, R., Effect of hydroxypropyl methylcellulose and lipid on mechanical properties and water vapor permeability of coated paper. *Food Research International* **2009**, *42* (2), 307-311.
- 35. Tambe, C.; Graiver, D.; Narayan, R., Moisture resistance coating of packaging paper from biobased silylated soybean oil. *Progress in Organic Coatings* **2016**, *101*, 270-278.
- 36. Jost, V.; Kobsik, K.; Schmid, M.; Noller, K., Influence of plasticiser on the barrier, mechanical and grease resistance properties of alginate cast films. *Carbohydr Polym* **2014**, *110*, 309-19.
- 37. Kopacic, S.; Walzl, A.; Zankel, A.; Leitner, E.; Bauer, W., Alginate and Chitosan as a Functional Barrier for Paper-Based Packaging Materials. *Coatings* **2018**, *8* (7).
- 38. Yang, J.; Li, H.; Lan, T.; Peng, L.; Cui, R.; Yang, H., Preparation, characterization, and properties of fluorine-free superhydrophobic paper based on layer-by-layer assembly. *Carbohydr Polym* **2017**, *178*, 228-237.
- 39. Bordenave, N.; Grelier, S.; Coma, V., Hydrophobization and antimicrobial activity of chitosan and paper-based packaging material. *Biomacromolecules* **2010**, *11* (1), 88-96.

- 40. Ham-Pichavant, F.; Sèbe, G.; Pardon, P.; Coma, V., Fat resistance properties of chitosan-based paper packaging for food applications. *Carbohydrate Polymers* **2005**, *61* (3), 259-265.
- 41. Reis, A. B.; Yoshida, C. M. P.; Reis, A. P. C.; Franco, T. T., Application of chitosan emulsion as a coating on Kraft paper. *Polymer International* **2011**, *60* (6), 963-969.
- 42. Zhang, W.; Xiao, H.; Qian, L., Enhanced water vapour barrier and grease resistance of paper bilayer-coated with chitosan and beeswax. *Carbohydr Polym* **2014**, *101*, 401-6.
- 43. Rabnawaz, M.; Liu, G.; Hu, H., Fluorine-Free Anti-Smudge Polyurethane Coatings. *Angew Chem Int Ed Engl* **2015**, *54* (43), 12722-7.
- 44. Rabnawaz, M.; Liu, G.; Hu, H., Fluorine-Free Anti-Smudge Polyurethane Coatings. *Angewandte Chemie* **2015**, *127* (43), 12913-12918.
- 45. Helling, R.; Mieth, A.; Altmann, S.; Simat, T. J., Determination of the overall migration from silicone baking moulds into simulants and food using 1H-NMR techniques. *Food Additives & Contaminants* **2009**, *26* (03), 13.

CHAPTER 2: LITERATURE REVIEW

This chapter provides a brief overview of the physical and chemical properties, applications as well as food safety and concerns of the polysaccharide and siloxanes. Special focuses have been placed on the definition, evaluation, and factors affecting water- and oil- resistance properties. Finally, various characterization approaches related to this thesis work are discussed.

2.1 Polysaccharide

2.1.1 Structure and properties of saccharide

Biobased polymers are defined as the polymers originates from renewable/biological resources. Based on the origin and production, biobased-polymers could be divided into three categories as shown in Figure 2.1¹⁻². The barrier properties, mechanical properties and thermal properties of biobased-polymers were previously reviewed and compared with petroleum-based materials². Polysaccharides are the most abundant biobased polymers, which are extracted from plants or marine animals². These polymeric carbohydrate molecules constituted by long chains of glycosidic bonded monosaccharide units. A variety of polysaccharides has been applied for producing biodegradable films, membranes, and coatings used in various fields such as medical, pharmaceutical, and food packaging due to their excellent grease, gas, and aroma barrier properties.¹⁻²

The polysaccharide selected in this study is chitosan, which is obtained from the deacetylation of chitin. Chitin is an abundant biobased polymer existed in exoskeletons of arthropods (crustaceans and insects), cell walls of fungi, scales of lissamphibians and fish, etc. It is an acetylated polysaccharide with a formula of $(C_8H_{13}O_5N)_n$ and constituted of polymerized N-acetyl-D-glucosamine. Even though chitin is naturally partially deacetylated, it is insoluble in all common solvents³. Chitosan is a linear polymer composed of N-acetyl-D-glucosamine (acetylated

unit) and β -(1 \rightarrow 4)-D-glucosamine (deacetylated unit) that is produced by deacetylation of chitin as is shown in Figure 2.2. Chitosan is usually insoluble in water or organic solvents, but soluble in acidic medium (pH<6) because the amino groups (-NH₂) of chitosan are protonated to water-soluble cationic –NH₃⁺. Commercially, the molecular weight of chitosan is in the range of 50000-300,000 Daltons, and the degree of deacetylation is between 60% to 100%. Both chitin and chitosan are biodegradable owing to the widely existed chitinases in bacteria, fungi, animals, and plants³.

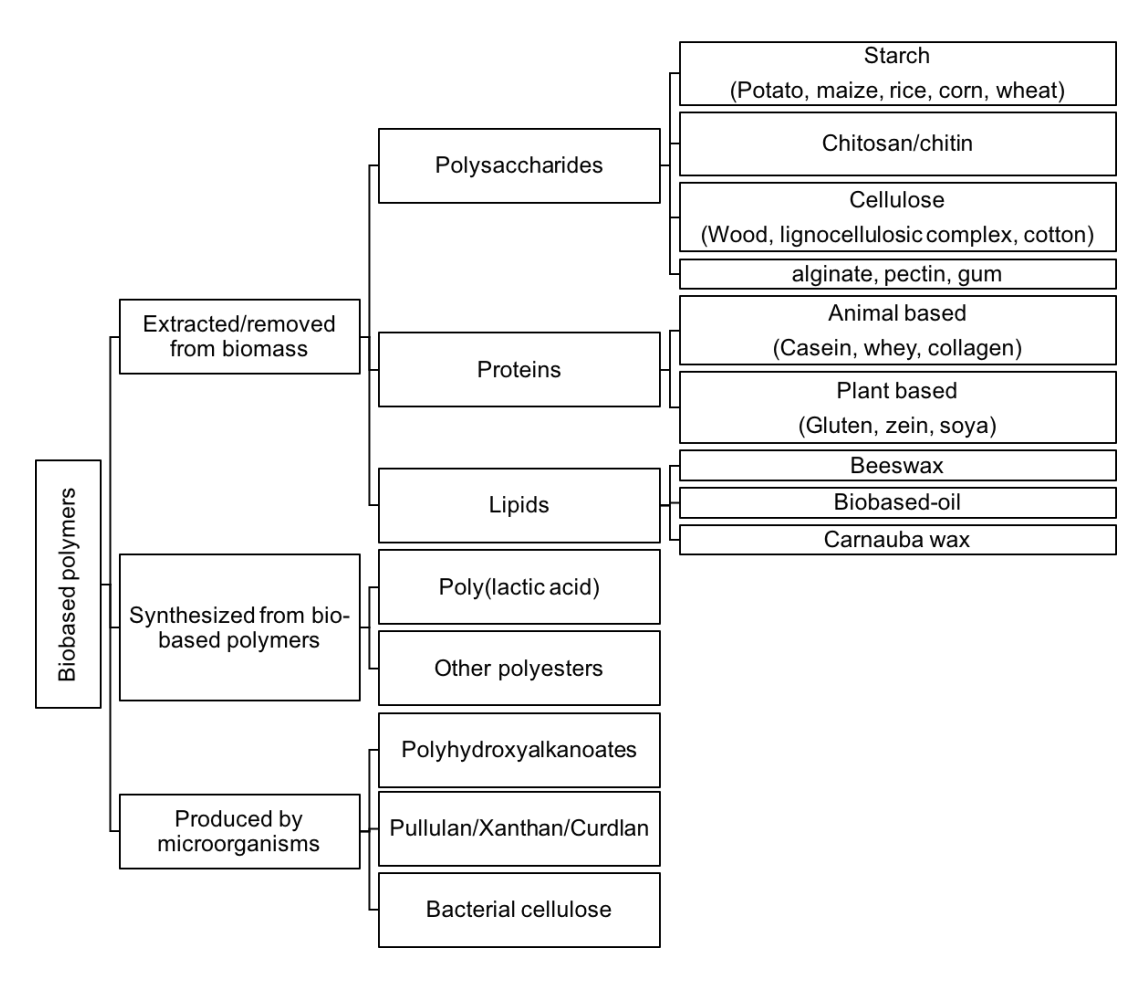


Figure 2.1 Categories of biobased polymers based on origin and production¹⁻²

Figure 2.2 Partial deacetylation of chitin to chitosan.

Chitosan is an ideal coating material for cellulosic materials because amine and hydroxyl groups develop strong interaction with hydroxyl groups of cellulose. The highly crystalline structure of chitosan along hydrogen bonds allows great oxygen properties. Chitosan has excellent film forming property with greater flexibility and mechanical properties, which are equivalent to those of some synthetic polymers². Kjellgren *et al.* studied the barrier properties of chitosan-coated paper. Great improvement of oxygen barrier property was obtained with a coat weight of 2.4 g/m² which was comparable to commercial PET liner. In addition, a significant increase of barrier properties against nitrogen and carbon dioxide was achieved with a coating weight of 5.2 g/m². Grease resistance was also excellent, whereas the obtained coating did not offer any barrier against water vapor and the water sorption was even greater than uncoated paper. This is mainly because the naturally hydrophilic structure can attract water molecules that unlocks the hydrogen bonds between chitosan chains, allowing the transport within macromolecules leading to insufficient

resistance against water⁵. Despite the outstanding performance of the chitosan coatings on cellulosic materials, the poor water resistance has limited its application.

2.1.2 Approaches to enhance water and oil properties of chitosan film/coating

To improve water-resistant properties, multi-layer, emulsion, chemical modification have been proposed to combine chitosan with other hydrophobic polymers.

2.1.2.1 Multi-layer and lamination approaches

The difference between multi-layer and lamination approaches is that multi-layer is a system prepared by subsequently applying two (or more) coating layers in multi-steps on the same substrate, whereas lamination is overlaying two (or more) pre-prepared independent films together⁶. In this approach, chitosan usually applied as the first layer on the paper substrates to cover the porous interfibrous structure due to the good film forming properties. A second layer, which is more resistant to water is generally applied on the top to guard the chitosan layer against water. The good affinity between chitosan and cellulose substrate also enhances the durability of the coating system. In general, materials obtained from multilayer and lamination approaches exhibit better water-resistant properties. ⁷⁻⁸

Caseinate, a milk protein, has also been applied along with chitosan for bi-layer coating on paper packaging materials, which yielded a reduction by 64% in the water vapors. ⁷. The introduction of beeswax to chitosan coating using a bi-layer approach has remarkably improved the WVTR (e.g., ~ 98%)⁵. Rivero et al. compared composite, bi-layer, and laminated films prepared using gelatin and chitosan⁶. Experimental findings revealed that both bi-layer and laminated films showed better water barrier properties (42.5% reduction of WVP) than the composite films.

2.1.2.2 Emulsion or blending

Blends of chitosan and other polymers such as palmitic acid⁹, curdlan¹⁰, starch¹¹ are also used for one-step coating on paper substrates. However, these methods have yielded a minor improvement in the water resistance. An emulsion of lipids/wax with polysaccharides or proteins have also been used to utilize the water resistance of lipid/wax and film-forming property of polysaccharides or proteins⁵. However, multiple parameters such as compatibility between hydrophobic and hydrophilic components, instability of the emulsion (phase separation), and the use of surfactant should be considered and to be carefully controlled during processing. More importantly, composite materials prepared via the emulsion approach are not as good as the multilayer approach in terms of improvement in water- and grease- resistance and barrier properties⁷⁻⁸. Also, the use of surfactant makes these coatings less stable against water because surfactant absorbs water and also have migration concerns from the films to the product.

2.1.2.3 Chemical modification

Cellulose has only hydroxyl groups, but chitosan has both hydroxyl and amino functional groups in the backbone due to the replacement of C-2 hydroxyl group in cellulose by an amine group. Both cellulose and chitosan could be chemically modified via etherification, esterification, acetylation due to the existence of hydroxyl. Besides, the amine groups of chitosan allow for chemical modifications through acetylation, quaternization, alkylation via Schiff's base, metal chelation, etc. The chemical modification of chitosan has been recently reviewed via high a focus on their applications in drug delivery, tissue engineering, biomedical, biosensor, and environmental application. However, our focus here is the chemical modification of chitosan to improve the water resistance of obtained film and coating.

To impart chitosan water-repellent properties, chitosan backbone is grafted with hydrophobic materials. The properties of resultant modified chitosan were affected by structure, length, and number (percentage or ratio) of side chains.

Bordenave etc. compared the emulsion and chemical modification approaches using chitosan and palmitic as a paper coating. Both approaches improved WVTR and grease resistance compared with chitosan coating alone. In another study, gallic acid was grafted to chitosan via a free radical initiated reaction for antioxidant and antimicrobial active food packaging materials. However, the mechanical properties and water resistance were reduced due to the hydrophilic structure of gallic acid. 15 Protocatechuic acid was also grafted to chitosan that led to improving the water vapor permeability and mechanical properties, but the water absorption was increased¹⁶. A double-network of chitosan/PVOH gel film was prepared using selectively cross-linking method¹⁷. Borate and tripolyphosphate were applied to impart cross-linking structure between chitosan and PVOH. The crosslinking helped to reduce the water vapor permeability. In other studies, hydrophobic chitosan film was prepared via grafting oleic acid onto chitosan coating in the presence of graphene oxide as nanofillers. 18 The obtained coating showed good barrier against oxygen by reducing the permeability up to 97%, and the water contact angle improved to 160°. Huang et al. functionalized graphene using tea polyphenols, which provided reactive oxygen sites allowing for chemical grafting to chitosan chains¹⁹.

Table 2.1 Literature data

Biopolymers	coating load (g/m2)	WVTR g/m²-d (decreased % b)	Cobb 60 g/m ² (decreased % ^b)	Kit rating	WCA°	approach
chitosan ²⁰	6	220 (68)	54 (-116)	6	70	-
chitosan ²¹	3.5	606 (44)	30.1 (23)	-	-	-
chitosan and palmitic acid ²¹	5.3	553 (48)	23 (41)	-	-	emulsion
chitosan ⁹	1.6	241 (62)	-	7	75	-
O,O'-dipalmitoylchitosan ⁹	1.6	441 (31)	-	6	117	chemical
chitosan and palmitic acid9	1.6	239 (63)	-	6	110	grafting emulsion
chitosan and caseinate ⁷	16	5 ^a (71)	-	-	-	bilayer
chitosan and beeswax ⁵	12	60 (98)	-	-	-	bilayer
chitosan and curdlan ¹⁰	5	500 (17)	3.2 (33)	-	-	emulsion
starch and chitosan ¹¹	5	495 (18)	2.8 (39)	-	-	emulsion

^a data with a subscript letter 'a' denotes WVP with a unit of g-mm/m²-d-kPa, otherwise data is the WVTR with a unit of g/m²-d b decreased % value was calculated by comparing coated-paper with uncoated-paper

2.2 Polysiloxane

2.2.1 Structure and properties

Polysiloxanes or silicones are a class of polymers with a silicone-oxygen (-Si-O-) backbone having organic moieties as the side group. Properties of polysiloxanes vary from liquid to hard plastics with different side groups, main chain length, and crosslinking extent. The most common is the poly(dimethylsiloxane) (PDMS), which has methyl groups as the side group as shown in Figure 2.3. PDMS has advantages of low toxicity, good chemical and thermal stability, biocompatibility, durability etc.²² PDMS shows great hydrophobicity and low surface tension due to the lack of polar groups in the structure. The specific silicone-oxygen backbone requires very low energy to rotate because the PDMS chains are highly flexible.²³ These unique properties are encouraging various applications for PDMS such as anti-adhesive (slip agent), hydrophobic/superhydrophobic surfaces/materials.²⁴

$$\begin{array}{c} H_3C \\ H_3C \\ \end{array} \\ \begin{array}{c} H_3C \\ \end{array} \\ \begin{array}{c} CH_3 \\ Si \\ \end{array} \\ \begin{array}{c} CH_3 \\ CH_3 \\ CH_3 \\ \end{array} \\ \begin{array}{c} CH_3 \\ CH_3 \\ CH_3 \\ \end{array} \\ \begin{array}{c} CH_3 \\ CH_3 \\ CH_3 \\ \end{array} \\ \begin{array}{c} CH_3 \\ CH_4 \\ CH_3 \\ CH_5 \\$$

Figure 2.3 Chemical structure of PDMS

2.2.2 Application of siloxane

Polysiloxane because of their lower surface tension than alkanes, render greater hydrophobicity of coatings than higher alkanes.²⁵ Sun et al. prepared a hydrophobic barrier coating on a steel panel with simple formulation include an amino-functional polysiloxane and titanium dioxide. The coating showed long term corrosion resistance and highly hydrophobic properties²⁶. Besides, polysiloxane could also be applied for synthesis superhydrophobic surface when used in

various thermosets such as epoxy and urethanes coatings. A mechanically durable superhydrophobic coating on fibrous cellulose surface using siloxane has been studied²⁷. The cellulose substrate was first dip-coated in PDMS/toluene solution, following the deposition of a layer of hydrophobic aerogel microparticles using an electrostatic powder spray method. Recently, an environmentally friendly superhydrophobic coating was prepared on polyester fabrics in three steps using water-based PDMS and commercial silica particles suspensions²⁵. The silica particles contributed to surface roughness as well as served as physical cross-linkers between PDMS chains, and the resultant coating showed good water repellency.

2.3 Fabrication of coating on paper-based materials

Three methods namely dip coating, rod coating, and spray coating are commonly used for paper coating (see Figure 2.4). These methods are discussed below.

2.3.1 Dip-coating

Dip coating is one of the most commonly applied approaches to apply a coating on a paper substrate. It typically requires three processing steps including dipping, drying, and curing. Coating slurry is usually prepared from hydrophobic compounds and one or a mixture of solvents. Particles of various sizes (nano/micro) can also be applied as if a rough surface is desirable. Dip coating is especially suitable for lab-scale research fabrication. However, it is difficult to control the thickness and coating loads, especially when the coating slurry is very viscous².

2.3.2 Rod coating

Rod coating is used both in labs as well as industry. It also involves three individual processing steps, i.e., coating, drying, and curing. Coating machines nowadays usually equipped with a series of rods with various groove depths giving to different coating thickness. The advantage of this approach is facile and easy to control the thickness of the coatings.

2.3.3 Spray coating

Spray coating is also a solvent-based coating approach which is efficient, facile and applicable for both laboratory and scale-up application. It works for almost all substrate materials even with irregular shapes. Thickness and coating load is also tunable by varying spraying amount and concentration of coating solution.

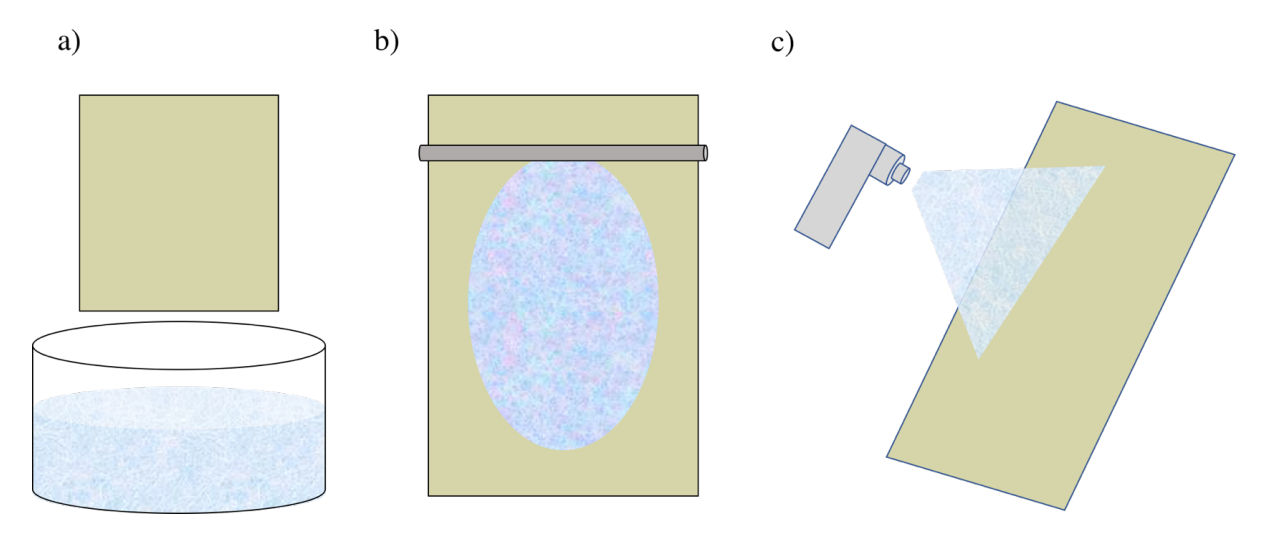


Figure 2.4 Approaches of coating fabrication: dip coating (a), rod coating (b) and spray coating (c)

2.4 Wettability

2.4.1 Static contact angle

Static contact angle describes the static behavior of a liquid droplet on a solid surface. It involved the interaction between liquid, solid surface and air/vapor, which is mainly affected by the chemical composition of the three phases as well as the morphology of the surface. When the surface is ideally smooth, chemically homogenous, the contact angle could be calculated using the Young equation (Equation 2.1):

$$cos\theta_Y = \frac{\gamma_{SV} - \gamma_{SL}}{\gamma_{LV}}$$
 Equation 2.1

where θ_Y is the contact angle, γ_{SV} , γ_{SL} and γ_{LV} are interfacial tensions between solid (S), vapor (V) and liquid (L) phases.

However, real surfaces are rarely perfectly smooth that almost all surfaces are with roughness in micro- and nano-scales. In this case, wetting could be described using two opposite states, i.e., Wenzel and Cassie states as is shown in Figure 2.5. In Wenzel state, the surface is completely wetted by liquid for which the contact angles are described by Wenzel equation (Equation 2.2):

$$cos\theta = r cos\theta_{Y}$$
 Equation 2.2

where θ is the apparent contact angle, θ_Y is the contact angle of an ideal smooth surface calculated using Young equation, which is also known as equilibrium contact angle, and r is the actual area divided by the geometrically projected area of the surface. Whereas in the Cassie state, the air is trapped in the rough texture and the surface is partially in contact with the liquid. The apparent contact angle could be evaluated using the Cassie-Baxter equation (Equation 2.3):

$$cos\theta = fcos\theta_{Y} + f - 1$$
 Equation 2.3

where f is the fraction of projected wetted area of the surface. Roughness enhances both wetting or repellency behavior, i.e., water contact angle decreases with an increase in roughness on a hydrophilic surface ($\theta_Y < 90^\circ$), and the angle increases with roughness on a hydrophobic surface($\theta_Y > 90^\circ$).

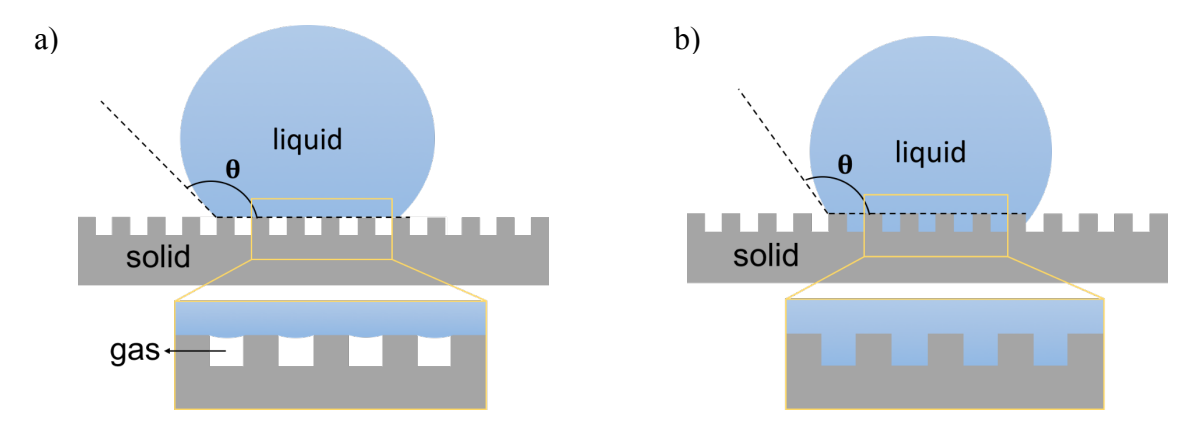


Figure 2.5 Liquid droplet in Cassie state (a) and Wenzel state (b)

When apparent water contact angle on a surface is below 10°, the surface is named as superhydrophillic that water spreads over the surface nicely. On the opposite, when the apparent water contact angle is above 150°, the surface is termed as superhydrophobic surface. The fabrication of superhydrophobic surface requires modification of both chemical composition and surface texture (highly rough-textured surface). In the case of a smooth surface, the water contact angle cannot exceed 120°. 42

For paper-based materials, monitoring the water contact angle (WCA) as a function of time is usually important since possibly it initially shows a high WCA due to the natural surface roughness followed by a sharp decrease due to the permeating of water into the paper substrate. Kopacic²⁰ monitored WCA of uncoated- and coated-paper as a function of time showing that WCA of uncoated-paper decreased until all water was absorbed by the paper substrate whereas WCA of the paper materials with a water-resistant coating decreased sharply within the first two seconds after applying the water droplet and kept constant after that. TAPPI offers standard testing method (T458 and T558) to study the surface wettability of paper based on monitoring contact angle after applying the liquid droplet for 5s and 60s.⁹

2.4.2 Sliding angle and contact angle hysteresis

For water- and oil-resistance, both contact angle hysteresis (CAH) and sliding angle (SA) are important criteria and need to be quantified. SA is the angle of the solid surface at which liquid droplet starts to slide down. Lower the sliding angles represent high repellency of the surface for that liquid. While CAH is defined as the difference between advancing and receding contact angles of a sliding droplet on a surface. CAH is an important physical phenomenon describing the antiwetting properties of a surface and giving a measurement of the adhesion strength of a droplet to a solid surface. The CAH could be described using equation 2.4²⁸:

$$mgsin\theta_{slide} = kw\gamma_{LV}(cos\theta_r - cos\theta_a)$$
 Equation 2.4

where m is the mass, g is the gravity, k is the constant, w is the contact diameter of the droplet and γ_{LV} is the surface tension, θ_{slide} is the sliding angle, θ_r and θ_a are the receding and advancing contact angles, respectively. Previous studies have shown that the hysteresis is influenced by the physical roughness as well as the chemical heterogeneities of the surface²⁸. Lower CAH indicates better liquid repellency and a weaker interaction between liquid and surface.

CAH is typically measured by two methods namely the tilted plane method and the sessile drop method.²⁹ In the tilted plane method, a droplet was placed on an inclined plane, and the advancing contact and receding contact angles were measured when the droplet starts sliding down as shown in Figure 2.6. In the sessile drop method, a droplet is applied on the solid surface, and a specific volume of that liquid is pumped into the droplet, and the advancing angle is recorded. Then, exactly the same amount of the liquid is pulled out from the droplet to record the receding angle.

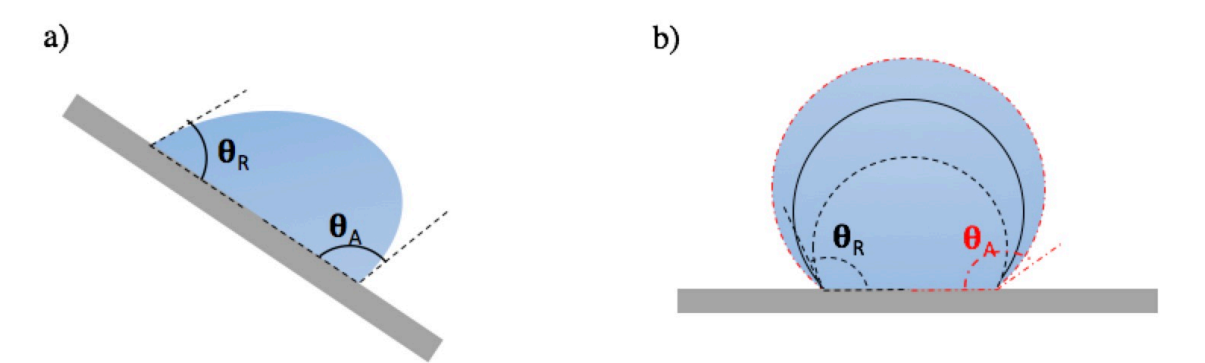


Figure 2.6 CAH measurement using a tilted plane method (a) and sessile drop method (b)

2.5 Barrier Properties

2.5.1 Water absorption

The interaction between liquid water and paper has been previously reviewed by Samyn et al.²⁸ It involves the interaction between water and cellulose fibers, and the interaction between water and paper webs, which are mainly driven by the intrinsic hydrophilic structure of cellulose fibers, and interfibre penetration, molecular diffusion, and capillary pressure.

Water absorption by paper, paperboard and the corrugated board could be determined using the Cobb Test according to standard tests ISO 535 and TAPPI 441, which quantifies the amount of water (in grams) absorbed by paper materials under a standard condition for a specific of time (60 s). During the test, an area of 100 cm² of paper material is exposed to 1-cm-depth DI water for 60 seconds, and the quantity of water absorbed by the paper material was calculated based on the weight of the paper material before and after the test. Water absorptiveness is expressed as Cobb value (g/m²) which is the mass in grams of water absorbed by a 1-m² paper material. Cobb Test requires paper sheets larger than 100 cm² and is commonly used in the industry.

For a smaller specimen, which is more common in the lab stage, soaking tests are usually applied. In the soaking test, a specimen with a specific size is soaked into the water, and the water absorbed by the specimen is monitored as a function of time. Water absorbance is described using the water gain (%) value calculated using the equation:

water gain % =
$$\frac{final\ weight-initial\ weight}{initial\ weight} \times 100$$
 Equation 2.5

This approach is more commonly used for samples prepared using dip coating approach of which all sides of the substrate are properly coated.

2.5.2 Water vapor transmission rate

The barrier property against water vapor is quantified as the water vapor transmission rate (WVTR) that is defined as the mass of total water vapor permeated through the materials per unit time and area under a specific relative humidity (RH) environment and usually expressed in a unit of g/m²-day. WVTR of paper-based materials could be determined according to standards such as the Technical Association of the Pulp and Paper Industry (TAPPI) 448 and American Society for Testing and Materials (ASTM) E96. Testing condition is usually set as 23 °C and 50% RH for the normal condition or 38 °C and 85-90% RH for extremely high RH conditions.

2.5.3 Oil/grease resistance

Oil/grease resistance could be evaluated using Kit Test as well as internal Fraunhofer IVV method³⁰. TAPPI also offers a standard test method named *Turpentine test for voids in glassine and greaseproof papers* (T 454), which is especially suitable for greaseproof paper materials. Kit Test (*Repellency of Paper and Board to Grease, Oil, and Waxes*) is an industry standard test (No. UM 557) offered by the Technical Association of the Pulp and Paper Industry (TAPPI). In internal Fraunhofer IVV method, a specimen with a 50 cm² area was covered with a fleece saturated with colored oil for 24 hours under 23 °C and 50% RH. The stained area on the specimen was counted and calculated as a percentage of the tested area. Kit Test is the most commonly applied method to evaluate oil resistant property of paper-based materials. A series of numbered solutions (NO.1-12) with different aggressiveness due to various surface tension and viscosity are prepared by mixing castor oil, n-heptane, and toluene in different ratios. Number 12 is the most aggressive, while 1 is the least. Solution droplets are sequentially applied on a specimen and cleaned with a clean tissue after 15 seconds. The tested area is examined immediately where the specimen is

regarded as failed if there are any darkened spots on the surface. The number of the most aggressive solution, which the specimen can support, is reported as "kit rating".

2.6 Mechanical properties

Mechanical properties of paper materials are defined and determined in TAPPI standards. Basically, the strength of paper materials under exposure to different force types such as stretching, crushing, bending, tearing, etc. could be evaluated using different approaches and standards as is shown in Table 2.2. Chitosan coating could increase the mechanical properties of paper substrate especially when the coating load is high.^{4,10-11} For some biopolymer such as starch a plasticizer is necessary for good mechanical strength and flexibility.³¹

Table 2.2 Mechanical properties, instruments and testing standards

Mechanical properties	Force type	Instruments	TAPPI standards	Quantification (unit)
Tensile strength	stretching	Instron testing machine	T 494	Tensile strength (lbs/in)
Compressing strength on the edge	crushing	TMI crush tester	T 822	Force value required to crush the sample (lbs)
Bending stiffness	bending	Taber stiffness tester	T 489	Bending moment (g cm)
Internal tearing resistance	tearing	Elmendorf-type tearing tester	T 414	Tearing force (g)

2.7 Recyclability

Recyclability of paper is one of the crucial parts when paper material being considered for real-world applications. Recycling of paper involves steps including the production of pulp (repulping), purification and cleaning of the recycled pulp, and manufacturing of paper from the recycled pulp.³² In the laboratory scale, a modified procedure is always applied to study the recyclability and repulpability. For example, Wenzel studied the repulpability of a recyclable and

compostable acrylic polymer/copolymer coated paper using a TAPPI disintegrator, and the obtained pulp slurry is made into a standard TAPPI handsheets.³³

2.8 Migration study

According to FDA regulations (1997 FDA Modernization Act), any substance which is intended to be used for food contact applications needs to be evaluated for their food safety. Packages that come in the direct contact of food, the migration of ingredients form packaging to food is possible. The quantity of a substance that migrates from the packaging materials to food products is an important factor for safety evaluation along with the toxicity profile of that substance.³⁴ Migration test is required by FDA in Code of Federal Regulation (CFR) Title 21 (Section 170, Volume 39),³⁵ while the migration testing and analytical methods are explained in guidance for industry offered by FDA.³⁶

Migration cell is designed such that a known surface area of samples is extracted with a known amount of food simulant to produce sufficient extractives for characterization. A two-sided migration cell³⁷ is recommended by FDA, however, which is not suitable for laminate constructions and coated-substrates.³⁶ When a material is thicker than 0.05 cm, migration needs to be considered independently from both sides; otherwise, migration will be considered from a single side of the specimen.

Per FDA guidance for industry related to migration tests of paper coating, a coating solution is coated on an inert substrate such as metal or glass to avoid the high level of extractives from paper substrates. Food simulants are selected that 10% ethanol for aqueous and acidic foods, 50% ethanol for low- and high- alcoholic foods, and food oil (corn oil), HB307 or Miglyol 812 for fatty foods. The solvent volume-to-exposed surface area ratio is 10 ml/in² which is equivalent to 10 g of the packaged product is in contact with 1 in² of packaging material. The guidance also

provides recommendations and protocols corresponding to materials with various conditions of use. An accelerated testing condition with 40 °C for 10 days is recommended, which is roughly equivalent to 20 °C for 6-12 months.

2.9 Characterization

2.9.1 Coating Load

A coating load represents the amount of coating in dry basis coated on the paper substrates. Coating load has a decisive role on the performance of the coated-paper. TGA can be applied where the degradation of coated paper is recorded against temperature profile. According to the TGA analysis of paper substrate (cellulose) and chitosan, both have a decomposition peak within the range of 200-300 °C.³⁸ This is the case with most of the biopolymers ^{39,41}. Another method to determine the coating load is the change in weight before and after coating using microbalance. Basis Weight is the weight of paper materials with a specific area, which could be expressed in grammage (g/m²) or lbs/ream. By comparing the basis weight of paper materials before and after applying the coating, the coating load can be obtained and converted to the unit of g/m².

2.9.2 Structure and morphology

Surface roughness could be characterized using optical profilometry or AFM, where optical profilometry is for microscale roughness and AFM is for nanoscale roughness. Electron microscopy is commonly applied to study the morphology of the surface. For example, Reis et al.²¹ studied the surface morphology of chitosan-coated paper using SEM.

REFERENCES

REFERENCES

- 1. Shalini, R.; Singh, A., Biobased Packaging Materials for the Food Industry. *Journal of Food Sceince & Technology Nepal* **2009**, *5*, 16.
- 2. Rastogi, V.; Samyn, P., Bio-Based Coatings for Paper Applications. *Coatings* **2015**, *5* (4), 887-930.
- 3. Rinaudo, M., Chitin and chitosan: Properties and applications. *Progress in Polymer Science* **2006**, *31* (7), 603-632.
- 4. Kjellgren, H.; Gällstedt, M.; Engström, G.; Järnström, L., Barrier and surface properties of chitosan-coated greaseproof paper. *Carbohydrate Polymers* **2006**, *65* (4), 453-460.
- 5. Zhang, W.; Xiao, H.; Qian, L., Enhanced water vapour barrier and grease resistance of paper bilayer-coated with chitosan and beeswax. *Carbohydrate Polymers* **2014**, *101*, 401-6.
- 6. Rivero, S.; García, M. A.; Pinotti, A., Composite and bi-layer films based on gelatin and chitosan. *Journal of Food Engineering* **2009**, *90* (4), 531-539.
- 7. Khwaldia, K.; Basta, A. H.; Aloui, H.; El-Saied, H., Chitosan-caseinate bilayer coatings for paper packaging materials. *Carbohydrate Polymers* **2014**, *99*, 508-16.
- 8. Khwaldia, K.; Arab-Tehrany, E.; Desobry, S., Biopolymer Coatings on Paper Packaging Materials. *Comprehensive Reviews in Food Science and Food Safety* **2009**, *9* (1), 82-91.
- 9. Bordenave, N.; Grelier, S.; Coma, V., Hydrophobization and antimicrobial activity of chitosan and paper-based packaging material. *Biomacromolecules* **2010**, *11* (1), 88-96.
- 10. Brodnjak, U. V., Experimental investigation of novel curdlan/chitosan coatings on packaging paper. *Progress in Organic Coatings* **2017**, *112*, 86-92.
- 11. Vrabič Brodnjak, U., Influence of ultrasonic treatment on properties of bio-based coated paper. *Progress in Organic Coatings* **2017**, *103*, 93-100.
- 12. Wang, J.; Wang, L.; Yu, H.; Zain Ul, A.; Chen, Y.; Chen, Q.; Zhou, W.; Zhang, H.; Chen, X., Recent progress on synthesis, property and application of modified chitosan: An overview. *Int J Biol Macromol* **2016**, *88*, 333-44.
- 13. Kurita, K., Controlled functionlization of the polysaccharide chitin. *Progress in Polymer Science* **2001**, *26*, 11.
- 14. Harish Prashanth, K. V.; Tharanathan, R. N., Chitin/chitosan: modifications and their unlimited application potential—an overview. *Trends in Food Science & Technology* **2007**, *18* (3), 117-131.

- 15. Wu, C.; Tian, J.; Li, S.; Wu, T.; Hu, Y.; Chen, S.; Sugawara, T.; Ye, X., Structural properties of films and rheology of film-forming solutions of chitosan gallate for food packaging. *Carbohydrate Polymers* **2016**, *146*, 10-19.
- 16. Liu, J.; Meng, C.-g.; Liu, S.; Kan, J.; Jin, C.-h., Preparation and characterization of protocatechuic acid grafted chitosan films with antioxidant activity. *Food Hydrocolloids* **2017**, *63*, 457-466.
- 17. Liang, S.; Liu, L.; Huang, Q.; Yam, K. L., Preparation of single or double-network chitosan/poly(vinyl alcohol) gel films through selectively cross-linking method. *Carbohydrate Polymers* **2009**, *77* (4), 718-724.
- 18. Fayyad, E. M.; Sadasivuni, K. K.; Ponnamma, D.; Al-Maadeed, M. A. A., Oleic acid-grafted chitosan/graphene oxide composite coating for corrosion protection of carbon steel. *Carbohydr Polym* **2016**, *151*, 871-878.
- 19. Huang, Q.; Hao, L.; Xie, J.; Gong, T.; Liao, J.; Lin, Y., Tea Polyphenol-Functionalized Graphene/Chitosan as an Experimental Platform with Improved Mechanical Behavior and Bioactivity. *ACS Appl Mater Interfaces* **2015**, *7* (37), 20893-901.
- 20. Kopacic, S.; Walzl, A.; Zankel, A.; Leitner, E.; Bauer, W., Alginate and Chitosan as a Functional Barrier for Paper-Based Packaging Materials. *Coatings* **2018**, *8* (7).
- 21. Reis, A. B.; Yoshida, C. M. P.; Reis, A. P. C.; Franco, T. T., Application of chitosan emulsion as a coating on Kraft paper. *Polymer International* **2011**, *60* (6), 963-969.
- 22. Blanco, I., Polysiloxanes in Theranostics and Drug Delivery: A Review. *Polymers* (*Basel*) **2018**, *10* (7).
- 23. Owen, M. J., Elastomers: Siloxane. In *Encyclopedia of Materials: Science and Technology*, Second ed.; Elsevier: 2003; pp 2480-2482.
- 24. Khorasani, M. T.; Mirzadeh, H.; Kermani, Z., Wettability of porous polydimethylsiloxane surface: morphology study. *Applied Surface Science* **2005**, *242* (3-4), 339-345.
- 25. Cai, R.; Glinel, K.; De Smet, D.; Vanneste, M.; Mannu, N.; Kartheuser, B.; Nysten, B.; Jonas, A. M., Environmentally Friendly Super-Water-Repellent Fabrics Prepared from Water-Based Suspensions. *ACS Appl Mater Interfaces* **2018**, *10* (18), 15346-15351.
- 26. Sun, X.; Turnage, S.; Iezzi, E. B.; Yang, Y.; Chang, B.; Muthegowda, N. C.; Balijepalli, S. K.; Dhuyvetter, N.; Wang, L. P.; Solanki, K. N.; Rykaczewski, K., Water permeation and corrosion resistance of single- and two-component hydrophobic polysiloxane barrier coatings. *Journal of Coatings Technology and Research* **2017**, *14* (6), 1247-1258.
- 27. Saadat-Bakhsh, M.; Ahadian, H. R.; Nouri, N. M., Facile, robust and large-scale fabrication method of mechanically durable superhydrophobic PDMS/aerogel coating on fibrous substrates. *Cellulose* **2017**, *24* (8), 3453-3467.

- 28. Samyn, P., Wetting and hydrophobic modification of cellulose surfaces for paper applications. *Journal of Materials Science* **2013**, *48* (19), 6455-6498.
- 29. Eral, H. B.; Mannetje, D. J. C. M. t.; Oh, J. M., Contact Angle Hysteresis: a Review of Fundamentals and Applications. *Colloid Polymer Science* **2013**, *291* (2), 14.
- 30. Jost, V.; Kobsik, K.; Schmid, M.; Noller, K., Influence of plasticiser on the barrier, mechanical and grease resistance properties of alginate cast films. *Carbohydr Polym* **2014**, *110*, 309-19.
- 31. Guazzotti, V.; Limbo, S.; Piergiovanni, L.; Fengler, R.; Fiedler, D.; Gruber, L., A study into the potential barrier properties against mineral oils of starch-based coatings on paperboard for food packaging. *Food Packaging and Shelf Life* **2015**, *3*, 9-18.
- 32. Bajpai, P., Process Steps in Recycled Fiber Processing. In *Recycling and Deinking of Recovered Paper*, Elsevier: MA, USA, 2014; p 55.
- 33. Wenzel, D. J.; Bartholomew, G. W.; Quick, J. R.; Delozier, M. S.; Klass-Hoffman, M. Recyclable and Compostable Coated Paper Stocks and Related Methods of Manufacture. US5837383, 1994.
- 34. Questions & Answers on Bisphenol A (BPA) Use in Food Contact Applications. https://www.fda.gov/food/ingredientspackaginglabeling/foodadditivesingredients/ucm355155.ht m (accessed 4-15).
- 35. 21CFR170.39. Food and Drug Administration: 2018.
- 36. Guidance for Industry: Preparation of Premarket Submissions for Food Contact Substances (Chemistry Recommendations). Food and Drug Administration: 2007.
- 37. Snyder, R.; Breder, C., New FDA migration cell used to study migration of styrene from polystyrene into various solvents. *Association of Official Analytical Chemists* **1985**, *68* (4), 5.
- 38. Li, Z.; Rabnawaz, M.; Krishna, A.; Sirinakbumrung, N.; Khan, B.; Kamdem, D. P., A Closed-Loop and Sustainable Approach for the Fabrication of Plastic-Free Oil- and Water-Resistant Paper Products. *Green Chemistry* **2019**, *submitted*.
- 39. Velásquez Herrera, J. D.; Lucas Aguirre, J. C.; Quintero Castaño, V. D., Physical-chemical characteristics determination of potato (Solanum phureja Juz. & Bukasov) starch. *Acta Agronómica* **2017**, *66* (3), 323-330.
- 40. Giita Silverajah, V. S.; Ibrahim, N. A.; Yunus, W. M.; Hassan, H. A.; Woei, C. B., A comparative study on the mechanical, thermal and morphological characterization of poly(lactic acid)/epoxidized Palm Oil blend. *Int J Mol Sci* **2012**, *13* (5), 5878-98.
- 41. Zhou, H.; Long, Y.; Meng, A.; Chen, S.; Li, Q.; Zhang, Y., A novel method for kinetics analysis of pyrolysis of hemicellulose, cellulose, and lignin in TGA and macro-TGA. *RSC Advances* **2015**, *5* (34), 26509-26516.

42. Contact Angle of Water on Smooth Surfaces and Wettability, http://www.uskino.com/article/113.html. (accessed on February 13, 2019)

CHAPTER 3: FABRICATION OF FOOD-SAFE WATER-RESISTANT PAPER COATINGS USING A MELAMINE PRIMER AND POLYSILOXANE OUTER LAYER

A version of this chapter is published as:

Li, Z.; Rabnawaz, M., Fabrication of Food-Safe Water-Resistant Paper Coatings Using a Melamine Primer and Polysiloxane Outer Layer. ACS Omega 2018, 3 (9), 11909-11916.

3.1 Abstract

Paper-based materials are highly desirable as packaging materials due to their numerous advantages that include low cost, renewability, and biodegradability. However, their hydrophilicity has limited their range of applications. Reported herein is a facile and economical approach for the preparation of biodegradable water-resistant paper for food contact applications. Commercial printing paper and cup papers are coated with melamine, which is FDA approved for food contact applications. Subsequently, a water-repellent outer layer is applied using polydimethylsiloxane-isocyanate (PDMS-NCO). A relationship between the PDMS concentration and water contact angles (WCAs) of the obtained coating was studied. Typically, the coated cup paper and printing paper had coating loadings of 1.61 ± 1.10 and 0.93 ± 0.74 wt%, respectively. After the coatings had been applied, the WCAs were very high (>125°), and water-absorption had decreased by 70% for printing paper and by 35% for cup paper. Considering the facile fabrication method and the low-cost food-safe raw materials herein, this approach will have great potential for the large-scale production of materials for use in food- and non-food contact applications.

3.2 Introduction

The annual production of plastic has reached 407 million tons globally. Approximately 80% of all plastics produced are used in the packaging sector because of their excellent properties. Meanwhile, ~244 million tons of plastic annually are disposed of either in landfills or ends in the ocean. To address this problem, greener alternatives such as biodegradable plastic and paper-based packaging materials are highly desirable.

Paper, paperboard and corrugated board are widely used materials in the packaging and distribution sectors due to their numerous advantages including their low cost, reliance on renewable feedstocks and their biodegradable nature. Approximately 40 million tons of paper and

paperboard were generated in 2014, of which 75.4% was recycled and composted in the United States according to U.S. Environmental Protection Agency.² Despite the low cost and environmental benefits of paper and paper-based materials, they have limited applicability due to their poor water resistance.

A common approach to improve the water resistance of paper-based materials is to laminate them with a plastic film. For example, disposable paper cups bear a water-resistant low-density polyethylene (LDPE) inner liner that prevents the direct contact between a liquid and the water-absorbing paper.³ However, after use, the separation of paper from plastic is difficult and thus paper cups end up in landfills or in the ocean. Biobased plastic such as polylactic acid (PLA) inner layers are also used as alternatives to LDPE.⁴⁻⁵ However, PLA and paper cellulose biodegrades in different environments because PLA is compostable (biodegradable under industrial compost conditions only) at temperature 60°C in a week.⁶ Wax is also commonly used to enhance the water resistance, but wax has poor crack-resistance as well as low thermal resistance.⁷⁻⁸ Thus, challenges still remain with the development of environmentally friendly water-resistant paper-based materials

Recently, research interest has grown in the development of recyclable and biodegradable (being decomposed into basic molecules by microorganisms), and thus they can reduce the strain on our landfills) paper-based materials with good water-resistance properties for use in packaging, the medical industry, food storage, bioassay devices or microfluidics. ^{9,10,11} Considerable research have been undertaken through various approaches such as paper sizing, ^{12-14,15,16} chemical modification (layer-by-layer, ¹⁷⁻¹⁸ grafting approach, ¹⁹⁻²¹ etc.) and physio-chemical modification (plasma etching, laser, etc.)²² However, most of these techniques are not applicable for practical large-scale production due to their time-consuming processes, reliance on costly raw materials, non-suitability

for food contact applications, and the use of environmentally harmful chemicals. Thus, the development of a facile, low-cost, safe for food contact, and scalable approach remains as a critical practical challenge.

The coating of paper with water-repellent materials is considered as a simple and commercially viable approach to develop biodegradable water-resistant paper. Typically, compounds with low surface energies such as fluorinated polymers, polysiloxanes²³⁻²⁴ or higher alkanes are applied to fabricate a hydrophobic coating for paper. Although fluorochemicals render excellent water resistance due to their low surface energies, demands have arisen for the phasing out of these materials from use in paper coatings due to their toxicity and environmental concerns.²⁵⁻²⁶ Alternatively, polysiloxanes and higher alkanes have attracted great attention due to their nontoxic nature, affordability, and environmental friendliness.²⁷ Due to their lower surface tension, polysiloxanes render greater hydrophobicity than is offered by higher alkanes.²⁸ For example, a mechanically durable superhydrophobic coating has been applied onto fibrous cellulose surfaces.²⁹ Considering the global importance of plastic-free water repellent paper, Kotkamills' has introduced a new plastic-free and easily recyclable paper AEGLETM Barrier Light.³⁰ To the best of our knowledge, however, have been no prior reports on the fabrication of water-resistant paper using fully biodegradable, low-cost materials, with suitability for food contact applications.

In this study, water-resistant coatings for paper are reported. These coatings rely on polysiloxanes, which are affordable and biocompatible materials³¹ that biodegrade into non-toxic silicate minerals,³²⁻³⁴ and thus are safe for food processing.³⁵⁻³⁷ To promote firm binding of the PDMS onto paper substrates, melamine was used as a primer. Melamine is a FDA approved material for food contact applications (tolerable level is 0.63mg/kg of body weight, per day),³⁸ that exhibits superior binding to paper because it is a strong hydrogen donor as well as an acceptor,

thus providing it with excellent performance as a primer. Meanwhile the use of PDMS-NCO enables the chemical grafting of PDMS to melamine via a biodegradable urea linkages formed as a result of a reaction between the NCO and amine groups of PDMS and melamine, respectively.³⁹ In the absence of melamine, the bonding between PDMS and paper would be weak and the PDMS could be readily washed away from the paper. As a result, water-resistant coated paper bears PDMS as its outer layer that is firmly held onto the paper substrate by an intermediate melamine layer. This method is facile, economical and suitable for large-scale production. The obtained melamine-PDMS coating exhibits excellent water-resistance.

3.3 Experimental

3.3.1 Materials

Melamine (purity 99%), acetone (purity 98%) and monoaminopropyl terminated polydimethylsiloxane (PDMS-NH₂) with a molecular weight of 2000 g/mol were purchased from Sigma Aldrich (MO, USA) and used without further purification. Polyisocyanate (HDIT) was supplied by a proprietary manufacture. Printing paper was purchased at a local supermarket. Cup papers were obtained from cup papers purchased from a local coffee shop (Spartan at Michigan State University, MI, USA). Prior to the application of the coating, the polymer layer on the commercial paper cups were carefully peeled off.

3.3.2 Methods and Characterization

3.3.2.1 Fabrication of water-resistant paper

Figure 3.1 shows the fabrication of two-step approach used to achieve the desired water-resistant paper. First, melamine was applied as a primer layer. In the next step, PDMS-NCO solution was applied.

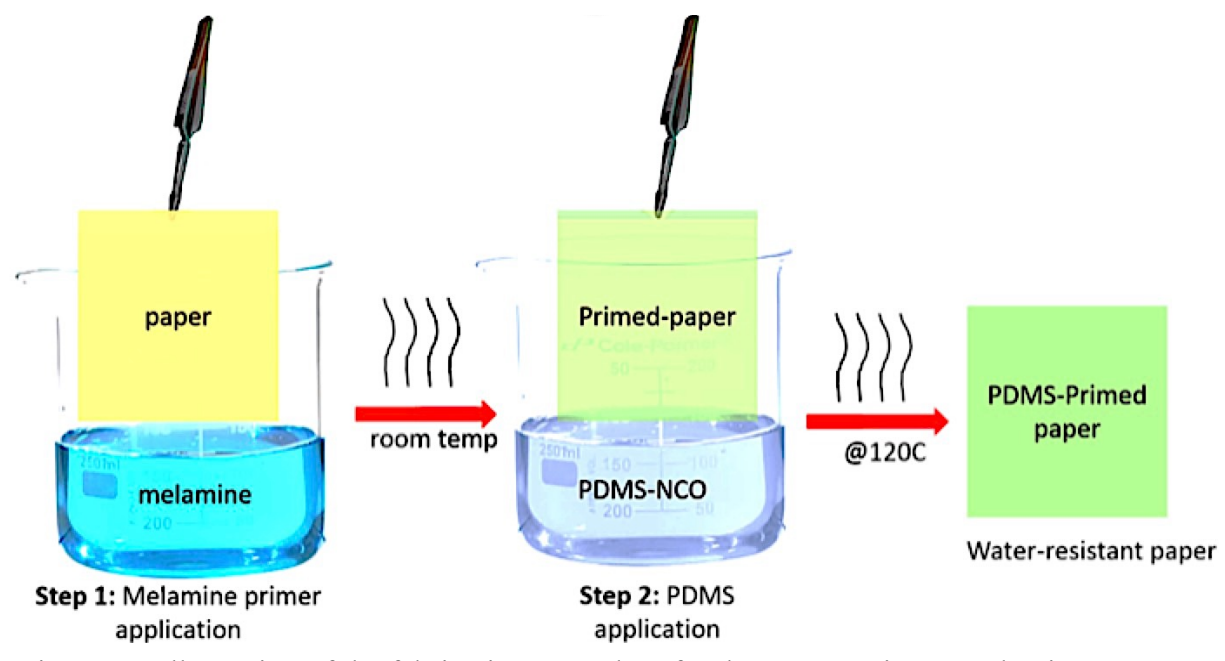


Figure 3.1 Illustration of the fabrication procedure for the water-resistant melamine-PDMS primed paper.

- a) Preparation of PDMS-NCO solution: First, HDIT (100 mg) was dissolved in acetone (5 mL). Subsequently, PDMS-NH₂ (200 mg PDMS-NH₂ in 5 mL acetone) was added into the HDIT solution and homogenized using a vortex mixer for 30 sec. The concentration of obtained PDMS-NCO solution was recorded as the concentration of PDMS, i.e. 2% in this case. All the characterization and testing was based on the formulation of 2% PDMS-NCO coating. Moreover, in order to study the effect of PDMS-NCO concentration on coating properties, PDMS-NCO solution with various concentration (0.1%, 0.5%, 1%, 2%, 4% and 8%) was prepared by varying the amount HDIT and PDMS-NH₂ proportionally but keeping the amount of acetone constant.
- b) Coating application: Printing paper and cup paper were cut into 1×1 in² sections prior to coating. Aqueous melamine solutions were prepared by dissolving melamine in hot water at a concentration of 0.20 wt%. Paper substrates were immersed into the melamine solution for 10 s, and they were then left under ambient conditions for 5 min to enable solvent evaporation. These paper samples were then dipped in a PDMS-NCO solution for 10 sec. The paper samples were

subsequently allowed to dry in open air for 5 min prior to heating at 120 °C for 1 h. The resultant coated paper samples are referred to as melamine-PDMS primed paper.

c) Preparation of reference coated papers (without PDMS): Samples that were only coated with the melamine solution are from here onwards referred to as melamine primed paper. Meanwhile, samples that were dipped into the melamine solution and subsequently in the HDIT solution are from here onwards referred to as melamine-HDIT primed paper.

3.3.2.2 Characterization

Fourier-transform infrared (FTIR) spectra of unmodified paper, melamine primed paper, melamine-HDIT primed paper and melamine-PDMS primed paper were recorded using a Shimadzu IR Prestige21 FTIR spectrometer (Shimadzu Co., Columbia, MD) equipped with an Attenuated Total Reflection (ATR) attachment (PIKE Technologies, Madison, WI). A total number of 64 scans with a spectral range of 4000-400 cm⁻¹ and a resolution of 4 cm⁻¹ were recorded for each sample.

Thermogravimetric analysis (TGA) was recorded to determine the thermal stability and weight gain of the coated paper in reference to the uncoated paper. The TGA was performed using a Q-50 thermogravimetric analyzer (TA Instruments, New Castle, DE). The weight loss exhibited by the samples was recorded as a function of the temperature range from 23 to 600 °C at a ramp rate of 10 °C/min under a nitrogen flow with a flow rate of 40 mL/min.

The weight gain by paper as a result of the application of the coatings was quantified via gravimetric methods. The weight of solution absorbed by paper substrates was recorded, and the theoretical loading of the coating was calculated based on the solution absorbed by the paper and their corresponding concentration. The experimental load of coating was quantified by calculating the difference between the weight gain of the coated paper and that of the corresponding control.

The weight before and after coating was recorded using a microbalance. To minimize the experimental error, the control paper substrates were dipped into pure water, and subsequently into acetone. Both the control group and the coated samples were dried under identical conditions.

In order to study the safety of melamine in paper coating, the theoretical melamine loading on paper coating was studied using gravimetric approach similarly to the above-mentioned weight gain analysis. Paper substrates were dipped into pure water as a control. Experimental melamine loading was not studied because melamine loading was too little that there was no significant difference before and after melamine primer was applied according to preliminary test.

3.3.2.3 Water resistance tests

Prior to testing, all of the samples were preconditioned by drying at 70 °C under vacuum for 1 h to remove moisture. Water-gain tests were conducted by dipping preconditioned samples into deionized water for periods of 0.5, 1, 2, 3, 5 and 24 h. The weight of each sample was recorded after wiping excess water from the surface with a clean tissue. Water-gain was calculated using the equation 1:

$$watergain\% = \frac{final\ weight\ -\ initial\ weight}{initial\ weight} \times 100$$
 (Equ. 1)

3.3.2.4 Water contact angles (WCAs)

Water contact angles (WCAs) were measured using a 590-U1 Advanced Automated Goniometer with DROPimage Advanced software (Ramé-hart Instrument Co., NJ, USA). 10 μ L deionized water droplet was placed onto the sample and allowed the droplet to sit for 3 min before contact angle was measured. The reported WCA values are the average of three measurements on different areas on the surface of each sample.

3.3.2.5 Scanning electron microscopy (SEM)

JEOL 6610 SEM, (JEOL Ltd., Japan) system was used for the SEM analysis. Samples were mounted on aluminum discs and coated with gold layer (10-nm-thickness) using a sputtering approach. All samples were examined with an accelerating voltage of 15 kV.

3.4 Results and Discussion

In this study, a novel fabrication approach has been developed to prepare a biodegradable water-resistant paper from low-cost raw materials. To obtain biodegradable water-resistant paper via this strategy, paper (cellulose) is coated with biodegradable melamine and PDMS using a dual-layer fabrication approach (see Figure 3.1). Melamine is selected because it binds strongly to the paper via hydrogen bonding. In addition, one or more of the three NH₂ moieties on the triazine core of each melamine react immediately with the NCO group of the PDMS-NCO, and thus the PDMS chains bind firmly to the paper through the melamine primer. The PDMS-NCO was chosen because NCO reacts with the NH₂ groups of melamine cleanly and efficiently even in the presence of water. As it is critical that each PDMS-NCO chain should have at least one NCO group to react with melamine, PDMS-NCO was thus prepared by mixing PDMS-NH₂ with a 10-fold excess of NCO groups. It is important to note that the low-cost and commercial availability of the raw materials (melamine, paper, PDMS), this approach is commercially viable for numerous real-world applications

FTIR analysis was performed to confirm the successful application of PDMS onto the paper. Figure 3.2 shows the FTIR spectra of the printed paper (a) and cup paper (b) at various stages during the fabrication process. The melamine C-N stretching in IR for the melamine-primed paper overlapped with that from the uncoated paper at 1553cm⁻¹. The melamine-PDMS primed paper exhibits several characteristic peaks corresponding to the PDMS. For example, the peak at

1260 cm⁻¹ corresponds to the stretching vibration of the –CH₃ groups in the Si-CH₃ moieties of PDMS, while the peak at 798 cm⁻¹ represents the –CH₃ rocking and Si-C stretching of PDMS. Thus the FTIR spectrum indicated that PDMS had been successfully applied onto the paper substrate.

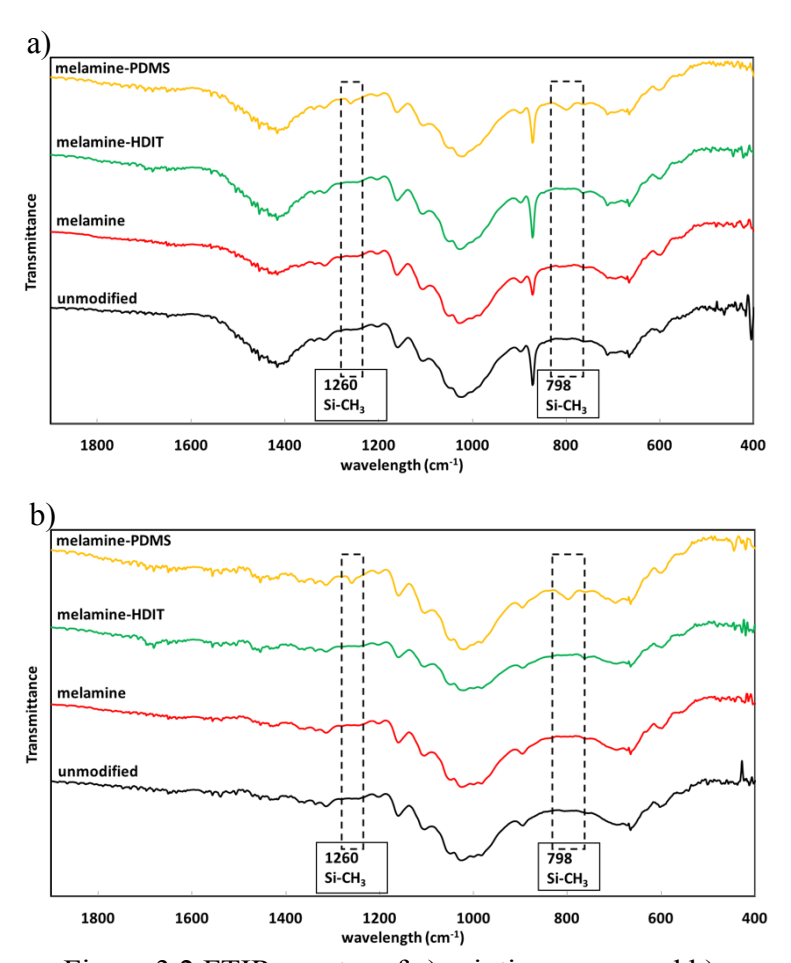


Figure 3.2 FTIR spectra of a) printing paper and b) cup paper.

Thermogravimetric analysis (TGA) was used to evaluate the thermal stability of the coating. As shown in Figure 3.3, the initial weight loss observed below 120 °C was attributed to the moisture loss. Meanwhile, the weight loss encountered between 200-270 °C was attributed to the decomposition of melamine,⁴⁰ whereas the decomposition of PDMS occurred over the temperature range of 400-500 °C.⁴¹ The absence of peaks between 200-270 °C suggests the

absence of free melamine presumably underwent reaction with the terminal -NCO group of PDMS-NCO. Overall, the TGA indicated that the coated paper had greater thermal stability than that of the uncoated paper, and thus the thermal stability of paper was improved after the coating. This also suggests that the coated paper is suitable for applications in which the material may be exposed to temperatures reaching up to ~220 °C as it is thermally stable up to this temperature.

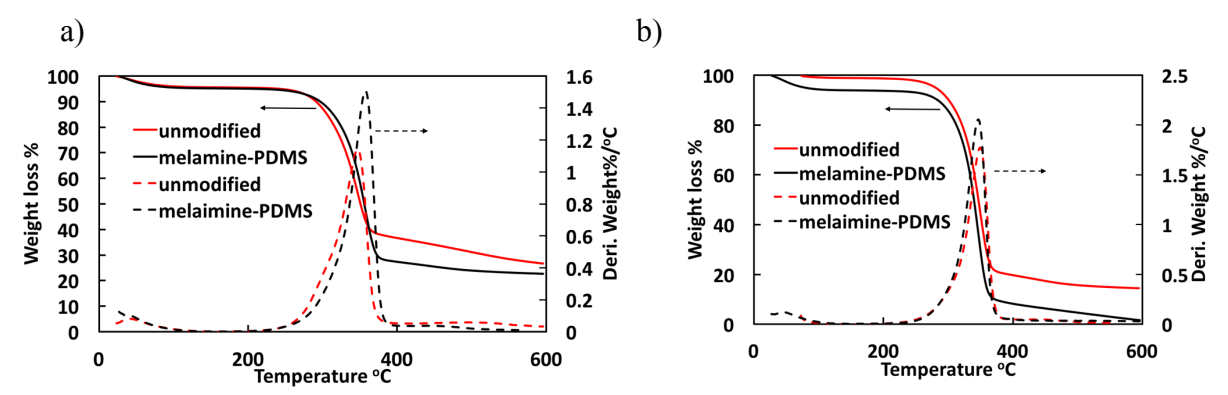


Figure 3.3 TGA traces of unmodified paper and melamine-PDMS primed paper under nitrogen for a) printing paper, b) cup paper.

The theoretical and experimental loading of the coating is shown in Table 1. The theoretical load value is not as accurate as the experimental load value because paper substrates were sequentially immersed into two solutions in which there was an uncontrollable loss of substances (moisture, fillers, and sizing agent) from paper into the coating solutions. To account for the uncontrolled loss, the weight loss caused by the dipping into the acetone and water solutions was quantified using uncoated paper. In future, the authors intend to develop spray method as that will overcome the above problem. The experimental loads were determined by comparing the weight gain by the coated paper and including the weight losses during the immersion into solutions. Based on these experimental results, the net coating applied onto the cup paper and printing paper, was 1.61 and 0.93 wt%, respectively. Melamine load are 0.39 and 0.16 wt% for

cup paper and printing paper, respectively. And we believe that the melamine load should be lower than the obtained result because of weight loss during dipping into the PDMS-NCO solution. Unfortunately, we tried to study the weight increase before and after applying melamine primer, but there is no statistically significant change.

Table 3. 1 Theoretical and experimental coating load and melamine load of cup paper and printing paper.

Sample	Theoretical coating load (%)	Experimental coating load (%)	Melamine load (%)
cup paper	12.20 ± 0.47^a	1.61 ± 1.10^a	0.39 ± 0.045^a
printing paper	3.64 ± 1.49^a	0.93 ± 0.74^a	0.16 ± 0.062^a

^a Values are shown as mean \pm standard deviation.

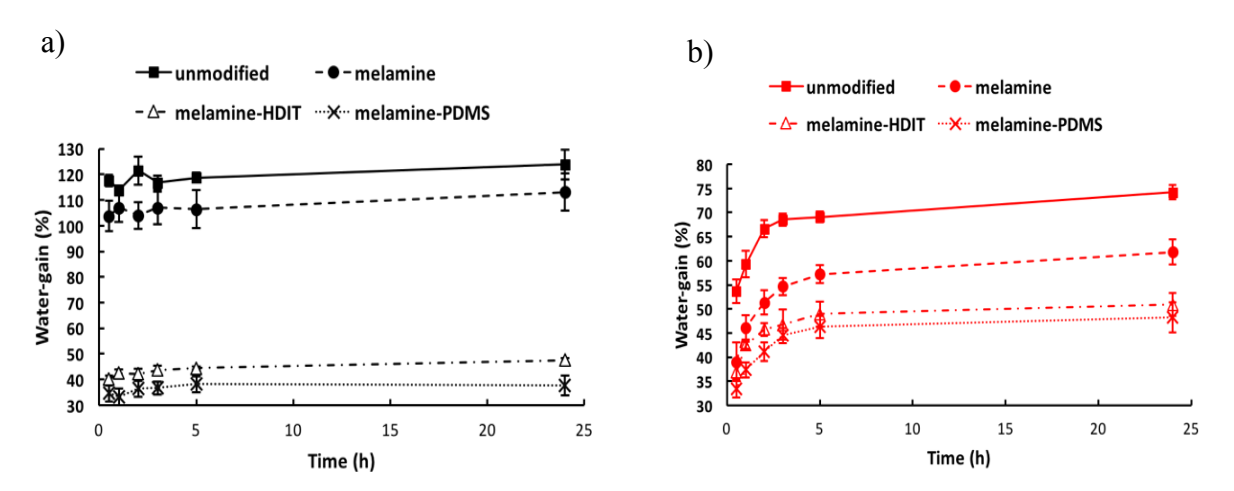


Figure 3.4 Water uptake profile of a) printing paper and b) cup paper.

Figure 3.4 a and b show the water-absorbance profile for printing paper and cup paper, respectively. It is apparent that printing paper absorbed more water compared to the cup paper, possibly because printing paper had a more porous structure. As anticipated, the unmodified printing paper water-gain was 123.96% for the first 0.5 h and subsequently plateaued for 24 h (the duration of water-gain test). Meanwhile, the unmodified cup paper slowly absorbed water and

reached 74.22% after 24 h. For the printing paper, the melamine primed paper (without PDMS) also showed a high water-gain of ~110 wt% after 24 h, which was due to the hydrophilic nature of melamine.

The water-gain exhibited by melamine-HDIT primed paper was reduced down to 47.51% and 48.23% for printing paper and cup paper, respectively. This was due to the relatively hydrophobic nature of the HDIT. As expected, the best water resistance among the tested samples were observed among the samples of melamine-PDMS primed paper. For example, the watergain was reduced down to 37.77% for the printing paper and 48.23% for cup paper. Also, the water uptake profile indicates slow water absorption by the melamine-PDMS primed paper, thus suggesting that this sample exhibited improved and robust water resistance.

The water contact angles (WCAs) were also determined for paper samples at various stages of fabrication (see Figure 3.5). The results indicate that unmodified printing paper was hydrophilic and showed poor resistance to water because the water droplet slowly permeated into the paper. Meanwhile, even though unmodified cup paper had a certain degree of water resistance (with a WCA of ~100°), some water marks remained on the sample after 3 min of contact with water, indicating that water had diffused into the paper substrate. We observed that the printing paper was even more hydrophobic as treatment of this printing paper with melamine reduced the WCA even further from 89° for unmodified printing paper to below 65° for melamine-primed paper. To our surprise, the WCA for the cup paper was improved after melamine treatment. We suspect that printing paper is highly porous, which upon coating with melamine allowed water to easily permeate into the bulk of the paper and thus causing a decrease in the WCAs. While the cup paper is thicker with low porosity that suppressed water permeation into the bulk of the paper. Considering water-gain of the printing and cup paper were reduced by the melamine coating, the

decrease for the printing paper is likely originated from the highly porous structure of printing paper. Both melamine-HDIT and melamine-PDMS primed paper showed high WCAs. For example, in the cases involving melamine-PDMS primed paper, the WCAs were >125° for both types of paper, thus indicating that they exhibited excellent water resistance. These findings were also consistent with the results obtained from the water-gain tests. The enhanced performance that was exhibited by the PDMS-coated paper is due to the strong water repellency of PDMS. It is noteworthy that both melamine-HDIT and melamine-PDMS primed papers showed no noticeable change in the WCA over time, indicating that these coated paper samples exhibited long-term water-resistance.

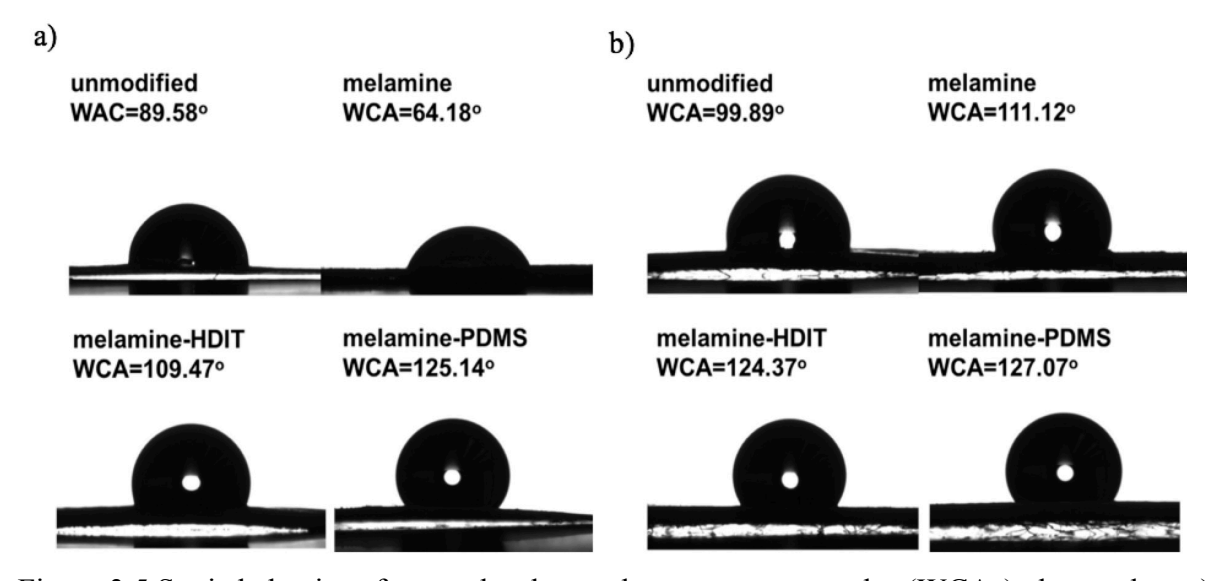


Figure 3.5 Static behavior of water droplets and water contact angles (WCAs) observed on a) printing paper and b) cup paper.

In order to investigate the effect of PDMS-NCO concentrations on the WCAs of the resultant coatings, both printing and cup papers were coated in PDMS-NCO solutions at different concentrations. Figure 3.6 demonstrates the effect of increasing the concentrations of the coating solutions and their influence on the WCAs. Initially the WCAs were improved with an increase in the PDMS concentration. For example, the highest hydrophobicity for the cup paper was

achieved at a 0.5 wt% PDMS-NCO concentration, while for the printing paper the highest WCA was achieved at 0.1 wt% of PDMS-NCO. However, with further increases in the concentration of PDMS, the WCAs gradually began to decrease. This unexpected decrease in the WCAs with an increasing PDMS concentration can be attributed to the fact that WCAs are influenced by surface roughness as well as surface energy. Initially, increasing the PDMS concentration yielded higher WCAs because it provided a lower surface energy while the roughness of the paper surface was retained. However, further increases in the PDMS concentration beyond a certain value also likely reduced the surface roughness due to the greater number of liquid-like PDMS chains on the surface. Therefore, it is apparent that an optimum PDMS concentration exists at (below 1 wt%) at which the surface energy can be reduced while the roughness of the surface can be retained to provide the maximum repellency. Interestingly, the observation of the highest WCAs at a low PDMS concentration strengthens our claim regarding the low-cost of this coating strategy.

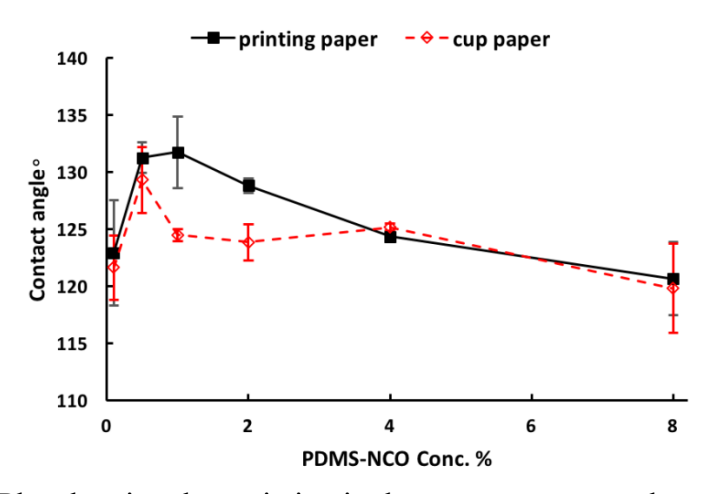


Figure 3.6 Plot showing the variation in the water contact angles with the concentration of the PDMS-NCO coating solution.

SEM images of cup paper at different stages of fabrication are shown in Figure 3.7. Inset images are taken to get a close-up view of the samples. The unmodified cup paper is comprised of a network of fibers (Figure 3.7a). After the melamine coating, there is no noticeable change in the

paper texture (Figure 3.7b); however, fiber surface became smoother upon melamine-HDIT coating (Figure 3.7c). It is possibly due to the flexible aliphatic HDID chains on the surface. Melamine-PDMS (Figure 3.7d) has fibers with much smoother texture caused by the liquid-like PDMS chains on the surface.

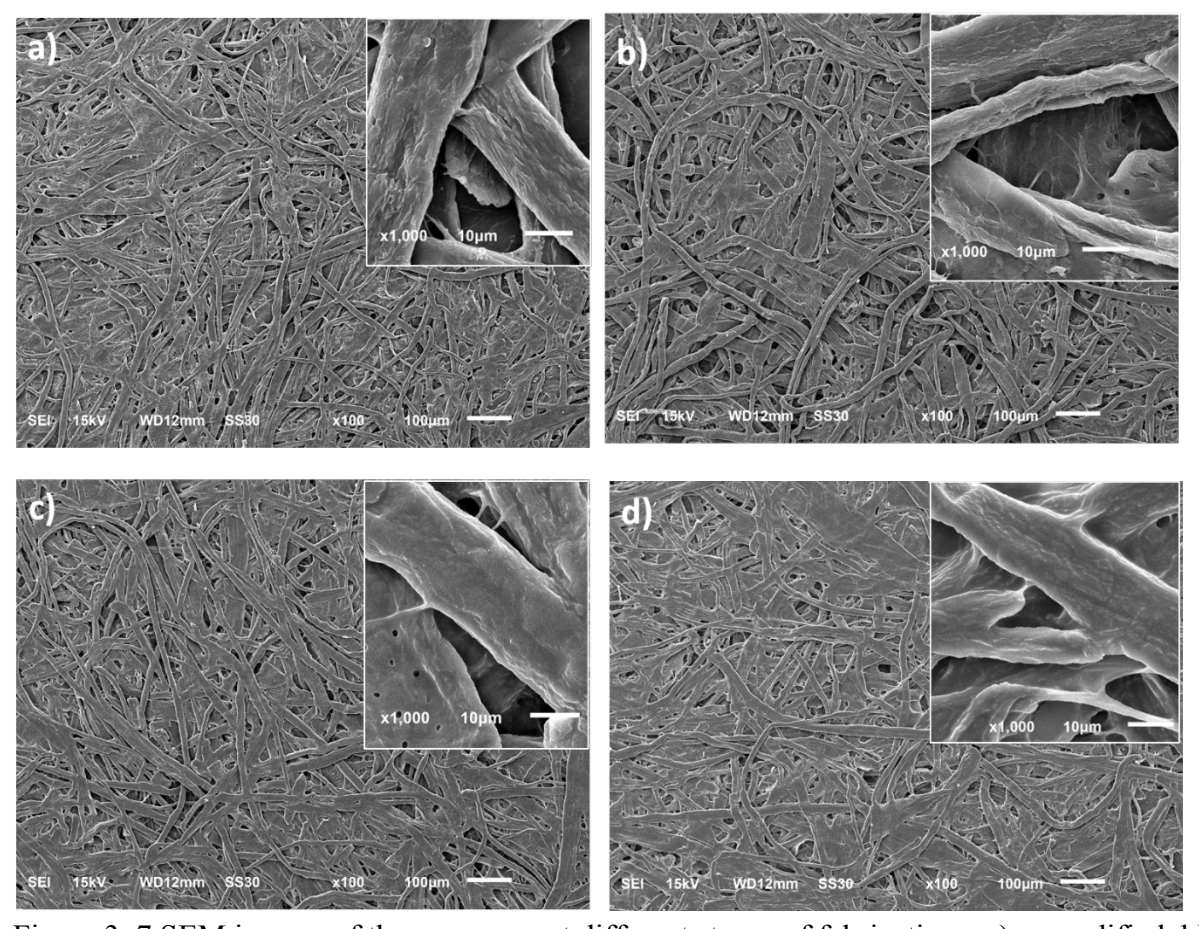


Figure 3. 7 SEM images of the cup paper at different stages of fabrications. a) unmodified, b) melamine coated, c) melamine-HDIT, and d) melamine-PDMS coated paper. The inset images are taken at 1000X magnification.

SEM images of printing paper at different stages of fabrications are shown in Figure 8. The unmodified cup paper is comprised of cellulosic fibers of various diameter. Except for melamine-PDMS (Figure 3.8d) coated paper, where the surface texture is smooth due to PDMS chains, the uncoated (Figure 3.8a), melamine coated (Figure 3.8b), melamine-HDIT coated (Figure 3.8c) print papers had rough textures.

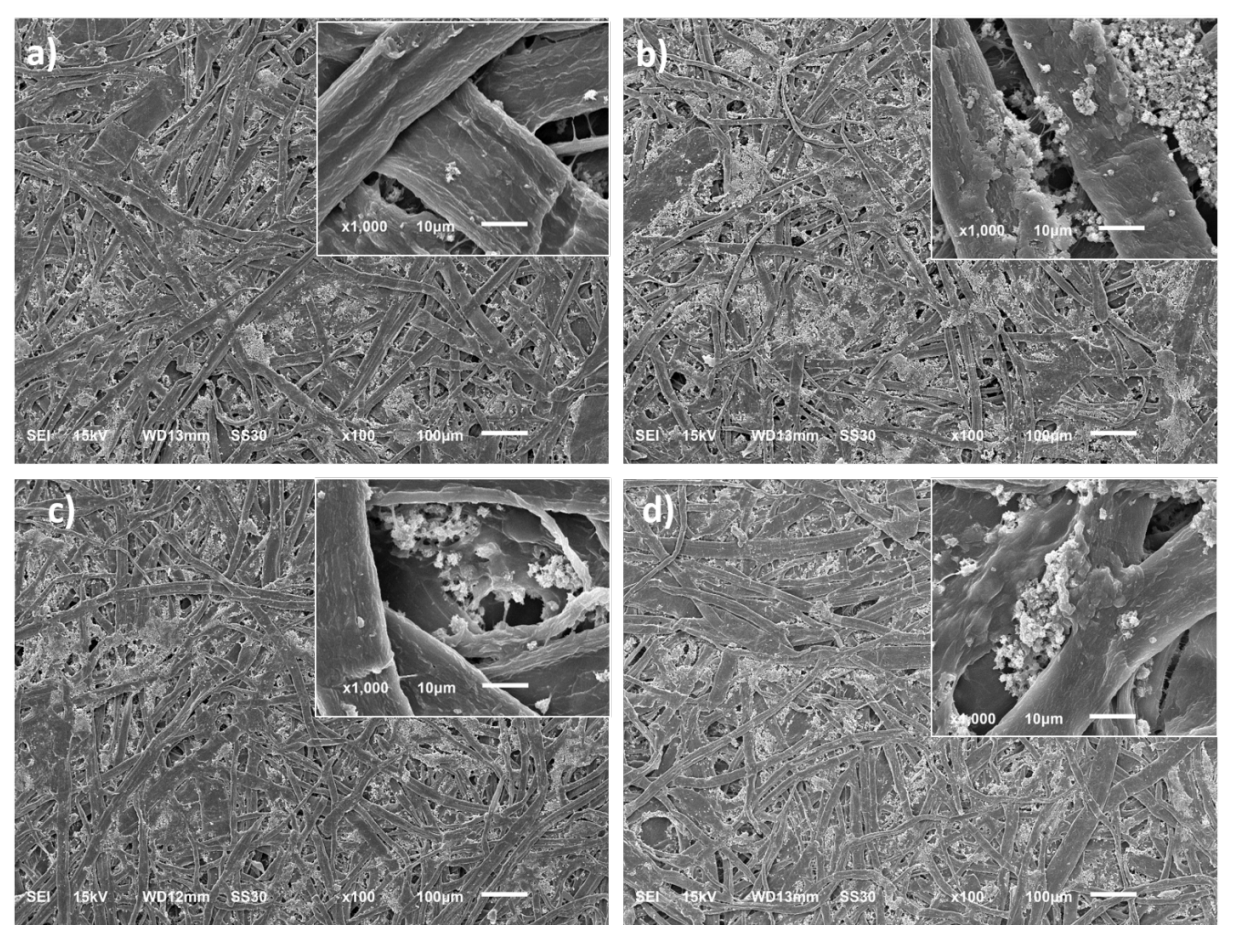


Figure 3. 8 SEM images of the printing paper at different stages of fabrications. a) unmodified, b) melamine coated, c) melamine-HDIT, and d) melamine-PDMS coated papers. The inset images are taken at 1000X magnification.

One key aspect of this coating is the proposed biodegradability of coated paper. Based on the nature of the materials (PDMS, Melamine) used for the coating, we expect that the coated papers are biodegradable. Also, linkage formed by the reaction of PDMS-NCO and melamine is urea bond, and urea bonds biodegradable. Coated paper fabricated in this study has some degree of crosslinking due to the multifunctional nature of melamine and HDIT trifunctionalties, however, even cross-linked polyurea is known to biodegrade though the at a slower rate. In the future, the biodegradability aspect of the coated papers will be explored.

3.5 Conclusions

In this study, we successfully applied a facile and economical approach for the preparation of biodegradable water-resistant paper coatings. A simple two-step dip-coating approach was used to fabricate the coated paper. The obtained surface exhibited hydrophobic properties with WCAs exceeding 125° at a 1 wt% loading of the coating. The water absorbed by the coated papers were significantly reduced in comparison with their uncoated counterparts, and also the water-gain time was enhanced, thus confirming the high water resistance of the coated paper. This novel approach can be extended to other types of papers and cellulose-based materials. Considering the biocompatibility and full biodegradability of these coatings as well as the low cost of the raw materials, this strategy provides a viable green route for the fabrication of disposable cups and corrugated packages.

REFERENCES

REFERENCES

- 1. Rabnawaz, M.; Wyman, I.; Auras, R.; Cheng, S. A roadmap towards green packaging: the current status and future outlook for polyesters in the packaging industry. *Green Chemistry* **2017**, *19*, 4737-4753.
- 2. EPA, U., Advancing sustainable materials management: 2014 fact sheet. **2015**.
- 3. Martin Jr, L. L. Paper laminate and method for producing the laminate and paperboard containers. Google Patents: 1989.
- 4. Cleveland, C. S.; Reighard, T. S.; Marchman, J. I. Biodegradable paper-based laminate with oxygen and moisture barrier properties and method for making biodegradable paper-based laminate. Google Patents: 2014.
- 5. Yamamatsu, T.; Uemura, M. Paper cup comprising a sheet of polylactic acid laminated paper. Google Patents: 2008.
- 6. Wong, C. K.; Wadsworth, L. C. Degradable Recycling Material. Google Patents: 2015.
- 7. Oswald, R. G.; Harvey, W. T.; Johnson, H. L. Wax-coated paper. Google Patents: 1966.
- 8. Knights, E. F. Wax coated paper of improved water resistance. Google Patents: 1975.
- 9. Samyn, P. Wetting and hydrophobic modification of cellulose surfaces for paper applications. *J. Mater. Sci.* **2013**, *48*, 6455-6498.
- 10. Liu, H.; Gao, S.-W.; Cai, J.-S.; He, C.-L.; Mao, J.-J.; Zhu, T.-X.; Chen, Z.; Huang, J.-Y.; Meng, K.; Zhang, K.-Q. Recent progress in fabrication and applications of superhydrophobic coating on cellulose-based substrates. *Materials* **2016**, *9*, 124.
- 11. Zhao, C.; Li, J.; He, B.; Zhao, L. Fabrication of hydrophobic biocomposite by combining cellulosic fibers with polyhydroxyalkanoate. *Cellulose* **2017**, *24*, 2265-2274.
- 12. Wurzburg, O. B. Paper sizing process using a reaction product of maleic anhydride with a vinylidene olefin. Google Patents: 1976.
- 13. Mazzarella, E. D.; Wood Jr, L. J.; Maliczyszyn, W. Method of sizing paper. Google Patents: 1977.
- 14. Guo, Y.-h.; Guo, J.-j.; Miao, H.; Teng, L.-j.; Huang, Z. Properties and paper sizing application of waterborne polyurethane emulsions synthesized with isophorone diisocyanate. *Prog. Org. Coat.* **2014**, *77*, 988-996.
- 15. Hubbe, M. A. Paper's resistance to wetting—A review of internal sizing chemicals and their effects. *BioResources* **2007**, *2*, 106-145.

- 16. Dang, C.; Xu, M.; Yin, Y.; Pu, J. Preparation and Characterization of Hydrophobic Non-Crystal Microporous Starch (NCMS) and its Application in Food Wrapper Paper as a Sizing Agent. *BioResources* **2017**, *12*, 5775-5789.
- 17. Liu, C.-F.; Zhang, A.-P.; Li, W.-Y.; Yue, F.-X.; Sun, R.-C. Homogeneous modification of cellulose in ionic liquid with succinic anhydride using N-bromosuccinimide as a catalyst. *J. Agric. Food. Chem.* **2009**, *57*, 1814-1820.
- 18. Yang, J.; Li, H.; Lan, T.; Peng, L.; Cui, R.; Yang, H. Preparation, characterization, and properties of fluorine-free superhydrophobic paper based on layer-by-layer assembly. *Carbohydr. Polym.* **2017**, *178*, 228-237.
- 19. Kitaoka, T.; Isogai, A.; Onabe, F. Chemical modification of pulp fibers by TEMPO-mediated oxidation. *Nord. Pulp Pap. Res. J.* **1999**, *14*, 279-284.
- 20. Hon, D.-S., Chemical modification of lignocellulosic materials. Routledge: 2017.
- 21. Roy, D.; Semsarilar, M.; Guthrie, J. T.; Perrier, S. Cellulose modification by polymer grafting: a review. *Chem. Soc. Rev.* **2009**, *38*, 2046-2064.
- 22. Dimitrakellis, P.; Travlos, A.; Psycharis, V. P.; Gogolides, E. Superhydrophobic paper by facile and fast atmospheric pressure plasma etching. *Plasma Processes Polym.* **2017**, *14*.
- 23. Xing, C.; He, T.; Peng, Y.; Li, R. Synthesis and characterization of poly (methyl methacrylate)/polysiloxane composites and their coating properties. *J Appl. Polym. Sci.* **2018**, *135*, 46358.
- 24. Osawa, Y.; Yamamoto, K.; Watanabe, Y. Coating emulsion composition, and water/oil-repellent paper and making method. Google Patents: 2017.
- 25. Rosenmai, A. K.; Taxvig, C.; Svingen, T.; Trier, X.; Vugt Lussenburg, B.; Pedersen, M.; Lesné, L.; Jégou, B.; Vinggaard, A. Fluorinated alkyl substances and technical mixtures used in food paper packaging exhibit endocrine related activity in vitro. *Andrology* **2016**, *4*, 662-672.
- 26. Zhang, X.; Wang, H.; Liu, Z.; Zhu, Y.; Wu, S.; Wang, C.; Zhu, Y. Fabrication of durable fluorine-free superhydrophobic polyethersulfone (PES) composite coating enhanced by assembled MMT-SiO 2 nanoparticles. *Appl. Surf. Sci.* **2017**, *396*, 1580-1588.
- 27. Li, Y., et al. "One-step spraying to fabricate nonfluorinated superhydrophobic coatings with high transparency." J. Mater. Sci. **2016**, *51*, 2411-2419.
- 28. Rabnawaz, M.; Liu, G.; Hu, H. Fluorine Free Anti Smudge Polyurethane Coatings. *Angewandte Chemie* **2015**, *127*, 12913-12918.
- 29. Saadat-Bakhsh, M., Ahadian, H. R., & Nouri, N. M Facile, robust and large-scale fabrication method of mechanically durable superhydrophobic PDMS/aerogel coating on fibrous substrates. Cellulose, **2017**, *24*, 3453–3467. https://doi.org/10.1007/s10570-017-1359-x.

- 30. Kotkamills Kotkamills' new plastic-free and easily recyclable consumer board AEGLE barrier light is now ready for world domination. <a href="https://www.google.com/url?sa=t&rct=j&q=&esrc=s&source=web&cd=1&cad=rja&uact=8&ved=2ahUKEwjSzfPT5bTcAhWJYJoKHWbXC44QFjAAegQIABAB&url=https%3A%2F%2Fwww.epressi.com%2Ftiedotteet%2Fpaperiteollisuus%2Fkotkamills-new-plastic-free-and-easily-recyclable-consumer-board-aegle-e2-84-a2-barrier-light-is-now-ready-for-world-domination.html&usg=AOvVaw0FUXLp9vfNaNJ7w_I8nOiA (accessed August 3).
- 31. Neu, T.; Van der Mei, H.; Busscher, H.; Dijk, F.; Verkerke, G. Biodeterioration of medical-grade silicone rubber used for voice prostheses: a SEM study. *Biomaterials* **1993**, *14*, 459-464.
- 32. Ceseracciu, L.; Heredia-Guerrero, J. A.; Dante, S.; Athanassiou, A.; Bayer, I. S. Robust and biodegradable elastomers based on corn starch and polydimethylsiloxane (PDMS). *ACS Appl. Mater. Interfaces* **2015**, *7*, 3742-3753.
- 33. Anderson, C.; Hochgeschwender, K.; Weidemann, H.; Wilmes, R. Studies of the oxidative photoinduced degradation of silicones in the aquatic environment. *Chemosphere* **1987**, *16*, 2567-2577.
- 34. Fendinger, N.; McAvoy, D.; Eckhoff, W.; Price, B., Environmental occurrence of polydimethylsiloxane. *Environmental science & technology* **1997,** *31*, 1555-1563.
- 35. FAO, Eighteenth Report of the Joint FAO/WHO Expert; World, C. o. F. A. J. G.; Health Organization)
- 36. FAO, JECFA Evaluations, January, P-9.
- 37. Mojsiewicz-Pieńkowska, K.; Jamrógiewicz, Z.; Łukasiak, J. Determination of polydimethylsiloxanes by 1H-NMR in wine and edible oils. *Food Addit. Contam.* **2003**, *20*, 438-444.
- 38. Healthknot FDA "dosing" melamine for infants and adults. http://www.healthknot.com/fda_melamine.html (accessed August 7th).
- 39. Tang, D.; Chen, Z.; Correa-Netto, F.; Macosko, C. W.; Hillmyer, M. A.; Zhang, G. Poly(urea ester): A family of biodegradable polymers with high melting temperatures. *J. Polym. Sci., Part A: Polym. Chem.* **2016,** *54*, 3795-3799.
- 40. Pareek, K.; Zhang, Q.; Rohan, R.; Cheng, H. Highly selective carbon dioxide adsorption on exposed magnesium metals in a cross-linked organo-magnesium complex. *J. Mater. Chem. A* **2014**, *2*, 13534–13540. https://doi.org/10.1039/C4TA01364F.
- 41. Guo, J.; Wang, J.; Zhang, S.; Ma, X.; Qiu, Z.; Peng, X.; et al. One-step modification of PU sponges for selective absorption of oil–water mixtures. New J. Chem. **2007**, *41*, 90–96. https://doi.org/10.1039/C6NJ03239G.

- 42. Teisala, H.; Tuominen, M.; Kuusipalo, J. Superhydrophobic Coatings on Cellulose-Based Materials: Fabrication, Properties, and Applications. Adv. Mater. Interfaces **2014**, *I*, 1–20. https://doi.org/10.1002/admi.201300026.
- 43. Cakić, S. M.; Ristić, I. S.; Jašo, V. M.; Radičević, R. Ž.; Ilić, O. Z.; Simendić, J. K. B., Investigation of the curing kinetics of alkyd–melamine–epoxy resin system. *Prog. Org. Coat.* **2012**, *73*, 415-424.
- 44. Yiamsawas, D.; Baier, G.; Thines, E.; Landfester, K.; Wurm, F. R., Biodegradable lignin nanocontainers. *RSC Adv.* **2014**, *4*, 11661-11663.

CHAPTER 4: OIL- AND WATER-RESISTANT COATINGS FOR POROUS CELLULOSIC SUBSTRATES

A version of this chapter is published as:

Li, Z.; Rabnawaz, M., Oil- and Water-Resistant Coatings for Porous Cellulosic Substrates. ACS Applied Polymer Materials, 2019, 1 (1), 103–111, DOI: 10.1021/acsapm.8b00106.

4.1 Abstract

Water- and oil-resistant materials are useful for many application but turning polar and porous cellulosic substrates such as paper, corrugated board, cardboard, and fabrics into a water- and oil-resistant is very challenging. Herein, we report an innovative method for fluorine-free water- and grease-resistant surface fabricated from a fully-porous cellulosic substrate. A chitosan coating was applied to fill the pores of the paper, followed by a polydimethylsiloxane (PDMS) coating to render paper water and oil-resistant. A Response Surface Methodology (RSM) was applied to optimize the concentrations of chitosan and PDMS to obtain the desired water- and oil/grease-resistant properties. Paper coated with a load of 8.6 wt% of chitosan and 2.2% of PDMS showed an excellent grease/oil kit rating value of 12/12 (maximum fat resistance) as well as excellent water resistance (water contact angles of 95.2°). The coating is robust as confirmed by solvent extraction tests of the coated paper. This coating approach was also successfully demonstrated for paperboard. Due to the simplicity of the coating application method and fluorine-free coating ingredients, these coatings will find many applications in real-world related to paper, corrugated board, cardboard, and fabrics.

Keywords: water resistant, oil resistant, paper, porous cellulosic substrates, fluorine-free

4.2 Introduction

Water and oil-resistant surfaces are of immense interest for many industrial applications ranging from anti-fouling medical devices and marine-equipment to self-cleaning glass and energy efficient distillations and fuel transport. Two common models based conceptually on lotus leaves, and pitcher plants are widely employed for the fabrication of synthetic water- and oil-resistant surfaces. The Lotus leaf model is typically used to prepared the surface with liquid contact angles >150°, which are achieved by creating textured surfaces that were modified with

fluorinated materials.⁴⁻⁵ For example, candle soot has been used a template for a transparent, robust superamphiphobic coating.⁶ Smooth surfaces bearing low-surface-tension liquid polymers on their surfaces have been fabricated as water- and oil-repellent surfaces.^{2,7,12,13} However, here a key requirement is water and oil-slides on their surface if the surface is perfectly smooth and non-porous.

Numerous substrates of commercial significance have porous textures such as paper, corrugated board, cardboard, fabrics, and foams. Due to their porous nature, liquids particularly oils readily diffuse into the bulk of these materials. To make porous substrate water- and oilresistant, a common approach is to fill the pores to avoid liquid permeation into the bulk and use low surface energy materials to repel water and oil-concurrently. Liu et al.8 reported water- and oil-resistant paper by first coating silicon particle with a fluorinated block copolymer, and the subsequent application of these particles on paper but this approach is expensive and less viable for real-world applications. Aizenberg et al. ² reported Slippery Liquid-Infused Porous Surface(s) (SLIPS) in 2011, which were inspired by the Nepenthes pitcher plants. The study involved the infusion of a fluorinated-oil into a porous matrix made of fluorinated materials. Test liquids can easily slide on these surfaces while the contact angle hysteresis values are typically very low. Meanwhile, the infused liquid preferentially remains in the porous matrix because of the greater affinity of the infused liquid and the matrix. However, because of non-covalent bonding, the infused liquid can leach out from the SLIPs. Previously, a grease-resistant porous substrate (paper) was prepared by the application of chitosan coatings, but these surface were non-water resistant. Recently, we also developed a water-resistant paper using polydimethyl siloxane(PDMS). 10 However, due to the porous nature, low surface tension oil permeated into the paper. Attanasio et al. demonstrated a waterproof cellulose fiber network using ethyl-cyanoacrylate monomer. ¹¹ Also,

biobased polyhydroxylated fatty acid has been applied onto cellulose by melt-processing, and subsequent addition of carnauba wax to improve the water and oxygen barrier properties.¹² However, in both cases, the coated substrate was not oil resistant. On the other hand, paraffin wax and poly(dimethylsiloxane)-*b*-poly(ethylene oxide) diblock copolymer coating on fibers were used to prepare oil repellent fibers for oil and water emulsions. However, in this case, the fibers were not water repellent.¹³ Recently, poly(methyl methacrylate) (or PMMA) coating was applied on paper to render them water and oil resistant using a significant amount of PMMA (~10wt%) in a thickness of 40 μm. PMMA is brittle, and applying this on flexible paper would adversely affect the crack resistance. Also, PMMA does not have a covalent bond with the paper, therefore, their delamination can be an issue.¹⁴

In this study, we report a unique approach to turn a porous cellulosic substrate into water and grease resistant. Paper is used porous model substrate. Chitosan was used to fill/mask the pores of the paper, and subsequent modification with PDMS to render the porous paper both grease- and water-resistant. The chitosan was applied using an aqueous chitosan solution to ensure that the surface of the paper was smooth, while the PDMS was applied as a second layer to render the paper water-repellent as well as to further enhance its grease-resistance. Chitosan is selected because it is a non-toxic, low-cost and fully-biodegradable polymer. While PDMS is an inert material, has low surface energy and is available at a low-cost. While this approach can offer a good alternative to the existing fluorinated paper used where water- and grease-repellency is required because fluorinated materials have growing environmental concerns and there is a push to phase-out fluorinated materials form the coatings especially paper coatings. Consequently, this fluorine-free coatings can find real-world applications in the paper-based products fabrications.

4.3 Experimental

4.3.1 Materials.

Acetone (Fischer Scientific, 99.7%), monoaminopropyl-terminated polydimethylsiloxane (PDMS-2K, $M_n = 2000$ g/mol, GELEST, Inc.) and chitosan (Sigma, $M_n = 50,000-190,000$ g/mol) were purchased and used without further purification. Hexamethylene diisocyanate trimer (HDIT) was provided by a proprietary manufacturer (see Figure 4.4). Printing paper was purchased from a local supermarket.

4.3.2 Methods and Characterization

4.3.2.1 Fabrication of chitosan-PDMS coated paper

A chitosan solution was prepared by dissolving a desired amount of chitosan in 2% (v/v) acetic acid solution via stirring for 12 h at room temperature. Meanwhile, a PDMS-NCO solution was prepared in a similar manner as described in a previous study. Briefly, PDMS-NH₂ was dissolved in acetone and was added dropwise into an HDIT solution that was also prepared in acetone. For example, in order to prepare PDMS-NCO at 5 wt%, a PDMS-NH₂ solution (0.5g of PDMS-2K in 5.0 mL of acetone) was added dropwise to an HDIT solution (0.25 g of HDIT in 5.0 mL of acetone). Freshly prepared PDMS-NCO solutions were used in all of the experiments.

In this study, the paper was coated in two steps. First, a paper substrate was coated with a chitosan solution on both sides using a rod coating machine (Model K303, RK PrintCoat Instruments Ltd, UK), and dried under ambient conditions for 1 h. The chitosan-coated paper was subsequently cut into 0.5×1 or 1×1 inch² pieces, and completely soaked in a PDMS-NCO solution for 30 s prior to curing at 120 °C in an oven for 1 h. The resultant coated paper is thus referred to as chitosan-PDMS-coated paper. The concentrations of chitosan and PDMS-NCO solutions were varied according to the experimental design described in Section 2.2.3. For

reference, paper coated with only chitosan was cured at 120 °C for 1 h, and is denoted as chitosan-coated paper. In addition, the unmodified paper was employed as a blank control.

4.3.2.2 Water-resistance tests

Water-gain tests were used to evaluate the water-resistance of the paper samples. First, paper samples were preconditioned at 70 °C under vacuum for 1 h and edges of each specimen were dipped into wax to avoid unexpected water diffusion from the edges. The weight of each sample was recorded with an analytical microbalance as the initial weight. Samples were then soaked in distilled (DI) water for 24 h, and subsequently weighed using the analytical microbalance after excess water had been wiped away from the surface with tissues to yield the final weight. The water-gain (g/m²) value was then calculated using Equation 4.1.

$$watergain (g/m^2) = \frac{final \ weight (g) - initial \ weight (g)}{area \ (m^2)}$$
 (Equation 4.1)

4.3.2.3 Oil/grease-resistance tests

Oil/grease-resistance tests were performed in accordance with a standard method, namely T 559 pm-96. A series of numbered solutions (1-12) with various surface tensions and viscosities (aggressiveness) were prepared by mixing specific proportions of castor oil (surface tension: 39.0 mN·m⁻¹, viscosity: 889.3 mPa·s, at 20 °C)²⁰, *n*-heptane (surface tension: 19.65 mN·m⁻¹, viscosity: 0.387 mPa·s, at 25 °C)²¹, and toluene (surface tension: 27.93 mN·m⁻¹, viscosity: 0.56 mPa·s, at 25 °C)²¹. Higher numbered solutions are more aggressive with lower surface energies (i.e., solution #1 is the least aggressive oil while #12 is the most aggressive oil). A test specimen was placed on a black bench, and various test solutions were gently allowed to drop onto the surface of this specimen from a height of 0.5 inches and quickly removed with a clean tissue after 15 s. The tested area was examined immediately, and a specimen with darkened spots was considered to have failed the test. The number of the most aggressive solution that remained on the surface of a

specimen without causing any failure was reported as the "kit rating." Therefore, a higher kit rating indicates that the paper has a stronger grease-resistance.

4.3.2.4 Experimental design and statistical study

The response surface methodology (RSM) was employed to determine the optimum concentrations of chitosan and PDMS-NCO coating solutions to obtain coatings with the best water- and oil/grease-resistance. Central Composite Design (CCD) with three levels, two factors including the concentrations of the chitosan (X_1) and PDMS-NCO (X_2) solutions was performed using JMP Statistical Software (SAS Institute Inc., NC, USA).²² CCD was chosen because it's an ideal option for second-order RSM model for continuous variables combining axial points, center points as well as a two-level fractional factorial. Preliminary experiments were performed to determine a reasonable range of the two independent variables. The concentrations of the chitosan solutions were varied within the range of 1-4 wt% such that the best oil/grease-resistance was obtained without hindering their application onto paper substrates to yield coatings. Meanwhile, the concentrations of PDMS were varied between 0-10 wt%. Twelve experiments were completed: 3×3 full design was performed, plus 3 more replicates at central points were accomplished to estimate residual variance. Results from the oil/grease-resistance and water-resistance tests were selected as responses. A full second-order (quadratic) model (Equation 4.2) was predicted using the Fit Least Squares program by JMP to study relationships between factors and responses:

$$Y_i = b_0 + b_1 X_1 + b_2 X_2 + b_{11} X_1^2 + b_{22} X_2^2 + b_{12} X_1 X_2$$
 (Equation 4.2)²²

where Y_i are the responses, X_i are the factors, and b_0 is the intercept, while b_i , b_{ii} , and b_{ij} are linear, quadratic and interactive regression coefficients, respectively. Estimated responses were converted into a scale-free value (named desirability) using the desirability function approach for

multi-response optimization. Desirability lies within the range of 0-1 with 0 indicating unacceptable and 1 indicating ideal formulation.

4.3.2.5 Extraction of coated paper

Coated paper $(0.5 \times 1 \text{ in}^2)$ was soaked into 5.0 mL of hexane and was gently shaken for 3 min. The hexane solution was then concentrated via rotary evaporation and characterized by NMR spectroscopy. For comparison, controlled samples were also extracted with hexane, and their NMR spectra were recorded.

The hexane-extracted paper specimens were dried at 70 °C for 1 h and were tested for their water- and oil-resistance. The chitosan-coated paper and unmodified paper were tested in a similar manner as was employed to test a reference.

4.3.2.6 Effect of NaHCO₃ treatment

To neutralize the protonated chitosan coating, chitosan (1.0 wt%) coated paper was dipped into a 25 mL NaHCO₃ solution (0.25 M) twice for 5 s each time, and subsequently rinsed twice with DI water. This NaHCO₃ treated chitosan-coated paper was then soaked in a 5.0 wt% PDMS solution to obtain the top coating layer. These samples were subsequently subjected to water- and oil/grease-resistance tests. Also, these samples were extracted with hexane and the changes in the water- and oil/grease-resistance were measured.

4.3.2.7 Chitosan-PDMS coated paperboard

In order to demonstrate the feasibility of chitosan-PDMS coating on other porous cellulosic substrates, paperboard, an important material for packaging, was applied as for chitosan-PDMS coating, and the corresponding water and oil resistance properties were studied.

4.3.2.8 Characterization

FTIR analysis: IR spectra of unmodified paper, chitosan-coated paper, and chitosan-PDMS-coated paper were recorded using a Shimadzu IR Prestige 21 FTIR spectrometer (Shimadzu Co., Columbia, MD) with an attenuated-total-reflection (ATR) accessory (PIKE Technologies, Madison, WI). A total of 32 scans with a resolution of 4 cm⁻¹ over a spectral range of 4000-400 cm⁻¹ were performed for each sample.

Thermogravimetric analysis (TGA): TGA analysis was performed using a Q-50 thermogravimetric analyzer (TA Instruments, New Castle, DE) to investigate the thermal stability and composition of the coated paper. Weight loss (%) was recorded as a function of the temperature between 23-600 °C. All of the samples were heated at a constant heating ramp rate of 10 °C/min under a nitrogen flow (40 mL/min).

Also, gravimetric (basis weight) analysis was employed to determine the amount of chitosan and PDMS used to achieve the best water- and oil-resistance properties. For basis weight analysis, paper specimens with dimensions of 1×1 inches² were weighted before and after the coating with a microbalance. The weight gains were calculated following Eq. 3 and were expressed in grams per square meter (g/m²). Coating loadings were calculated separately based on the results obtained via TGA measurements and basis weight analysis.

basis weight =
$$\frac{weight(g)}{area(m^2)}$$
 (Eq. 3)

Scanning electron microscopy (SEM): The SEM analysis was performed using a JEOL 6610 SEM, (JEOL Ltd., Japan) system to investigate changes in the surface morphology of the paper at different stages of the coating process. Samples were mounted on aluminum discs with a carbon tab and coated with a 10-nm-thick gold layer using a sputtering approach. All samples were examined with an accelerating voltage of 15 kV.

Contact angles (CAs) and surface tension: The CA measurements were conducted using a 590-U1 Advanced Automated Goniometer (Ramé-hart Instrument Co., NJ, USA) with DROPimage Advanced software. Water and castor oil droplets with volumes of 5 µL were applied on the surface of a specimen. Images of the droplets were taken 30 s and 5 min after their application onto the surface. Three measurements were performed on different areas of each sample, and the results are reported as the average of these three values. To determine the surface energies of the coated papers, the contact angle for two different liquids with different surface tension (water and diiodomethane) were applied, and then surface tension was given by the DROPimage Advanced software. Contact angle hysteresis was studied using a tilted plane method with the help of the Goniometer. The sample was taped on a glass slide, one droplet (5 µL) of water was carefully applied on the surface. The glass slide was tilted and advancing and receding angles were measured using Goniometer for the sliding water droplet.

Water vapor transmittance (WVTR): The WVTR were determined in g/m²day at 23 °C and 50% RH using a Permatran-W (Model 3/34, Mocon Inc. MN, USA) system, and the result was compensated to the WVTR value under 100%RH. Samples with a size of 1×1 inch² were masked in an aluminum sheet with a 5-mm-diameter circle opening in the middle to fit the sample holder. Samples were preconditioned under the testing condition for 1 h prior to characterization. The carrier gas was nitrogen with a flow rate of 12 SCCM. To further compare the barrier properties between chitosan-coated paper and chitosan-PDMS-coated paper, coated-samples with thicker coating layer was prepared by applying three layers of chitosan coating on the same paper substrate which is noted as 3Lchitosan-coated paper. The 3Lchitosan-coated paper was then dip coated into 5.0% PDMS-NCO solution followed by drying under 120 °C for 1 h, which is noted as 3Lchitosan-PDMS-coated paper. The samples were tested under the same condition.

4.3.3 Statistical analysis

The oil/fat and water resistance properties of PDMS-chitosan coated paper prepared using different procedures were compared by one-way analysis of variance (ANOVA) Tukey's tests using SAS (Statistical Analysis System Institute Inc., Cary, NC).

4.4 Results and Discussion

Reported herein is fluorine-free water- and oil/grease-resistant coating for a porous paper substrate. The materials (PDMS, chitosan) used for these coatings are environmentally friendly. In addition, this coating process is simple and convenient (see Figure 4.1). The paper substrate was firstly coated with chitosan on both sides to fill the pores of the paper (see SEM images). Once the chitosan coating was air-dried, then hydrophobic PDMS was applied via dip-coating.

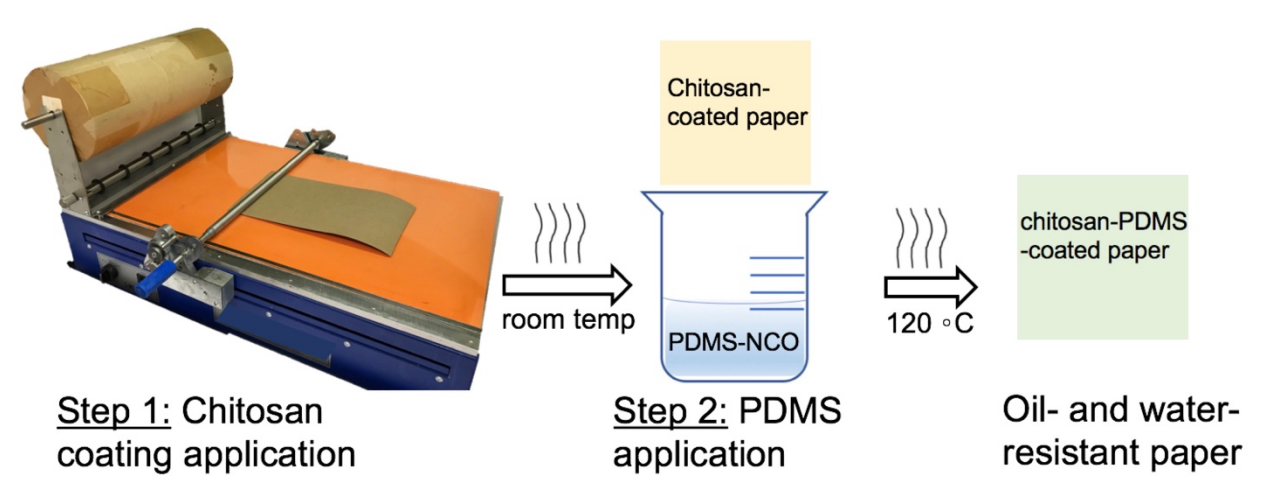


Figure 4. 1 Illustration of preparation procedure of water and oil/grease resistant chitosan-PDMS coated paper

To covalently graft PDMS onto chitosan-coated paper, we selected PDMS-NCO because the NCO groups (of PDMS) and the amines (of chitosan) should react efficiently and rapidly reacts with one another. Bearing this in mind, we prepared PDMS-NCO via the reaction shown in Figure 4.2. PDMS-NH₂ (see Figure 4.3 for the ¹H NMR spectrum) was used at a low molar ratio relative

to the HDIT (see Figure 4.4 for the ¹H NMR spectrum), to ensure that all PDMS chains carry one or more NCO as they are the part of HDIT. In this study, the term PDMS-NCO refers to the PDMS chains, which bear one or two NCO groups (see Figure 4.2).

OCN(
$$H_2C$$
)₆ NCO
$$(CH_2)_6NCO$$

$$HDIT (4.0 equ.)$$

$$R-(H_2C)_6$$

$$(CH_2)_6NCO$$

$$(CH_2)_6NCO$$

$$(CH_2)_6NCO$$

$$(CH_2)_6NCO$$

$$(CH_2)_6NCO$$

$$PDMS-NCO$$

$$R=R'=PDMS-NHC(O)-O$$

$$R=NCO, R'=PDMS-NHC(O)-O$$

$$R=R'=NCO, R'=PDMS-NHC(O)-O$$

$$R=R'=NCO, R'=PDMS-NHC(O)-O$$

Figure 4.2 Synthesis of PDMS-NCO.

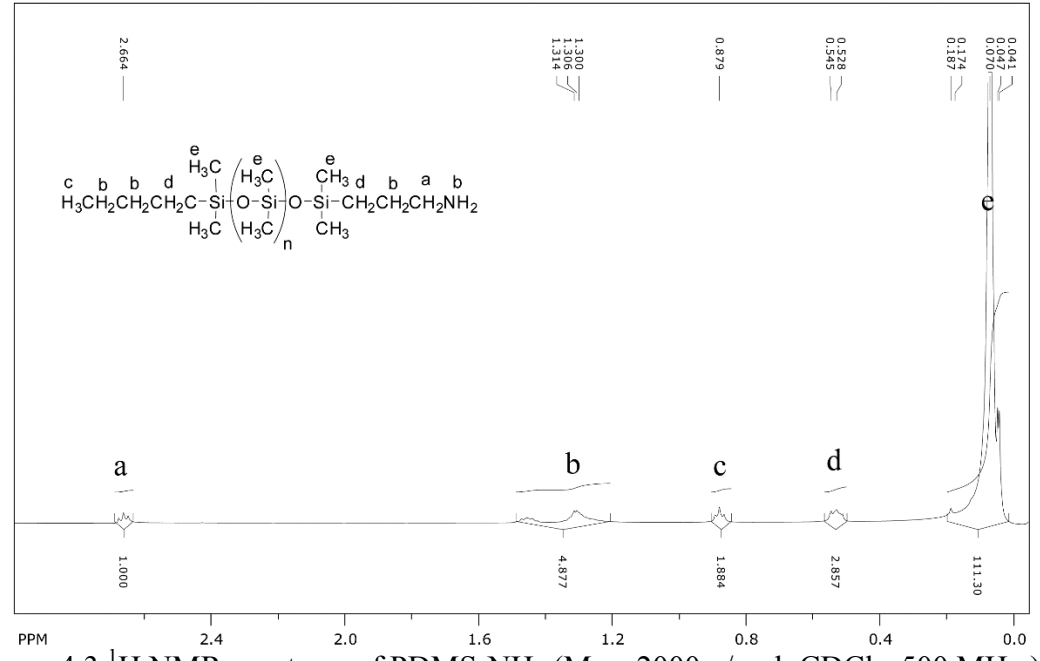
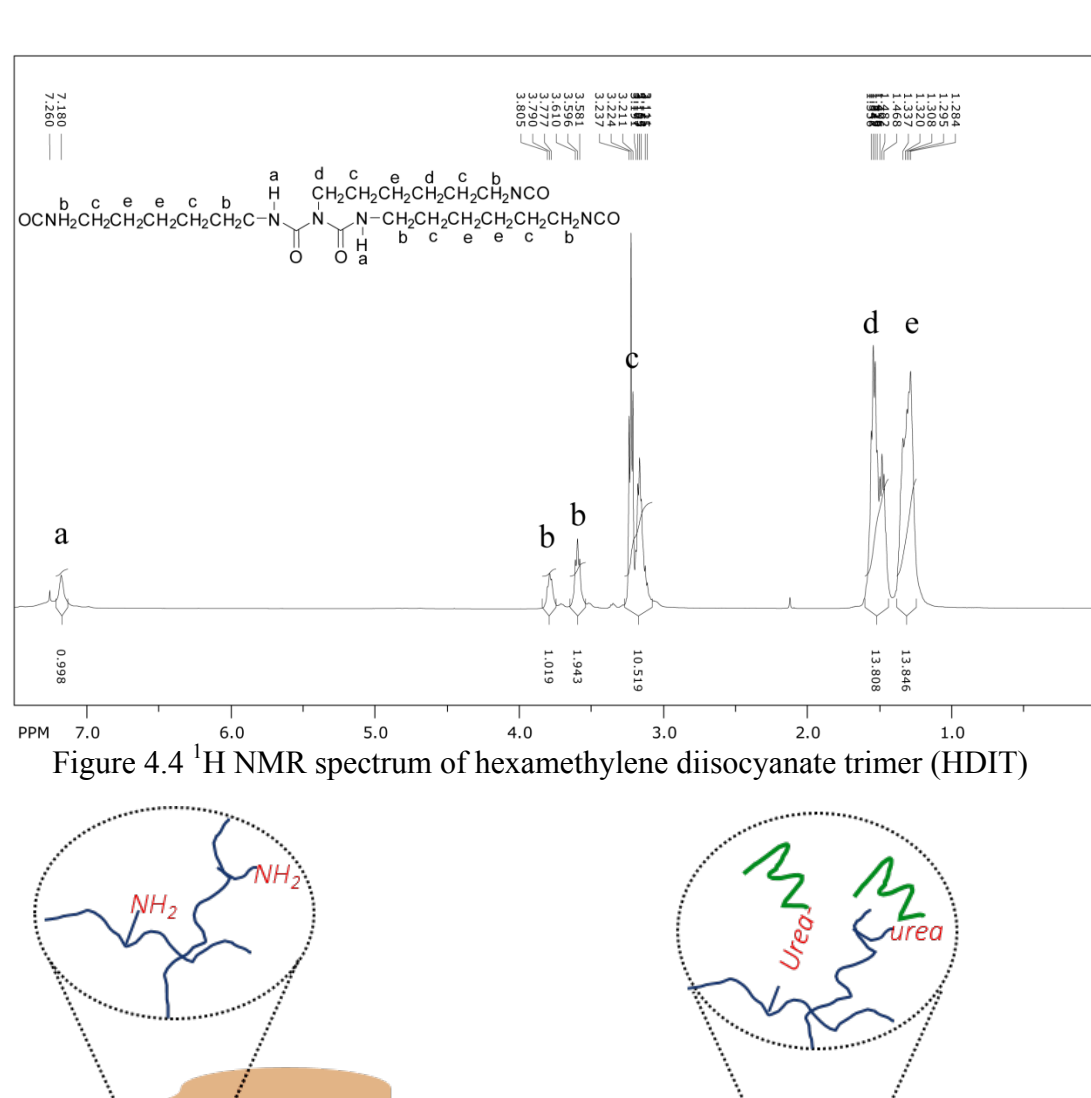


Figure 4.3 1 H NMR spectrum of PDMS-NH₂ (M_n = 2000 g/mol, CDCl₃, 500 MHz).



Chitosan-coated paper

Chitosan-PDMS coated paper

Chitosan-PDMS coated paper

Figure 4.5 Schematic illustration of the coated paper before and after PDMS-NCO application.

Once PDMS-NCO was prepared and then applied to the chitosan-coated paper, the reaction between the amine and NCO groups occurs to form highly stable urea bonds (Figure 4.5). Based on the weight of PDMS-NCO (2.2 wt%) and chitosan (8.6 wt%) added onto the paper during the

coating process and the considering the molecular weight of the chitosan monomer (159.1 g/mol), the number of NH_2 moieties was ~12 times that of the NCO moieties of the PDMS-NCO. The full-consumption of NCO was confirmed via IR analysis by the absence of the NCO peak at 2270 cm⁻¹. In one instance, the chitosan-coated paper was neutralized with a NaHCO₃ solution. This was followed by dip-coating in a PDMS-NCO solution.

To confirm the non-leaching of PDMS chitosan-PDMS-coated paper, ¹H NMR analysis was performed on the coated paper extracts to determine whether there were any traces of PDMS. ¹H NMR was chosen because this spectroscopic technique can easily detect organic compounds down to 0.1 µg/mL.²³ Therefore, we extracted coated papers at different stages of the fabrication process and recorded ¹H NMR spectra of their concentrates. Hexane was used as an extracting solvent due to the excellent solubility of PDMS in hexane. ¹H NMR analysis confirmed the absence of any PDMS peaks from the extract of PDMS-coated paper for both NaHCO₃-treated and untreated paper, which suggested that the PDMS chains were grafted onto the chitosan-coated paper (Figures 6-8).

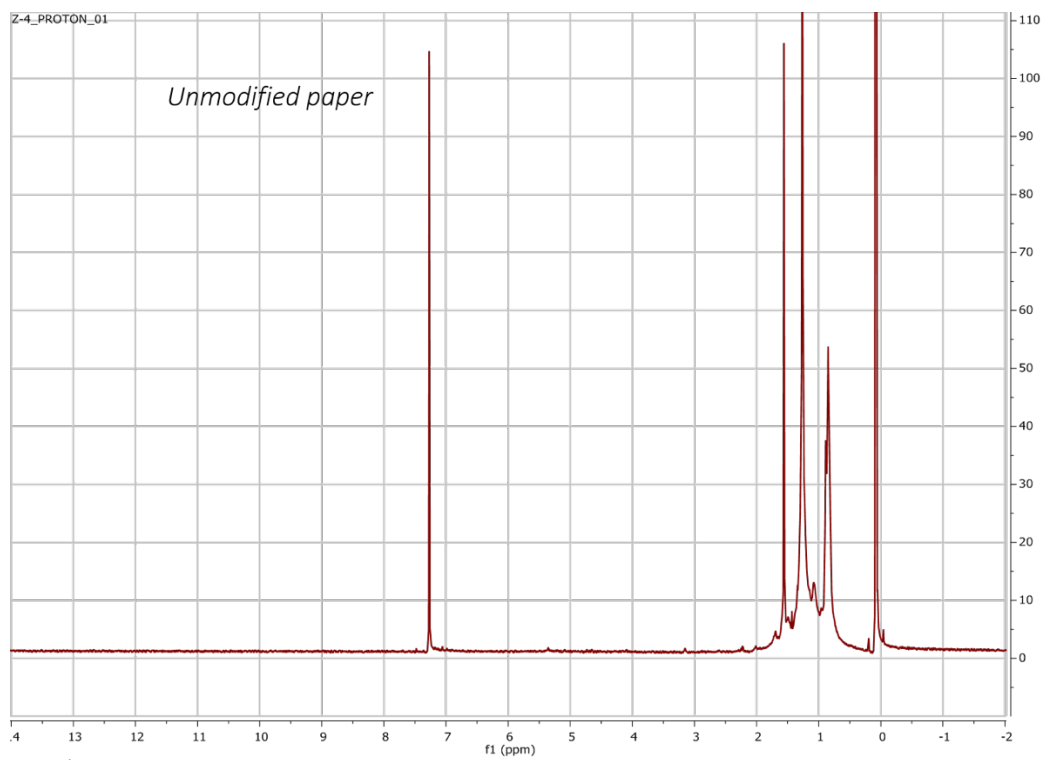


Figure 4.6 ¹H NMR spectrum the concentrated extract of the uncoated paper (CDCl₃, 500 MHz).

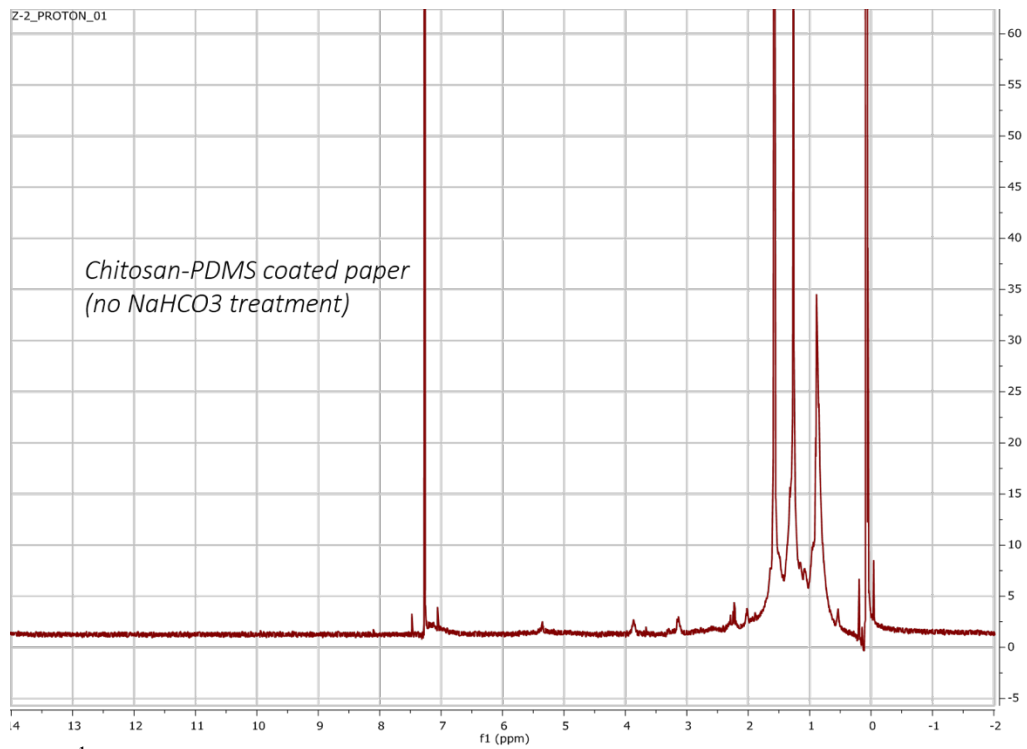


Figure 4.7 ¹H NMR spectrum of the concentrated extract of the Chitosan-PDMS coated paper (CDCl₃, 500 MHz).

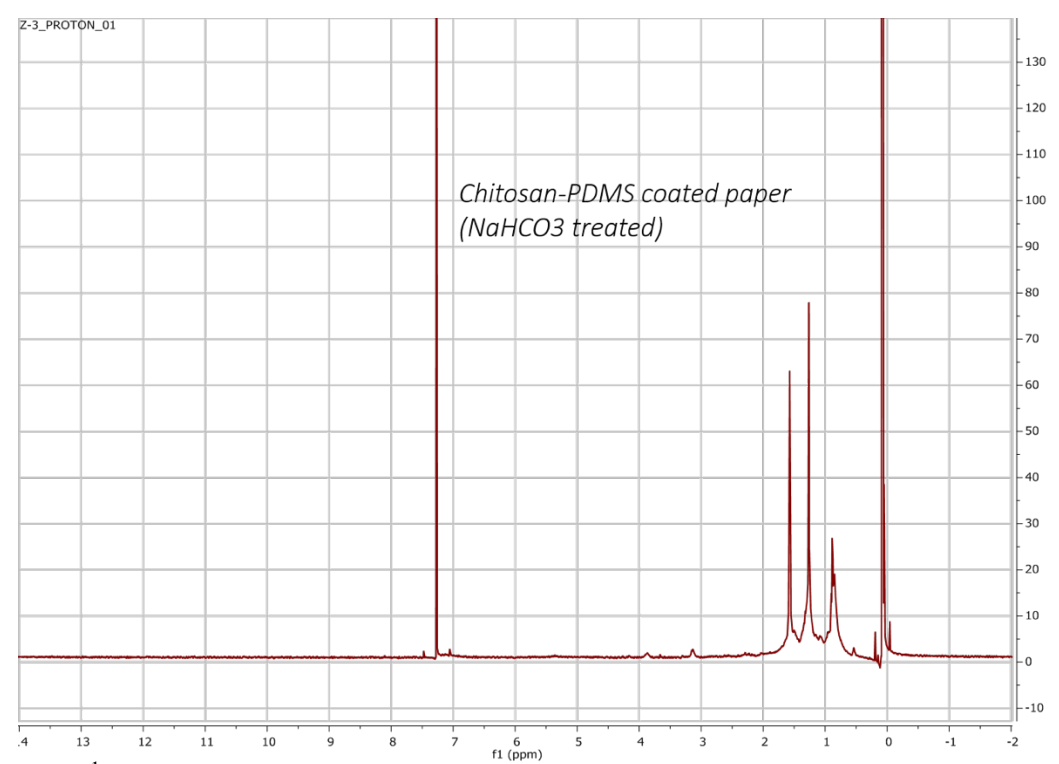


Figure 4.8 ¹H NMR spectrum of the concentrated extract of the Chitosan-PDMS coated paper treated with NaHCO₃ (CDCl₃, 500 MHz)

Table 4.1 shows the factors and experimental responses for coatings prepared under various conditions. Estimated regression coefficient values are shown in Table 4.2, and P-values from Student's T-test was employed to examine the significant effect of each coefficient. The response of water-gain, the regression coefficient (R^2) of the obtained second-order regression equation was 98%, indicating that the model could represent the experimental data. Also, all of the coefficients except the quadratic term of chitosan were significantly important indicating significant effects on the water-resistant properties. Whereas both chitosan and PDMS had positive effects on the kit rating value for oil-resistance, however, only the terms of intercept and interact between chitosan and PDMS were significant. Meanwhile, the obtained R^2 value was only 77%, indicating that the obtained regression formulation did not provide a reliable prediction of the experimental results. This could be explained when considering the experimental data, as all of the kit rating values were 12/12 except for one sample that had a kit rating value of 7/12. Also,

RSM analysis is based on polynomial regression, which could not accurately predict a data set distributed in this manner. However, all of the samples generally exhibited good oil resistance.

Response surfaces including three-dimensional response with the two-dimensional contour on the bottom were plotted in Figure 4.9 to study the effect of various factors and their interactions. The water-gain value increased with the concentration of chitosan but decreased with the concentration of PDMS, due to the hydrophilic nature of chitosan and ultrahydrophobic nature of PDMS. With regard to the oil/grease-resistance, the kit rating value increased with both the chitosan and the PDMS loadings. This occurred because chitosan is polar and has a low interaction with non-polar organic liquids. Similarly, PDMS has also shown good oil resistance against many organic liquids because of its very low surface tension.²⁴ According to the results, the optimal solution concentrations for the paper coatings were 1.0 wt% for the chitosan solution and 5.0 wt% for the PDMS solution with the desirability of water-gain of 0.99. For this formulation, the kit rating value was 12/12 according to the experimental data, and 11/12 according to the predicted data. Therefore, 1.0 wt% chitosan and 5.0 wt% PDMS was chosen as the optimum formulation for this study.

Table 4. 1 CCD experimental design and experimental responses

	Factors			Responses		
Run	Coded		uncoded (experime			
	X_1	X_2	conc. of chitosan (% w/w)	conc. of PDMS- NCO (% w/w)	water-gain (g/m²)	kit rating
1	-1	-1	1	0	96.98	7
2	0	-1	2.5	0	145.85	12
3	1	-1	4	0	177.04	12
4	-1	0	1	5	67.28	12
5	0	0	2.5	5	78.18	12
6	0	0	2.5	5	74.80	12
7	0	0	2.5	5	78.19	12
8	0	0	2.5	5	78.56	12
9	1	0	4	5	82.32	12
10	-1	1	1	10	72.17	12
11	0	1	2.5	10	73.30	12
12	1	1	4	10	77.06	12

Table 4. 2 Regression coefficients of the second-order polynomial model

Term	Estimate	Std. Error	t Ratio	<i>P</i> –value,		
				Prob. > F		
Water-gain						
Intercept	77.62	3.20	24.23	<.0001*		
chitosan (X_1) (1,4)	16.67	2.86	5.82	0.0011^*		
PDMS (X_2) $(0,10)$	-32.89	2.86	-11.48	<.0001*		
chitosan*PDMS	-18.79	3.51	-5.36	0.0017^{*}		
$(X_1 * X_2)$						
chitosan*chitosan	-3.20	4.30	-0.74	0.4849		
(X_1^2)						
PDMS*PDMS (X_2^2)	31.58	4.30	7.35	0.0003^{*}		
Kit rating						
Intercept	12.21	0.43	28.71	<.0001*		
chitosan (X_1) $(1,4)$	0.83	0.38	2.19	0.071		
PDMS (X_2) $(0,10)$	0.83	0.38	2.19	0.071		
chitosan*PDMS	-1.25	0.47	-2.68	0.0364^{*}		
$(X_1 * X_2)$						
chitosan*chitosan	-0.625	0.57	-1.10	0.3153		
(X_1^2)						
PDMS*PDMS (X_2^2)	-0.625	0.57	-1.10	0.3153		

^{*}Mean coefficient was significant at 95% confidential level (values of "Prob.>F" <0.05)

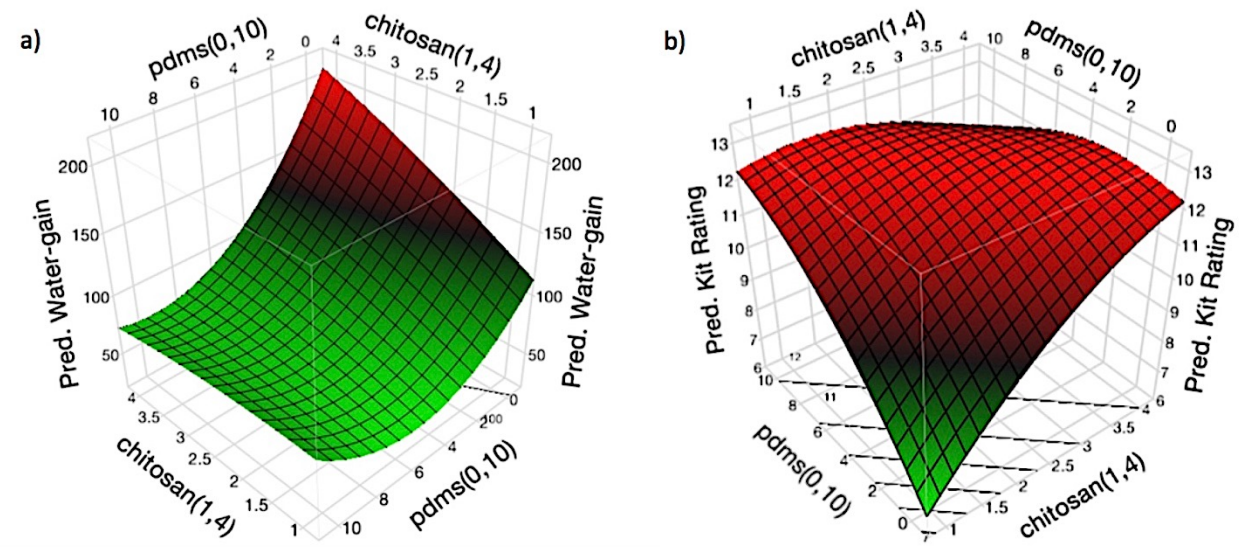


Figure 4. 9 Response surface plots of water-gain for water-resistance (a) and kit rating for oil-resistance (b). (Figure generated using JMP Statistical Software (SAS Institute Inc., NC, USA).

FTIR spectroscopy was used to validate the presence of chitosan and PDMS on the surfaces of the chitosan-coated and chitosan-PDMS-coated paper samples (see Figure 4.10). The IR spectra reveal the presence of many broad peaks between 3200-3600 cm⁻¹, which correspond to the stretching vibrations of the OH groups of the uncoated paper, the stretching frequencies of the OH and NH₂ moieties of the chitosan-coated paper, and the stretching frequencies the OH and NH₂ of the chitosan-PDMS-coated paper. The difference between uncoated and chitosan-coated paper is revealed by the presence of a peak at 1546 cm⁻¹ in the spectrum of chitosan-coated paper attributed to the N-H bending of the amino groups of chitosan, thus indicating successful loading of the chitosan onto the paper. Meanwhile, the chitosan-PDMS-coated paper exhibits a peak at 1257 cm⁻¹ representing a –CH₃ symmetric bending in Si-CH₃, and a peak at 800 cm⁻¹ corresponding to the bending in Si-O-Si of PDMS. Meanwhile, the spectrum of the chitosan-PDMS-coated paper also exhibits a peak at 1546 cm⁻¹ belonging to the C-N bending of the chitosan.

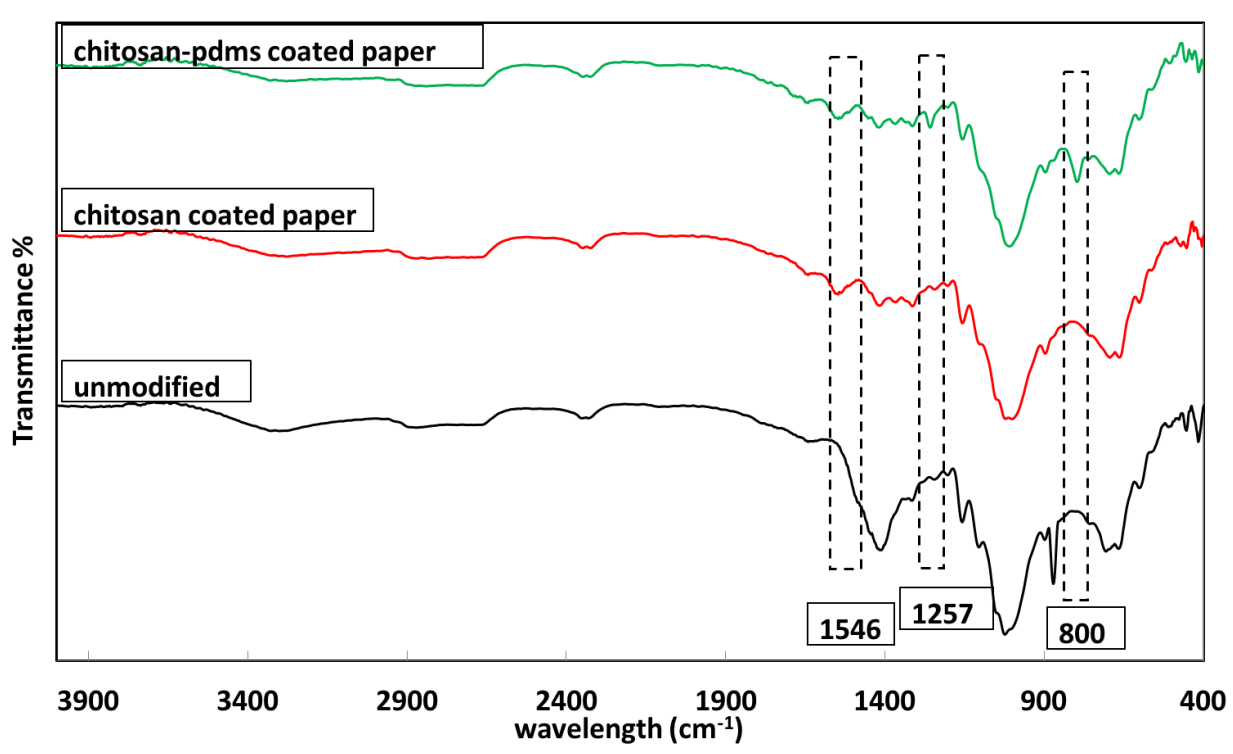


Figure 4.10 FTIR results of chitosan-coated and chitosan-PDMS-coated paper samples

TGA traces of the unmodified paper, chitosan-coated paper, and chitosan-PDMS-coated paper were recorded to investigate the thermal stability as well as to quantify the coating loading (as a wt%, see Figure 4.11). The weight loss below 120 °C can be attributed to the evaporation of moisture. Both chitosan and paper decompose at ~ 300 °C. One can see that the moisture contents of the chitosan-coated paper and chitosan-PDMS-coated paper were higher than that of the unmodified paper. A small peak at ~ 400 °C in the TGA trace of the chitosan-PDMS-coated paper corresponds to the weight loss of PDMS. This peak corresponds to a PDMS loading of ~ 2 wt%, which is calculated as the difference between the weight losses encountered in the range of 380-420 °C for the chitosan-coated paper and the chitosan-PDMS-coated paper. Since the weight loss of chitosan was overlapped with that of the paper substrate, chitosan loading was calculated based on the basis weights of the different materials.

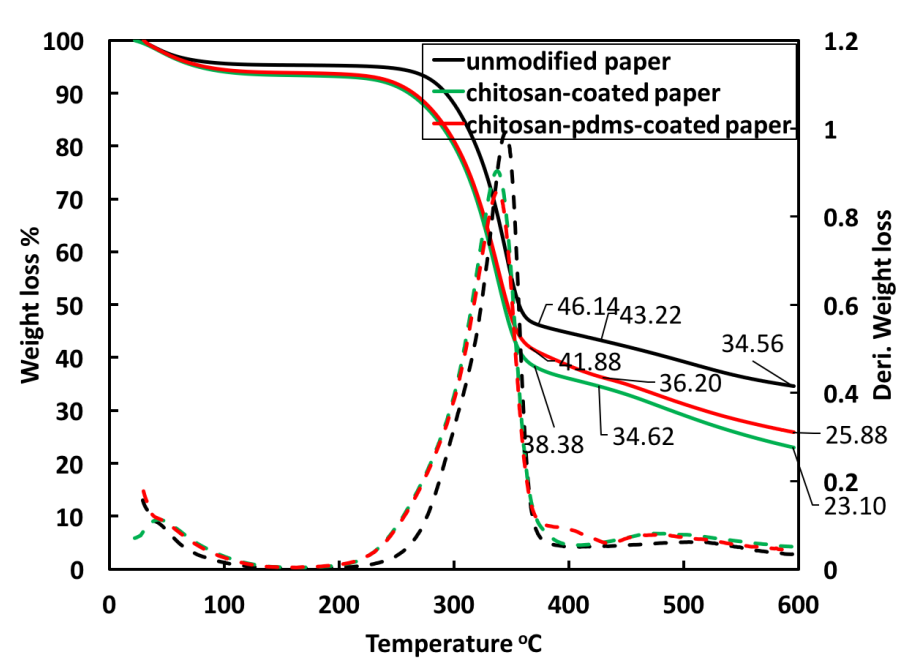


Figure 4.11 TGA traces of unmodified paper, chitosan-coated paper, and chitosan-PDMS-coated paper.

The basis weights of various materials are shown in Table 4.3. The chitosan-coated paper was dipped into acetone for 30 s as a control for this calculation. This dipping into acetone was performed because acetone was the solvent used for the coating solutions employed to prepare chitosan-PDMS-NCO. Therefore, this dipping step would help to eliminate inaccuracies arising from any potential leaching of material into acetone. The final PDMS loading was calculated as the difference between the loadings of the chitosan-PDMS coated paper and controlled chitosan-coated paper using Equation 4.5. Meanwhile, chitosan loading was calculated as the increased basis weight (%) after the chitosan coating was applied again using Equation 4.4. The weight gain analysis confirmed that the coating loadings were 8.6wt% and 2.2wt% for chitosan and PDMS, respectively.

Table 4.3 Basis weight of unmodified paper, chitosan-coated paper, and chitosan-PDMS-coated paper

	Unmodified paper	Chitosan-coated paper	Controlled chitosan- coated paper ¹	Chitosan-PDMS- coated paper
Grammage (g/m ²)	99.51 ± 1.25^2	108.84 ± 2.22^2	107.40 ± 0.69^2	109.84 ± 3.76^2

¹ chitosan-coated paper was dipped into acetone for 30 s as a control for the calculation of coating load; ² standard deviations.

$$chitosan\ loading = \frac{chitosan\ coated\ paper-unmodified\ paper}{chitosan\ coated\ paper} \qquad \text{(Equation\ 4.4)}$$

$$PDMS\ loading = \frac{chitosanPDMS\ coated\ paper-controlled\ chitosan\ coated\ paper}{chitosan-PDMS\ coated\ paper} \qquad \text{(Equation\ 4.5)}$$

The water contact angles (WCAs) and contact angles for castor oil of unmodified paper, chitosan-coated paper, and chitosan-PDMS-coated paper were also measured. One set of contact angles was obtained 30 s after the droplets had been applied onto paper, and the other set of contact angles was recorded 5 min after the application of the droplets (see Figure 4.12). Our results revealed that unmodified paper showed no resistance to water at all, and water permeated into the paper substrate in less than 5 min. In contrast, the chitosan coating imparted some water resistance to the paper, and the obtained WCA was 73.4° (after 30 s), which was decreased to 64° after 5 min. PDMS layer played an important role imparting hydrophobicity to the surface that the WCA of PDMS-coated paper was 118.9° after 30 seconds and 116.1° after 5 min. The WCA of chitosan-PDMS-coated paper was 113.4°, indicating that it possessed a hydrophobic surface, and the WCA decreased slightly to 107.2° after 5 min of contact. Meanwhile, the chitosan-coated paper showed a significant decrease in the contact angle, thus indicating that it had poor water-resistance. This decrease corresponds to the absorption of water by the chitosan-coated paper as shown in Figure 4.13. On the other hand, the unmodified paper showed no resistance to castor oil, whereas chitosan coating imparted some resistance with a contact angle of 40.2° (after 30 s) which slightly decreased to 37.0° after 5 min. Even though PDMS-coated paper and chitosan-PDMS coated paper showed similar contact angle against castor oil, the chitosan-PDMS coated paper showed great oil resistance as evident in Figure 4.12, where oil stayed on the surface without permeated into substrate whereas PDMS-coated paper failed because oil permeated into the paper substrate. This further proved that the application of PDMS improved both water and oil resistance of chitosan-coated paper. The surface energy of chitosan-PDMS coated paper was obtained as 22.40 mN·m⁻¹ with a WCA of 110.18° and contact angle for diiodomethane of 79.76°. For chitosan coated paper, the WCA was 73.6°, and contact angle for diiodomethane was 29.4°, and the obtained surface energy was 55.13 mN·m⁻¹. For the water contact angle hysteresis determination, results showed that even though the chitosan-PDMS coated paper was tilted to 90°, the water droplet still tended to stick on the surface indicating rather a high hysteresis.

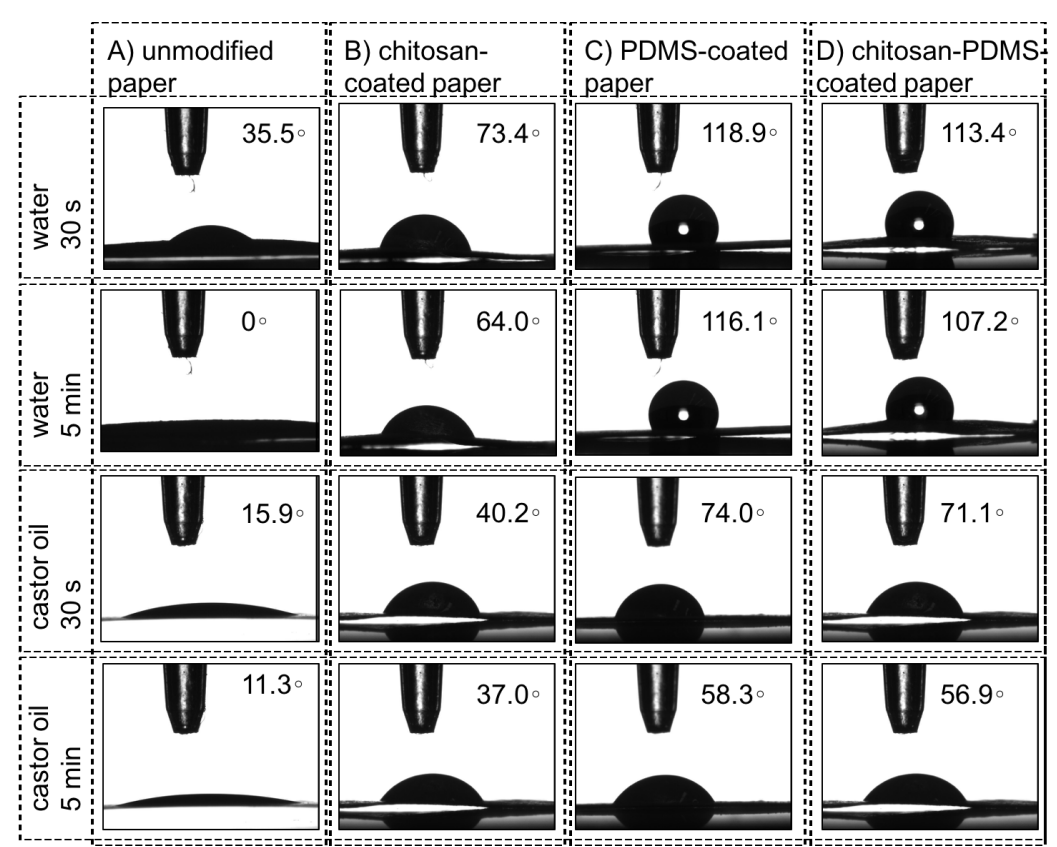


Figure 4.12 Contact angles of papers at different stages of fabrications. Water and castor oil droplets on uncoated paper (A), chitosan coated paper (B), PDMS coated paper (C), and chitosan-PDMS coated paper (D) and after 30 sec and 5-minute. Note: "PDMS coated" paper represents PDMS-HDIT coating applied on paper in the absence of chitosan.

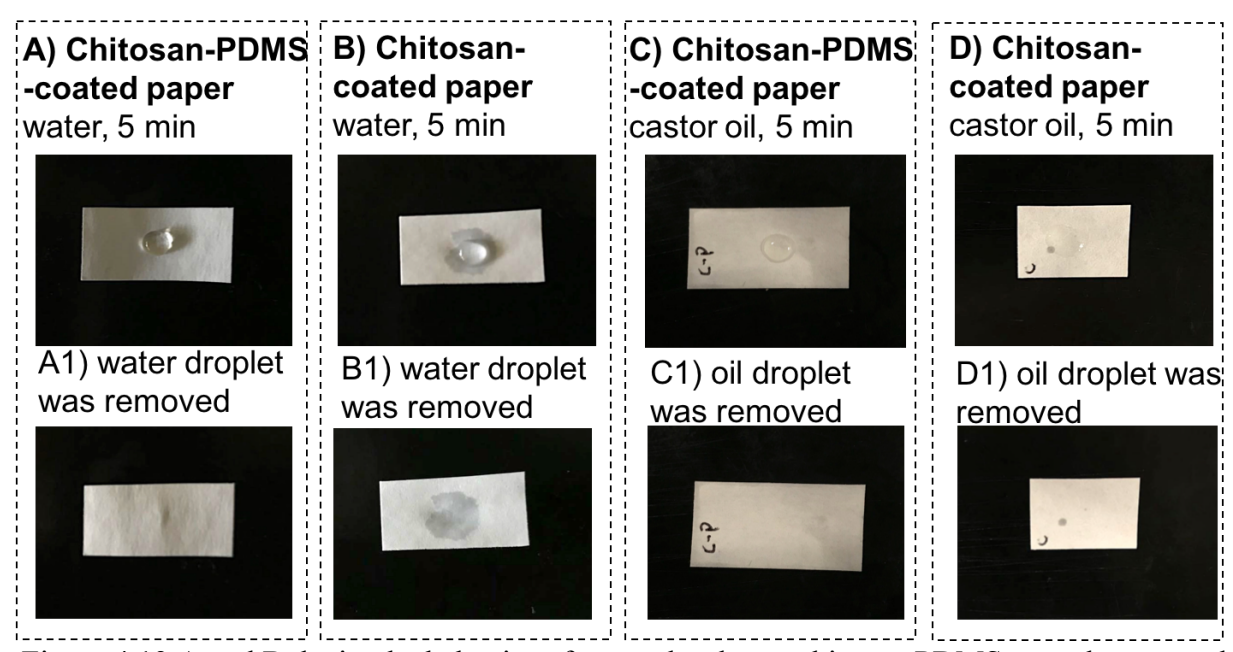


Figure 4.13 A and B depict the behavior of water droplet on chitosan-PDMS coated paper and chitosan coated paper, respectively. C and D show the behavior of castor oil droplet on chitosan-PDMS coated paper and chitosan coated paper, respectively. A1 to D1 represent images of the paper after water or oil droplets were removed after sitting for 5-min.

The hypothesis of this study was based on the fact that chitosan fills the pores on paper and renders the paper grease/fat-resistant, while PDMS renders chitosan-coated paper water-repellent and further enhances the oil-resistance. Therefore, SEM characterization was employed to observe the surface features of the unmodified paper, chitosan coated paper and chitosan-PDMS coated paper as shown in Figure 4.14. The pictures in the inset represent magnified images (by 1000×) that were used to study the structure of the fibers. The cellulose fibers, as well as the pores, were visible on the surface of the unmodified paper. After the chitosan coating, the cellulose fibers became smoother and were covered by a layer of chitosan, and the pores on the surface of the paper were filled (Figure 4.14b). In Figure 4.14c, it can be seen that the surface of the chitosan-PDMS-coated paper was even much smoother and more uniform, and no pores were visible. Thus, SEM analysis confirmed our predictions regarding the surface features. It is evident that

hydrophilic nature and the porous texture of the paper are responsible for its poor oil- and water-resistance, which were overcome by filling the pores and applying hydrophobic coatings.

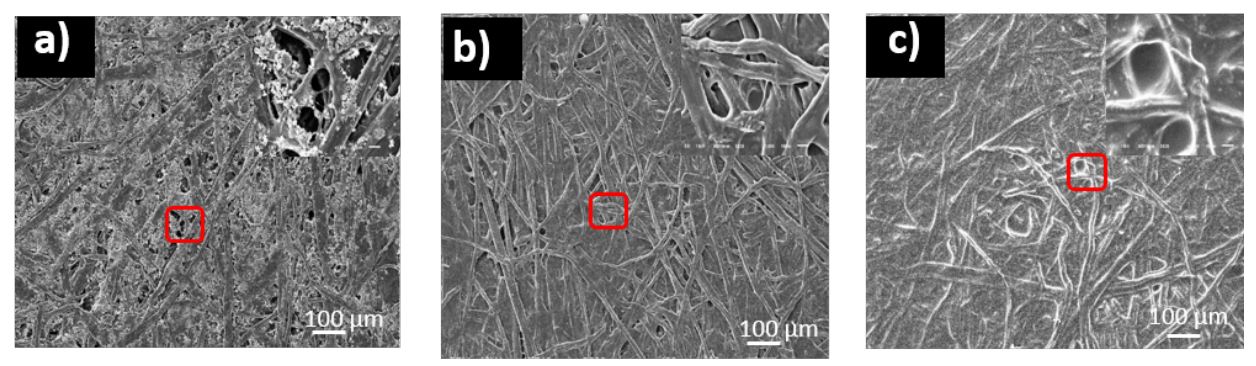


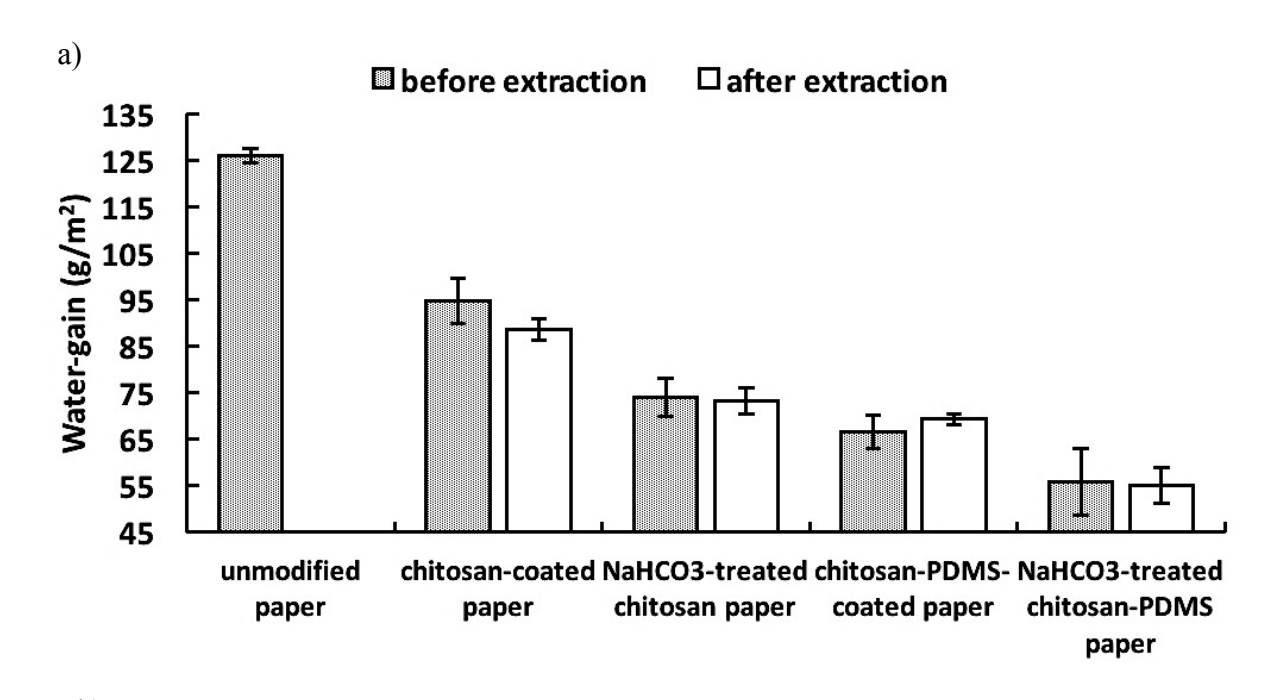
Figure 4.14 SEM images (100×) with zoomed-in pictures (1000×) shown as insets in the upper right corners for unmodified paper (a), chitosan-coated paper (b) and chitosan-PDMS-coated paper (c).

We also explored the effect of NaHCO₃ treatment before PDMS-NCO coating and compared their results with those obtained without NaHCO₃ treatment. NaHCO₃ treatment was applied as an attempt to deprotonate the -NH₃⁺ ions of the chitosan-acetic acid. The water- and oil-repellency of both the cationic- and NaHCO₃-treated samples were compared before and after extraction with hexane, as shown in Figure 4.15.

Figure 4.15a shows the water gain analysis of the paper samples that were conducted before and after extraction. Uncoated paper water gain was 125 g/m², which was reduced down to 60 g/m² for the chitosan-PDMS-coated paper. Similarly, the kit-rating values had increased from 0 to 12 for chitosan-PDMS-coated paper as shown in Figure 4.15b. After extraction with hexane, the water-gain was decreased slightly for both NaHCO₃-treated and untreated chitosan-coated paper. On the other hand, the oil-resistance of chitosan-PDMS-coated paper had decreased after extraction with hexane at a 95% confidence level based on Student's *t*-test.

Meanwhile, the water-gain value increased only slightly to 4.2% after extraction with hexane. A plausible explanation for this behavior is that some of the PDMS chains may have been

physically grafted onto the chitosan and were taken away during extraction with hexane. This presumably physical grafting can occur because of the low reactivity exhibited by $-\mathrm{NH_3}^+$ (due to the chitosan solution in acetic acid) towards NCO. However, the NMR spectra of the extracted samples did not show any PDMS peaks in the extract, possibly due to the very low concentration of PDMS (below $0.1~\mu\text{g/mL}$). To address the above problem, we applied NaHCO3 treatment to neutralize the protonated $-\mathrm{NH_3}^+$ groups and thus convert them into $-\mathrm{NH_2}$ moieties. As shown in Figure 4.15a and 4.15b, hexane extraction had virtually no effect on the NaHCO3-treated chitosan-PDMS-coated paper. Thus, NaHCO3 treatment strengthened the oil- and water-resistance of the chitosan-PDMS coatings.



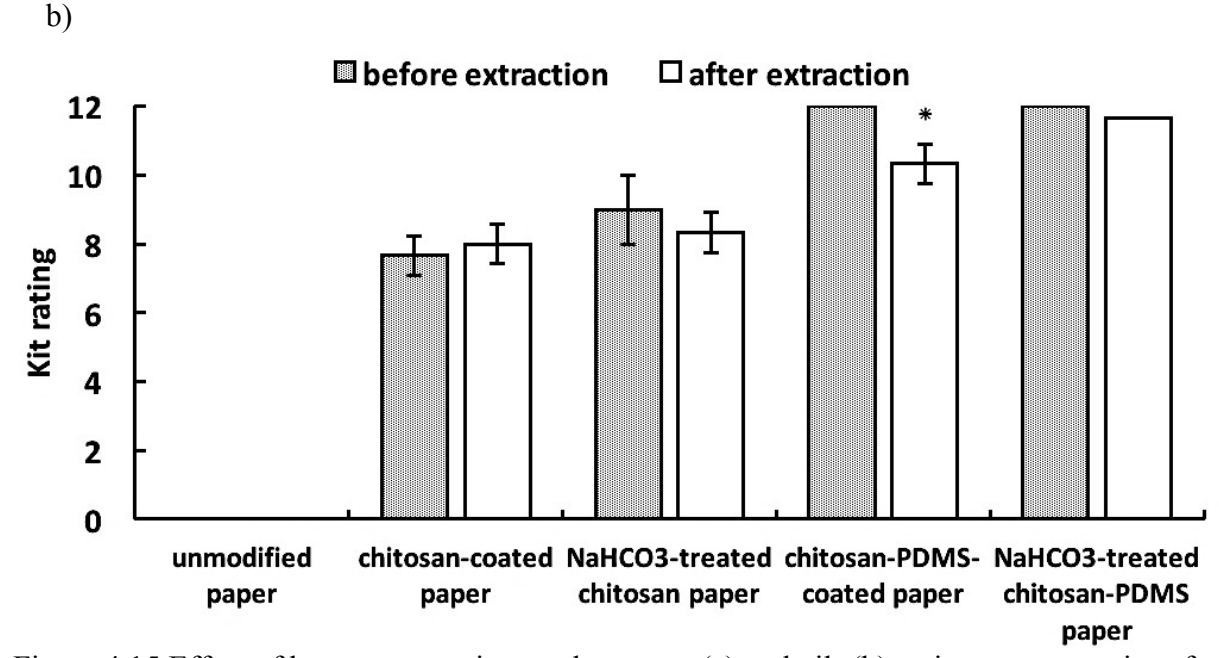


Figure 4.15 Effect of hexane extraction on the water- (a) and oil- (b) resistance properties of nonand NaHCO₃-treated paper coatings ("*" indicates a significant difference at the 95% confidential level based on Student's t-test).

To evaluate the effect of heating on the coated paper, some of the chitosan-PDMS-coated paper (Chitosan-PDMS room temperature) were dried at room temperature, and their water and oil-resistance were compared with those heated at 120°C. The room temperature Chitosan-PDMS coated paper showed an oil resistance of 4.33/12 after 1 day and 12/12 after 4 days, while water-

resistance after 1 day (as well as 4-day) was as good as the samples curing under 120 °C (Table 4.4). This room temperature drying with good water and oil resistance validates the feasibility of commercialization.

Table 4.4 Comparison of room temperature curing and heat-cured chitosan-PDMS coated papers

Curing condition	Room temp., 1 d	Room temp., 4 d	120 °C, 1h
Water-gain	63.15±2.64 ^a	61.78±1.97 ^a	66.53±3.62 ^a
Oil resistance	4.33 ± 0.58^{a}	12 ^b	12 ^b

Results were expressed as average value \pm standard deviation, values with different superscript letters "a" and "b" are significantly different (p<0.05)

The WVTR of paper (coated and uncoated) were also measured using a Mocon instrument (Figure 4.16). The thickness of the unmodified paper was 0.108 mm, and for chitosan-coated paper and chitosan-PDMS coated paper, the thickness was 0.127 mm. The WVTR for the uncoated paper and PDMS-coated paper (without chitosan) is almost 3-time higher than that of coated paper. This may correspond to the porous structure of the uncoated paper that allows easy passage of the water vapors. When chitosan coating was applied on the surface of the paper substrate, most of the pores were covered by a layer of chitosan film, and the WVTR decreased to 726 g/m²-day. The WVTR values were further reduced for chitosan-PDMS coated paper to 716 g/m²-day that did not decrease significantly compared with the chitosan-coated paper because this substrate still has some porosity that allows water vapors to pass through. When a thicker layer coating (with a thickness of 0.163 mm of the coated paper) was applied on the paper substrate, the chitosan-PDMS coating provided a higher barrier against water vapor compared with the chitosan coating alone due to the hydrophobicity, with a WVTR value of 322.16 g/m²-day compared with 628.63 g/m²-day.

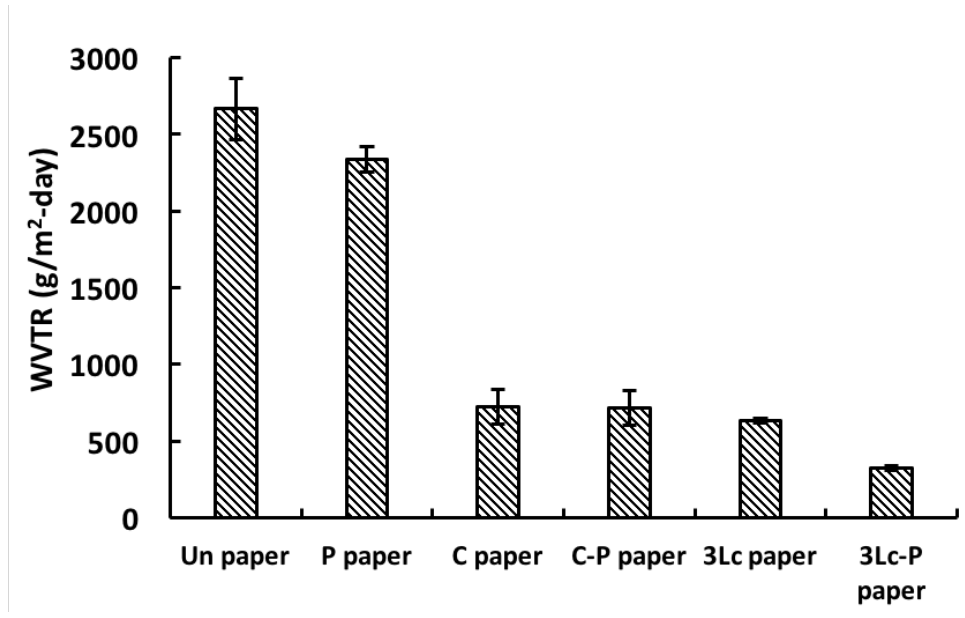


Figure 4.16 WVTR of unmodified paper (Un paper), PDMS coated paper (P paper), chitosan coated paper (C paper), chitosan-PDMS coated paper (C-P paper), 3 Layers chitosan coated paper (3Lc paper), and 3 Layers chitosan-PDMS coated paper (3Lc-P paper)

Paperboard was also used as a porous cellulose substrate to test the feasibility of chitosan-PDMS coating. The contact angle for water and castor oil is shown in Figure 4.17. Results indicate that chitosan-PDMS coating imparts both water and oil resistance to paperboard. As is shown in 4.18, applying PDMS onto the chitosan coated paper could both improve WCA as well as oil resistance. The kit rating of obtained chitosan-PDMS coated paper was 6/12, which is lower than 12 for printing paper in the previous study. This is mainly because the surface of paperboard is rougher and a thicker layer of coating is desired to improve the oil resistance.

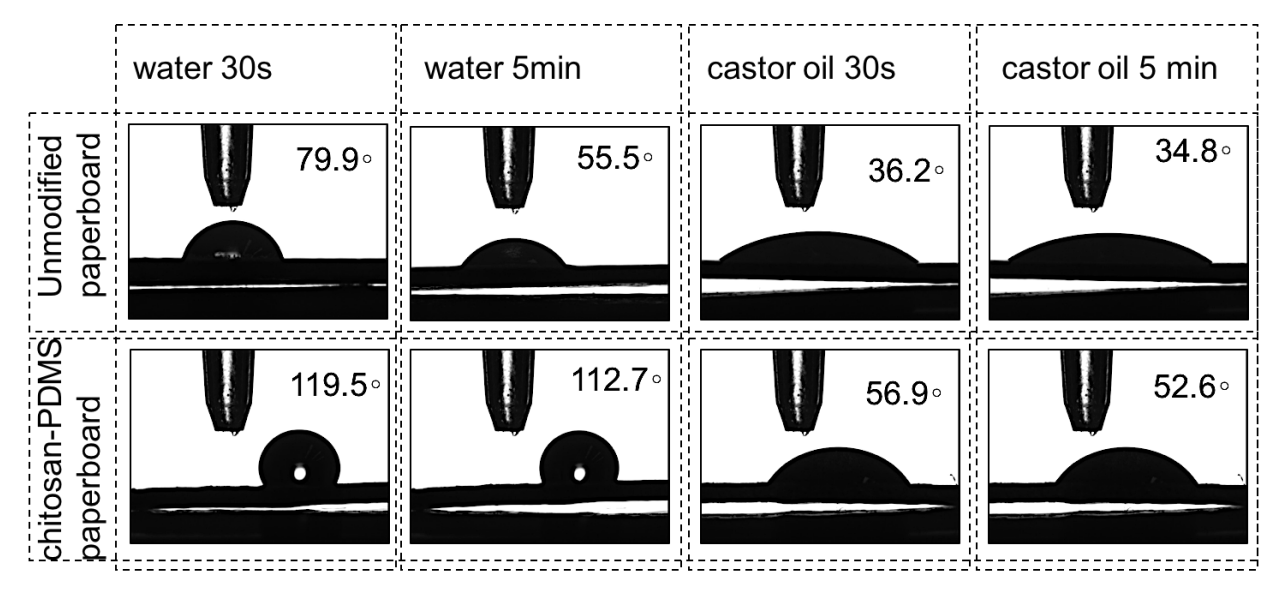


Figure 4.17 Contact angles of paperboards at different stages of fabrications. Water and castor oil droplets on uncoated paperboard and chitosan-PDMS coated paperboard and after 30 sec and 5-minute. Note: PDMS-coated paper without chitosan has poor water-resistance as reported by us previously.¹⁰

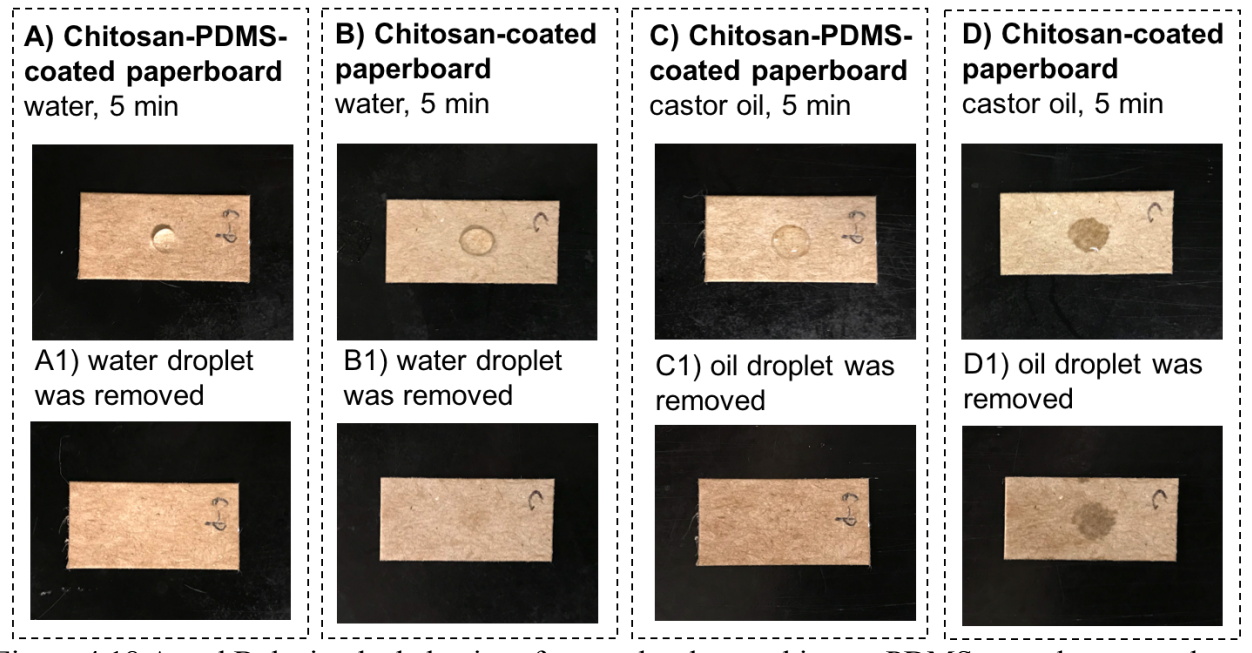


Figure 4.18 A and B depict the behavior of water droplet on chitosan-PDMS coated paper and chitosan coated paperboard, respectively. C and D show the behavior of castor oil droplet on chitosan-PDMS coated paper and chitosan coated paperboard, respectively. A1-D1 represent images of the paperboard after water or oil droplets were removed after sitting for 5-min.

4.5 Conclusions

In this study, we proved that porous substrate such as paper could be turned water- and oil-repellent, if the pores are masked with chitosan and the surface is modified with PDMS. Optimized concentrations of the coating solution were 1.0 wt% chitosan solution and 5.0 wt% PDMS. RSM was used to screen the optimized formulations. The oil/grease-resistant properties of the obtained coatings were due to the non-porous nature of the coated paper, and the hydrophobic nature of PDMS, as was confirmed by SEM analysis. NaHCO3 treatment was also utilized that helped to enhance the resistance of the coated paper against extraction with hexane. Considering the growing environmental concerns related to the use of fluorinated materials, this fluorine-free and low-cost approach will find many real-world applications. Also, paperboard was successfully fabricated by this approach suggesting the universality of this coating method for other porous cellulosic substrates such as sponges, fabrics, foams, and corrugated boxes.

REFERENCES

REFERENCES

- 1. Quéré, D., Wetting and roughness. *Annu. Rev. Mater. Res.* **2008,** *38*, 71-99.
- 2. Wong, T.-S.; Kang, S. H.; Tang, S. K.; Smythe, E. J.; Hatton, B. D.; Grinthal, A.; Aizenberg, J., Bioinspired self-repairing slippery surfaces with pressure-stable omniphobicity. *Nature* **2011**, *477* (7365), 443.
- 3. Barthlott, W.; Neinhuis, C., Purity of the sacred lotus, or escape from contamination in biological surfaces. *Planta* **1997**, *202* (1), 1-8.
- 4. Tuteja, A.; Choi, W.; Ma, M.; Mabry, J. M.; Mazzella, S. A.; Rutledge, G. C.; McKinley, G. H.; Cohen, R. E., Designing superoleophobic surfaces. *Science* **2007**, *318* (5856), 1618-1622.
- 5. Lu, Y.; Sathasivam, S.; Song, J.; Crick, C. R.; Carmalt, C. J.; Parkin, I. P., Robust self-cleaning surfaces that function when exposed to either air or oil. *Science* **2015**, *347* (6226), 1132-1135.
- 6. Deng, X.; Mammen, L.; Butt, H.-J.; Vollmer, D., Candle soot as a template for a transparent robust superamphiphobic coating. *Science* **2012**, *335* (6064), 67-70.
- 7. Cheng, D. F.; Urata, C.; Yagihashi, M.; Hozumi, A., A statically oleophilic but dynamically oleophobic smooth nonperfluorinated surface. *Angewandte Chemie International Edition* **2012**, *51* (12), 2956-2959.
- 8. Xiong, D.; Liu, G.; Hong, L.; Duncan, E. S., Superamphiphobic diblock copolymer coatings. *Chemistry of Materials* **2011**, *23* (19), 4357-4366.
- 9. Ham-Pichavant, F.; Sèbe, G.; Pardon, P.; Coma, V., Fat resistance properties of chitosan-based paper packaging for food applications. *Carbohydrate Polymers* **2005**, *61* (3), 259-265.
- 10. Li, Z.; Rabnawaz, Muhammad, Fabrication of Food-Safe Water-Resistant Paper Coatings Using a Melamine Primer and Polysiloxane Outer Layer. *ACS Omega* **2018**, 3 (9), 11909-11916.
- 11. Bayer, I. S.; Fragouli, D.; Attanasio, A.; Sorce, B.; Bertoni, G.; Brescia, R.; Di Corato, R.; Pellegrino, T.; Kalyva, M.; Sabella, S.; Pompa, P. P.; Cingolani, R.; Athanassiou, A., Water-Repellent Cellulose Fiber Networks with Multifunctional Properties. *ACS Applied Materials & Interfaces* **2011**, *3* (10), 4024-4031.
- 12. Heredia-Guerrero, J. A.; Benítez, J. J.; Cataldi, P.; Paul, U. C.; Contardi, M.; Cingolani, R.; Bayer, I. S.; Heredia, A.; Athanassiou, A., All-Natural Sustainable Packaging Materials Inspired by Plant Cuticles. *Advanced Sustainable Systems* **2017**, *I* (1-2), 1600024.
- 13. Paul, U.; Fragouli, D.; Bayer, I.; Athanassiou, A., Functionalized Cellulose Networks for Efficient Oil Removal from Oil–Water Emulsions. *Polymers* **2016**, *8* (2), 52.

- 14. Uttam, C. P.; Despina, F.; Ilker, S. B.; Elisa, M.; Chiara, C.; Roberto, C.; Sabrina, M.; Athanassia, A., Mineral oil barrier sequential polymer treatment for recycled paper products in food packaging. *Materials Research Express* **2017**, *4* (1), 015501.
- 15. Graiver, D.; Farminer, K. W.; Narayan, R., A Review of the Fate and Effects of Silicones in the Environment. *J. Polym. Environ.* **2003**, *11* (4), 129-136.
- 16. Schaider, L. A.; Balan, S. A.; Blum, A.; Andrews, D. Q.; Strynar, M. J.; Dickinson, M. E.; Lunderberg, D. M.; Lang, J. R.; Peaslee, G. F., Fluorinated compounds in US fast food packaging. *Environmental Science & Technology Letters* **2017**, *4* (3), 105-111.
- 17. Dassuncao, C.; Hu, X. C.; Nielsen, F.; Weihe, P. l.; Grandjean, P.; Sunderland, E. M., Shifting Global Exposures to Poly-and Perfluoroalkyl Substances (PFASs) Evident in Longitudinal Birth Cohorts from a Seafood-Consuming Population. *Environmental science & technology* **2018**, *52* (6), 3738-3747.
- 18. https://sustainablepackaging.org/events/spc-impact-2018/;
 https://news.starbucks.com/news/starbucks-and-closed-loop-to-develop-recyclable-compostable-cup-solution; accessed on July 10, 2019.
- 19. Technical Association of the, P.; Paper, I., *TAPPI standards and suggested methods:* tentative and official testing methods, recommended practices, specifications of the Technical Association of the Pulp and Paper Industry. The Association: New York U6 ctx_ver=Z39.88-2004&ctx_enc=info%3Aofi%2Fenc%3AUTF-
- $8\&rfr_id=info\%3Asid\%2Fsummon.serials solutions.com\&rft_val_fmt=info\%3Aofi\%2Ffmt\%3Akev\%3Amtx\%3Abook\&rft.genre=book\&rft.title=TAPPI+standards+and+suggested+methods\&rft.date=1949-01-$
- 01&rft.pub=The+Association&rft.externalDBID=I17&rft.externalDocID=b86936542¶mdic t=en-US U7 eBook, 1949.
- 20. Sunghwan Kim, P. A. T., Evan E. Bolton,* Jie Chen, Gang Fu, Asta Gindulyte, Lianyi Han, Jane He, Siqian He, Benjamin A. Shoemaker, Jiyao Wang, Bo Yu, Jian Zhang, and Stephen H. Bryant, PubChem Substance and Compound databases. *Nucleic Acids Res.* **2016 Jan 4**, *44*, D1202-1213.
- 21. Haynes, W. M., *CRC Handbook of Chemistry and Physics*. 95th Edition ed.; CRC Press: Boca Raton, 2014.
- 22. Nandane, A. S.; Dave, R. K.; Rao, T. V. R., Optimization of edible coating formulations for improving postharvest quality and shelf life of pear fruit using response surface methodology. *Journal of Food Science and Technology* **2016**, *54* (1), 1-8.
- 23. Creasy, W. R.; McGarvey, D. J.; Rice, J. S.; O'Connor, R.; Durst, H. D. *Study of Detection Limits and Quantitation Accuracy Using 300 Mhz NMR*; EAI CORP ABINGDON MD: 2003.
- 24. Rabnawaz, M.; Liu, G.; Hu, H., Fluorine-Free Anti-Smudge Polyurethane Coatings. *Angewandte Chemie* **2015**, *127* (43), 12913-12918.

- 25. Cardenas, G.; Miranda, S. P., FTIR AND TGA STUDIES OF CHITOSAN COMPOSITE FILMS. *Journal of the Chilean Chemical Society* **2004**, *49* (4), 291-295.
- 26. Park, J. K.; Ryu, J.; Koo, B. C.; Lee, S.; Kang, K. H., How the change of contact angle occurs for an evaporating droplet: effect of impurity and attached water films. *Soft Matter* **2012**, *8* (47), 11889-11896.

CHAPTER 5: A CLOSED-LOOP AND SUSTAINABLE APPROACH FOR THE FABRICATION OF PLASTIC-FREE OIL- AND WATER-RESISTANT PAPER PRODUCTS

A version of this chapter is published as:

Li, Z.; Rabnawaz, M.; Krishna, A.; Sirinakbumrung, N.; Khan, B.; Kamdem, D. P. A Closed-Loop and Sustainable Approach for the Fabrication of Plastic-Free Oil- and Water-Resistant Paper Products. *Green Chem.* **2019**, *21*, 5691-5700. DOI: 10.1039/C9GC01865D.

5.1 Abstract

The current open-loop practices employed to render paper substrates water- and oilrepellent for packaging and non-packaging applications have generated ocean pollution and have placed daunting burdens on landfills. In this study, we report a green, unique and facile approach for the fabrication of grease- and water-resistant paper products with 100% recyclability of the paper pulp. Low surface energy polydimethylsiloxane (PDMS) was grafted onto a biobased chitosan polymer via urea linkages to prepare the graft copolymer chitosan-graftpolydimethylsiloxane (chitosan-g-PDMS). Chitosan-g-PDMS was then applied as a coating onto an unbleached Kraft paper substrate from an aqueous solution. The coated paper substrates exhibited good hydrophobic properties with a water contact angle of $120.53 \pm 0.96^{\circ}$ and a Cobb 60 value of 9.89 ± 0.32 g/m². The coated paper substrates also showed good oil-resistance as evident from the kit rating value of 11.7/12. The tensile strength, crushing resistance, bending stiffness, and internal tearing resistance of the paper before and after coating treatment was determined. Scanning electron microscopy (SEM) analysis was used to characterize changes in the porosity of the paper before and after the coating. The pulp recyclability of the coated paper was validated by subjecting the coated paper samples to repulping and washing treatment. Overall migration study of siloxanes into two food simulants including 50% aqueous ethanol and Miglyol 812 were performed using ¹H-NMR. The migration didn't exceed 46.19 µg/ml (7.16 mg/dm²), which is well below the overall migration limit 60 mg/kg food (100 mg/dm²) by the Council of Europe's Resolution AP (2004). This novel and practical approach can provide significant environmental benefits by offering plastic-free, fluorine-free and fully-recyclable water- and grease-resistant paper; thus promoting sustainability due to its unique closed-loop nature.

Keywords: closed-loop system, plastic-free, water resistant, oil resistant, paper, porous cellulosic substrates, fluorine-free

5.2 Introduction

Paper products are widely used due to their desirable technical properties such as low-weight, renewability, biodegradability, food-safety, and good mechanical properties.^{1, 2}For example, in the packaging sector alone, paper products account for more than 50% (by mass) of the packaging materials. However, paper products have poor water- and oil-resistance due to the polar hydroxyl groups of the lignocellulose that comprises the paper as well as their porous structure, which allows the permeation of liquids and results in the swelling of cellulosic fibers. Various approaches have been used to enhance the water- and grease-resistance of paper, such as internal sizing during paper processing or external coating as further treatment.^{3, 4} These approaches are typically focused on the modification of the hydrophobic cellulosic fibers as well as the filling of the paper pores.

Lamination and coating treatment are common commercial practices to impart paper products with water- and oil-repellency. For lamination, low-density polyethylene (LDPE) liners are typically used in this regard.⁵ However, the laminated paper has limited recyclability, and thus enormous amounts of this material end up as municipal solid waste. For example, 22 million tons of plastic was dumped in landfills in 2017 in the U.S. alone.⁶ This waste of pulp is compensated for through the cutting down of additional trees, which places a staggering toll on the environment. Moreover, the polymers and coatings that are used to impart paper with water- and oil-resistance are typically non-degradable synthetic materials, and they also contribute to the 145 million tons of plastic that are sent to landfills each year.⁷⁻⁹ To minimize this environmental damage caused by laminated and coated paper, the EU parliament voted in 2018 to ban single-use plastics in

cutlery, plates, and straws, and also urged a reduction in the use of single-use cups and beverage containers.¹⁰

Non-degradable polymer latexes (e.g., styrene-butadiene latexes) are also used in paper coatings to enhance their water- and oil-resistance.¹¹ However, latex formulations possess polar/ionic groups that reduce their resistance against polar liquids such as water. Also, concerns exist regarding the migration or leaching of latex when it is used for food packaging applications.¹² Furthermore, non-degradable latex from coated paper ends up in the environment as microplastics with adverse effects on ecosystems.^{13, 14}

Biodegradable/compostable plastics such as polylactide (PLA) have also been used as liners for paper cups and plates. ^{1, 15, 16}However, as is the case with LDPE, it is difficult to separate PLA from paper substrates during the pulping process. Also, PLA is biodegradable under compost conditions, unlike paper that is biodegradable in the natural environment, which further complicates the recyclability of PLA-laminated paper. ¹⁷ In addition, PLA is not a good candidate for coating because of its thermal stability during processing and to package hot beverages or liquid. Polyaleuritate coatings with carnauba wax coatings have been used to improve the water-resistance of paper substrates. ¹⁸ Proteins ¹⁹⁻²² and lipids ²³⁻²⁵ have also been used as paper coatings, but they showed poor resistance against water and oil.

Another problem encountered with current industrial paper modification practices involves the use of fluorinated chemicals^{26,27} to render paper strongly water- and oil-resistant for applications such as disposable plates, take-out food containers, and fast food wrappers. However, due to their toxicity and environmental concerns, industry stakeholders and governments are seeking to phase out the use of fluorinated materials in coatings.^{28,29}

Silicone oils³⁰, which are inexpensive low surface energy materials with good environmental friendliness, is considered as a greener alternative for fluorochemicals. 30-32 For example, polydimethylsiloxane (PDMS) (surface energy = 20 mN/m)³³ renders non-porous substrates such as urethane and epoxy coatings water- and oil-resistant.³⁴ Whereas, not many researches have used PDMS for fabricating water- and oil- resistant cellulose-based materials. We have recently reported that the application of PDMS coatings on porous substrates such as paper only vielded water-repellent properties but did not impart oil repellency.³⁵ Interestingly, the incorporation of a chitosan layer prior to the application of a PDMS layer rendered paper both water- and oil-resistant because chitosan filled the paper's pores. However, these two studies are both in two steps with the final step relying on large amount of organic solvent, which thus limited the practical and environmental significance of these strategies for the paper coating industry. In addition, these two approaches lacked recyclability because PDMS was grafted to both the fibers and chitosan, and therefore, the separation of the coating from the paper presented a significant challenge. Consequently, these approaches offered only limited sustainability. Therefore, there is an urgent to replace organic solvent by water which is a big step aligned with Green Chemistry mission. Also, one-step approach and pulp-recovery are desired due to the practicability in terms of reducing cost, saving energy as well as maintaining sustainability.

Herein, we report a novel coating approach toward grease- and water-resistant paper products with 100% pulp recyclability. We used an aqueous micellar solution of chitosan-*graft*-polydimethylsiloxane (chitosan-*g*-PDMS) to coat paper substrates. The proposed study is a single-step coating approach without using organic solvent. After drying, the paper was investigated to evaluate its water- and oil-resistance. The recyclability of the coated paper was studied by separating the paper pulp from the coating via a repulping approach. The obtained chitosan-*g*-

PDMS-coated paper exhibited excellent grease- and water-resistance, and the coating could be fully washed away via a simple pulp-washing approach, thus offering an ideal scenario for sustainable practices.

5.3 Materials and Methods

5.3.1 Materials.

Polydimethylsiloxane (PDMS) monoaminopropyl-terminated ($M_{\rm w}=2000$ g/mol, PDMS-2K) was purchased from Gelest, Inc. and used without further purification. Chitosan ($M_{\rm w}=50,000-190,000$ g/mol), butyl acrylate (99%), ethanol (95%) and acetone (99.7%) were purchased from Sigma. Hexamethylene diisocyanate trimer (HDIT) was purchased from a local Sherwin-Williams store in Detroit Michigan, United States of America. Miglyol 812 was purchased from IOI Oleo GmbH (Witten, Germany). An unbleached Kraft paperboard with a basis weight of 147 g/m² (grammage) was selected as a paper substrate for coating.

5.3.2 Methods and Characterization

5.3.2.1 General procedure for Model Reactions

Model reactions between HDI and ethanolamine (HOEtNH₂) and ethanol were performed in order to prove the reaction between amino group (-NH₂) and the NCO in an aqueous acidic medium. Ethanolamine was chosen as a model substrate because of the presence of -NH₂ groups like chitosan, while ethanol was applied as the corresponding control. First, HOEtNH₂ (1.0 Equvi., 0.42 mL) was dissolved in water at 2wt% to simulate our chitosan solution concentration. Acetic acid was added to achieve pH ~5 was achieved. Then HDI (0.3 mL, 0.5 Equiv. of HOEtNH₂) was added. After ~1 min, IR was recorded and an additional 0.3 mL (0.5 Equiv. of HOEtNH₂ of HDI) was added. IR was again recorded after an additional 1 min stir, followed by the addition of additional 0.02 mL (0.03 Equiv.) to achieve slight excess of HDI. For ¹H NMR analysis, model

product was obtained by the extraction of crude reaction mixture with ethyl acetate. The separated model product was vacuum dried before ¹H NMR in DMSO-d6.

In another experiment, ethanol and HDI were reacted in the same conditions mentioned above for ethanolamine and HDI. Briefly, ethanol (0.4 mL) solution in water-acetic acid (10 mL). HDI (0.3 Ml, 0.5 Equiv. of ethanol) was added, and IR was recorded after ~1 and 25 min stirring. As there was no significant change in the NCO peak, therefore, stopped in the experiment.

Synthesis of Model PDMS-NCO: PDMS-NH₂ (1 mmol) was dissolved in acetone (~20wt/vol). HDI (1.5 mmol, 20wt% in acetone) was added dropwise into the PDMS-NH₂ solution. Once all HDI was added, the mixture was stir for 5 min. Then the crude PDMS-NCO was precipitated from 10 times excess acetonritile, and upon centrifugation, pure PDMS-NCO was obtained.

5.3.2.2 Paper coating procedure

First, a stock solution of PDMS-NCO was prepared via a literature method,^{34, 35} which is briefly described herein. PDMS-NH₂ (26.7 w/v% of PDMS-NH₂ in acetone, 133.5 mmol/L) was added dropwise into an HDIT solution (13.3 w/v% HDIT in acetone, 661.7 mmol/L) under stirring. The concentration of the prepared PDMS-NCO stock solution was 20 w/v% PDMS-NCO in acetone. A series of PDMS-NCO solutions with various concentrations (25, 50, 100, 200 and 400% w/v) was prepared by mixing the appropriate volume of PDMS-NCO stock solution with acetone.

Chitosan stock solution was prepared by dissolving 4.0 g of chitosan in 100 mL water in the presence of 2.0% (v/v) acetic acid, and subsequently stirring this solution for 24 h. The concentration of the final chitosan solution was adjusted by adding 3.5 mL of deionized water into 2.5 mL of the chitosan stock solution. Thus, the obtained solution contained 100 mg of chitosan per 6.0 mL of solution, thus having a concentration of 1.67 wt%.

The chitosan-*g*-PDMS solution was prepared via the dropwise addition of the PDMS-NCO solution into the chitosan solution. Once the addition was completed, the solutions were further stirred for 5 min and the NCO consumption was monitored by ATR-FTIR spectroscopy until the NCO peak had disappeared. The residual acetone was removed from the solution *via* bubbling with air. The obtained water-borne chitosan-*g*-PDMS solutions containing various amounts of PDMS (12.5, 25.0, 50.0, 100 and 200 mg) along with 100 mg of chitosan (see Table 5.1). For NMR analysis, the Chitosan-*g*-PDMS was dried at reduced pressure.

The above chitosan-*g*-PDMS coating solutions were applied onto one side of an unbleached Kraft linerboard using a K303 Multi Coater (RK PrintCoat Instruments Ltd, UK), and they were subsequently dried in air at room temperature for 24 h. All of the samples were preconditioned at 23 °C and at 50% relative humidity (RH) for 24 h prior to performance analysis.

Table 5. 1 Formulations and corresponding codes used in this article

Abbreviated name	PDMS-NCO (mg)	Chitosan (mg)
U-p ^a	-	-
C - p^b	-	100
P0.125C-p ^c	12.5	100
P0.25C-p	25	100
P0.5C-p	50	100
P1C-p	100	100
P2C-p	200	100

^aUnmodified paper (U-p); ^bchitosan-coated (C-p), ^cP0.125C-p (P denotes PDMS, 0.125C denotes the weight of the PDMS with respect to the weight of chitosan, which is expressed as C

5.3.3 Characterization

5.3.3.1 Dynamic light scattering (DLS) analysis

DLS characterization was employed to determine the average hydrodynamic diameter of the chitosan-*g*-PDMS micelles. The chitosan-*g*-PDMS coating solutions or chitosan solution (0.5 mL) were added into 50 mL of DI water and subsequently vortexed for ~1 min and then centrifuged at 5000 rpm for 5 min. The solution was subsequently analyzed using a Light Scattering Analytical Instrument (BI-200SM, Brookhaven Instrument, US).

5.3.3.2 Basis weight and thickness

The basis weights (mass per unit area of paper) of chitosan-*g*-PDMS-coated paper (PC-p), chitosan-coated (C-p) paper, and unmodified paper (U-p) were measured in accordance with the ASTM D646 protocol. Specimens with dimensions of 200 × 200 mm² were weighed with a microbalance. The basis weight was calculated via Eq. 1, and expressed in grams per square meter (g/m², grammage). Measurements were performed in triplicate for each type of paper material. Coating loadings were calculated based on the difference between the coated paper and the unmodified paper. The thickness of each sample was measured using a digital micrometer (Testing Machine Inc., New Castle, DE, USA) at ten different random locations on the same specimen.

basis weight =
$$\frac{weight(g)}{area(m^2)}$$
 (Eq. 1)

5.3.3.3 Water vapor transmittance rate (WVTR) and water absorption capacity (Cobb60 value)

The WVTR values of PC-p, C-p, and U-p were determined using a Permatran-W (Model 3/34, Mocon Inc. MN, USA) system. These measurements were performed at 23 °C and at 50% RH with nitrogen as the carrier gas (flow rate = 12 SCCM). Specimens with dimensions of $20 \times 20 \text{ mm}^2$ were masked in aluminum sheets with a 6-mm-diameter opening to fit the sample cell.

Water absorptions of PC-p, C-p, and U-p were determined according to their Cobb values via a TAPPI standard T441 om-09 protocol. A Cobb sizing tester (Büchel BV Inc. Utrecht, Netherlands) was employed to allow 100 mL of DI water to come into contact with a 100-cm² specimen for 60 s. The weight of the absorbed water was calculated as the difference in the weight of each specimen before and after the test. The Cobb60 value was expressed as the weight of water absorbed by the specimen in grams per square meter (g/m²).

5.3.3.4 Grease-resistance properties

The grease resistance was studied in accordance with a previous study and via a TAPPI T 559 pm-96 standard method.³⁵ The oil-resistance was quantified and scaled from 1-12 based on their "kit rating" values, where the kit-rating corresponded to the maximum oil resistance.

5.3.3.5 Contact angle (CA), sliding angle, and surface energy measurements.

The CAs of water and castor oil were measured with a 590-U1 Advanced Automated Goniometer (Ramé-Hart Instrument Co., NJ, USA). Droplets with a volume of 5 μ L were carefully applied onto the surface of a specimen, and the CAs were then measured and images were taken after 30 s and 5 min. These measurements were performed in triplicate on three random locations of each sample.

Sliding angles were determined by adding a 100 μ L droplet of the test liquid onto the surface of each coated paper specimen, which was affixed onto a wood plate. The angle of this wood plate with respect to the horizontal plane was then increased at a constant rate (2 °/s) until the water droplets began to slide. The angle of the wood plate at this point was recorded as the sliding angle of the specimen.

The surface tensions of coated and uncoated paper samples were determined with the use of DROPimage Advanced software (Ramé-Hart Instrument Co., NJ, USA) based on the CAs of water and diiodomethane.

5.3.3.6 IR analysis

A Shimadzu FT-IR spectrometer IR-Prestige21 (Shimadzu Co., Columbia, MD) equipped with an attenuated-total-reflection accessory (ATR, PIKE Technologies, Madison, WI) was employed to record IR spectra of PC-p, C-p, and U-p. Each spectrum was obtained with an average of 64 scans over a wavenumber range of 4000-600 cm⁻¹ with a resolution of 4 cm⁻¹.

5.3.3.7 Thermogravimetric analysis (TGA)

TGA measurements of PC-p, C-p, and U-p samples were performed using a Q-50 thermogravimetric analyzer (TA Instruments, New Castle, DE). Samples (6-10 mg) were heated under a nitrogen atmosphere (flow rate = 40 mL/min) from 23 to 600 °C at a rate of 10 °C/min. Derivative thermogravimetric (DTG) curves were plotted as first derivatives of the corresponding TGA curves.

5.3.3.8 Scanning electron microscopy (SEM)

The surface morphologies of the PC-p, C-p, and U-p samples were observed using a JEOL 6610 SEM (JEOL Ltd., Japan) system. The SEM instrument was operated at an accelerating voltage of 15 kV. Samples were affixed on aluminum stubs with a carbon double-sided tape and they were subsequently coated with a gold layer (15 nm thick) with the use of a sputter coating machine.

5.3.3.9 NMR characterization

¹H NMR analysis was conducted using a 500 MHz NMR spectrometer (Agilent, Santa Clara, CA, USA).

5.3.4 Recyclability

The recyclability of chitosan-*g*-PDMS-coated paper (PC-p) was studied using a repulping approach. Paper samples (P1C-p) with a weight of 3.0 g were chopped into 2 cm by 2 cm sections and soaked in warm water (~40 °C) for 30 min, and then the soaked paper samples were repulped using a blender. Half of the pulp suspension was made into paper by sequentially pouring this suspension onto the screen of a wood frame to allow filtration to occur, subsequently pressing it with an iron, and then drying the sample at 56 °C under vacuum for 1 h. The other half of the pulp was centrifuged and the supernatant was removed after this centrifugation treatment. Freshwater was added again and the sample was then centrifuged and the supernatant was removed again. This step was repeated one more time. The obtained pulp was used to fabricate paper again via the procedure described above. Paper made from the washed and unwashed pulp was analyzed via FT-IR-ATR spectroscopy by monitoring the disappearance of peaks corresponding to PDMS, which would indicate the presence or absence of the coating. Unmodified-paper (U-p) was recycled in a similar manner as the control samples.

5.3.5 Mechanical property tests

Bleached Kraft paper samples were coated with chitosan, P0.25C, and P0.5C polymers to study the effect of these coatings on the mechanical properties. Each test was performed in triplicate and in both the cross machine direction (CD) and machine direction (MD).

The tensile strength was studied following a TAPPI standard T 494 protocol using a 5565 Universal Instron testing machine (Instron, MA, USA). A specimen (1" × 11") was loaded on two clamps, where the gap between the clamps was 7.1". The specimen was stretched at a constant rate (0.5 in/min). A plot of the force versus extension was recorded with the use of the Bluehill

software package (Instron, MA, USA). Tensile strengths were calculated as the maximum tensile force divided by the width of the specimen.

The ring crush test (RCT) was performed using a TMI crush tester (Model 1210, Instron, MA, USA) following the TAPPI T822 protocol. RCT represents the compression strength of paper board when it stands on its edge, and therefore affects the edgewise compression strength of corrugated board and of a finished container made from this paperboard. Samples were cut into 0.5 inch by 6 inch sections using a standard sample cutter, and carefully slid into a sample holder so that these samples could stand on their edges. Force was applied on the edge of the paperboard, and the amount of force required to crush the sample was then recorded.

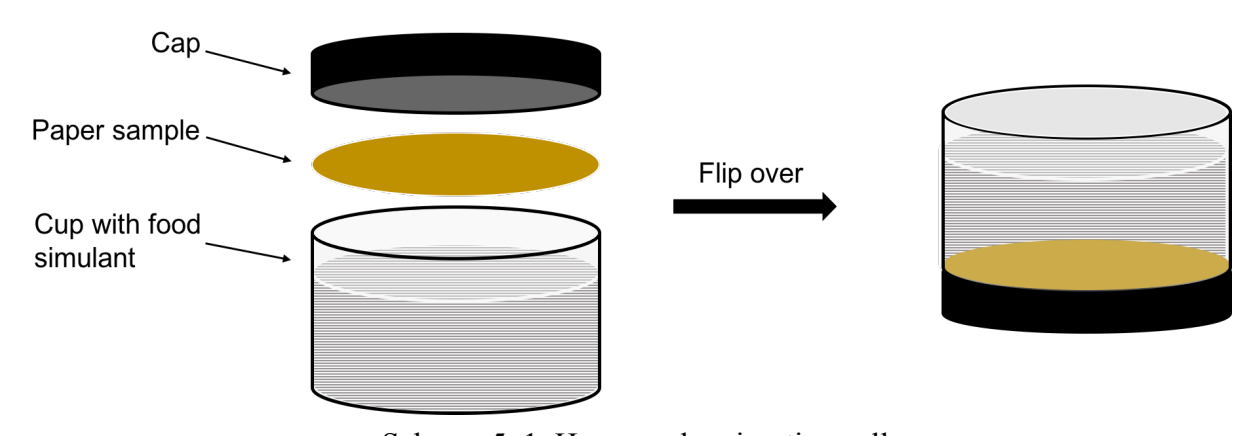
The bending stiffness (BS) was studied using a Taber stiffness tester (Model 150-D, Teledyne Taber, NY, USA) following the TAPPI T489 protocol. One end of the specimen (1.5 inches by 2.75 inches) was clamped in the tester, and a force (500 Taber stiffness units) was applied at the other end to bend the specimen by 15°. The bending stiffness was calculated as the average of left and right readings on the tester.

Internal tearing resistance (ITR) was analyzed following the TAPPI T414 protocol using an ME-1600 Manual Elmendorf-type tearing tester (Oakland Instrument Co, MN, USA). Two piles were loaded for each test and the tearing forces required to tear a single sheet was calculated.

5.3.6 Overall Migration Study

An overall migration study was performed to estimate the migration of PDMS in food simulants. One-sided liquid extraction experiment was performed using a homemade migration cell as is shown in Scheme 5.1. Basically, the paper sample (6 in²) is clamped as a liner in the cap which was then applied to a plastic cup which containing 60 ml food simulant. The obtained solvent volume-to-expose surface area ratio was 10 mL/in² as is recommended by United States

Food and Drug Administration (FDA) which represents most actual food packaging. The cup was then flip over allowing for continuous contact between paper sample and food simulant. The system was kept at 40 °C for up to 10 days of which the migration level is equivalent to 6-12 months' storage at 20 °C according to United States FDA recommendation. Miglyol 812 was applied to simulate fatty food and 50% aqueous ethanol to simulate low- and high-alcoholic food also according to FDA recommendation. Chitosan-g-PDMS-coated paper and Chitosan-coated paper were tested, and migration cell containing food simulant with no paper sample was tested as blank control to study the possible leaching from migration cell itself.



Scheme 5. 1 Homemade migration cell

5.3.7 Quantitative analysis of migrated silicone

Silicone concentrations in the solvent were quantified using ¹H-NMR techniques by a 500 MHz NMR spectrometer (Agilent, CA, USA). CDCl₃ spiked with butyl acrylate (1 mg/ml) as internal standard (I.S.) was applied as solvent. Calibration curve was generated from PDMS standards in CDCl₃ (with butyl acrylate I.S.) solution at various concentrations 0 – 400 μg/ml. The peak area at 6 ppm of butyl acrylate I.S was chosen as reference peak (regarding as 1), and the relative peak area at 0 ppm of PDMS was the target peak area. For the 50% aqueous ethanol exact,

rotary evaporator was applied to remove solvent (both water and ethanol) from the 3ml extract, followed by dissolving the residue using 1 ml CDCl₃ with I.S. The mixture was then analyzed by NMR, and the silicone concentration in the mixture was calculated based on the calibration curve, which equals to three times of the silicone concentration in the 50% aqueous ethanol extracts. The Miglyol 812 final exacts (0.4 ml) was mixed with 0.4 ml CDCl3 with I.S. followed by NMR analysis. Recovery study was performed by adding known amount of PDMS in both food simulants (150 μg/ml in Miglyol 812, 100 μg/ml in 50% aqueous ethanol), followed by same pretreatment and ¹H-NMR analysis as the real sample.

5.4 Results and Discussion

To prepare chitosan-g-PDMS, PDMS-isocyanate (PDMS-NCO) was reacted with chitosan, which was dissolved in 2 wt% acetic acid aqueous solution (pH 4.5). The acidic medium was used because chitosan is water soluble at a lower pH (e.g., 4.5). However, in acidic conditions, the amines of the chitosan should exist in the protonated form, and therefore, we were not certain whether the amines would be available for reaction with PDMS-CNO. As amines are weak bases and their protonation with a weak acid (acetic acid) should be a reversible reaction, we thus contemplated that at any instant, the mixture of acetic acid and chitosan should contain some free amines even at a pH of 4.5. These free amines should react faster with the PDMS-NCO groups than with the OH moieties of the water medium and the chitosan backbone. To demonstrate this, we performed model experiments at pH 5 in acidic water medium between hexamethylene diisocyanate (HDI) and ethanolamine (HOEtNH₂) as well as HDI and ethanol (EtOH), and the reactions were monitored via IR analysis.

Figure 5.1a shows an ATR-FTIR analysis of the reaction between HOEtNH₂ and HDI in acetic acid aqueous medium at pH \sim 5. When HDI (0.3 mL, 0.5 Equiv. of HOEtNH₂) was added,

even after ~1 min, no NCO peak at 2270 cm⁻¹ was observed presumably due to the immediate reaction between amine and NCO. When another batch of HDI was added such that NCO and amine identical molar ratio was achieved, there was almost no change in peak at 2270 cm⁻¹. Interestingly, when further NCO was added in slight excess (0.03 Equvi. more than the amine groups of the HOEtNH₂), a strong peak ~2270 cm⁻¹ corresponding to the unconsumed NCO peak appeared, which confirmed that amine reacts very fast with the NCO even in the acidic aqueous medium. Another identical model reaction was executed between ethanol and HDI to further ensure that ethanol (OH) does not react fast with NCO, and that amine reaction with NCO is the dominant one in the presence of OH groups. The IR analysis for ethanol and HDI are shown in Figure 5.1b. After the addition of half of the amount of NCO with respect to OH of ethanol, even after 25 min of stirring, an intense peak at 2270 cm⁻¹ owing to the NCO was present. The above experiments with model compounds validated the swift reaction between amine and NCO in the acetic-acid aqueous medium. The findings of these model reactions form a strong basis for the grafting of PDMS-NCO onto chitosan in acetic acid-water medium.

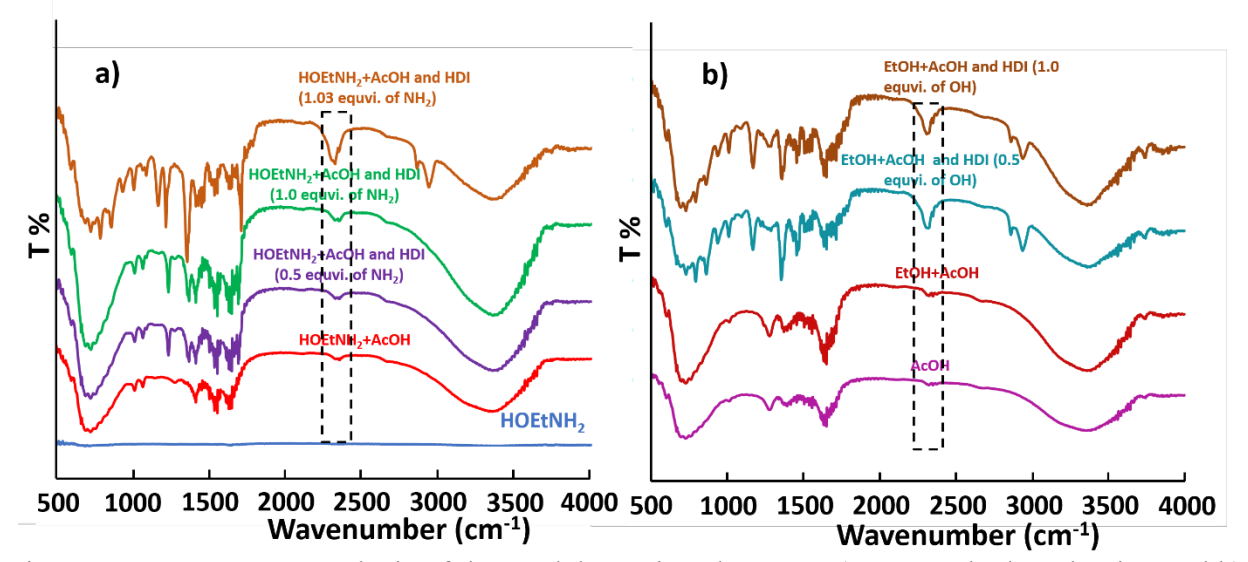


Figure 5. 1 ATR FTIR analysis of the model reactions between a) HDI and ethanolamine and b) HDI and ethanol. In "a", IR is recorded 1 min after the addition of HDI, in "b" IR was recorded after 25 min of the addition of HDI.

The model reactions of HDI with ethanolamine under acidic conditions (pH 4.5) was also studied by ¹H NMR spectroscopy (see **Figure 5.2**). The product of the model reaction ethanolamine and HDI was isolated by extraction with ethyl acetate against water. The peak at ~3.4 ppm for the **CH**₂NCO of the HDI disappeared completely. Similarly, peak at 2.5 ppm for the **CH**₂NH₂ of the ethanolamine also completely disappeared after the reaction. It shows that amine that reacts with the NCO of the HDI rather the OH. New peaks for the product of the model reactions also appeared (see **Figure 5.2C**) for example, the appearance of NH peak of the urea group at ~7.8 ppm. In addition, characteristic peaks for the **CH**₂-NH(CO) also appeared at ~3.0 ppm.

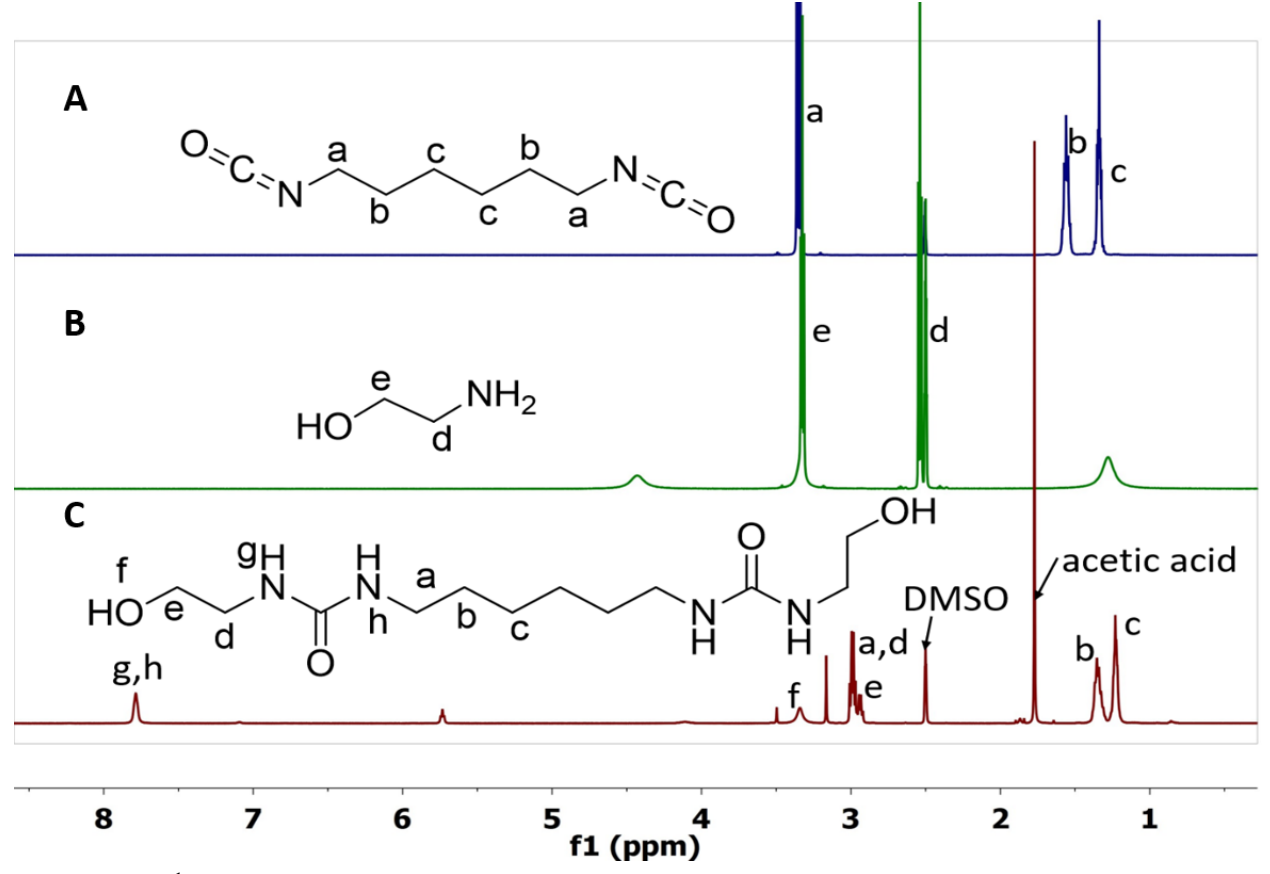


Figure 5. 2 ¹H NMR (recorded in DMSO-d6) of the: A) HDI, B) ethanolamine, and C) product of the urea product of the ethanolamine and HDI.

For the grafting to the chitosan, first PDMS-NCO was prepared by reaction of PDMS-NH₂ with HDIT. While HDIT is a commercial materials with some solvents peaks around 4 ppm, therefore, we utilized HDI, a solvent-free isocyanate, for ¹H NMR spectral analysis. The stoichiometric ratio was adjusted such that 3-time more NCO was used to ensure PDMS is capped with NCO groups. The crude PDMS-NCO was precipitated from acetonitrile. ¹H NMR analysis are shown in **Figure 5.3** for the PDMSNCO and its precursors. It is evident that **CH**₂-NH₂ peak at ~2.65 ppm completely disappeared after reaction with HDI. The characteristic peak for methylene protons (**-CH**₂-NH-CO-NH-**CH**₂-) in the urea linkage as a result of PDMS-NH₂ and NCO reaction, appeared as multiplet at 3.14 ppm. One can also see a peak at 3.3ppm corresponing to the NCO of the PDMS-NCO. Thus, ¹H NMR successfully confirmed the synthesis of PDMS-NCO.

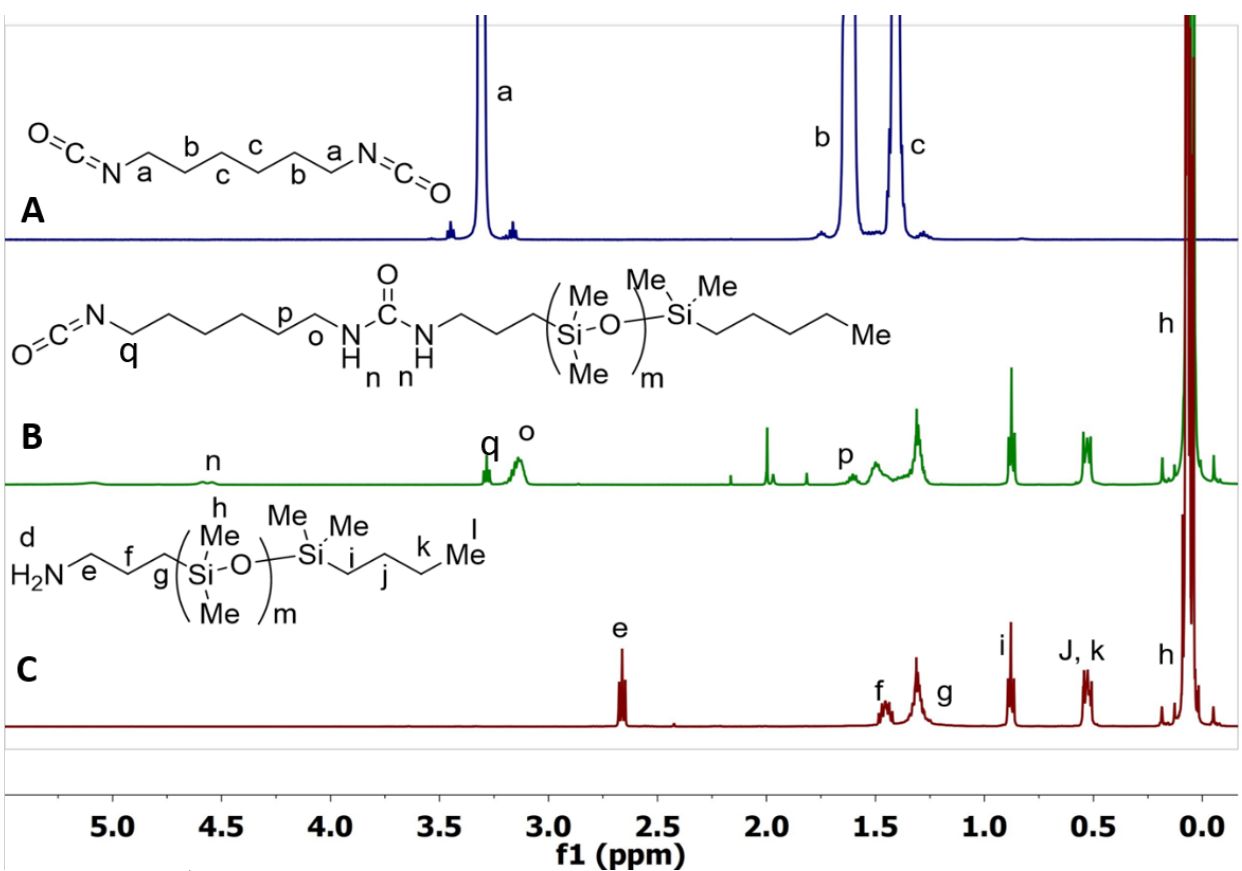


Figure 5. 3 ¹H NMR spectra of PDMS-NH₂ (A), HDI (B), and PDMS-NCO (C) (recorded in CDCl₃).

As the model reactions confirmed that -NH₂ group can react with NCO in aqueous acidic medium (pH ~4.5); therefore the chitosan-g-PDMS samples were synthesized in the water at a pH of 4.5. Using water as reaction solvent for this particular step is indispensable because chitosan is soluble in water at pH ~ 4.5. PDMS-NCO and Chitosan were mixed in different weight ratios (from Table 5.1). The lowest PDMS to chitosan ratio was 1:7 by wt., and the highest was 2:1. ¹H NMR analysis at various stages of the grafting are shown in Appendix A-C. Chitosan shows a prominent peak at ~3 ppm corresponding to the CH-NH₂. After reaction with PDMS-NCO, peak at 2.80ppm corresponding to CH₂ next to the newly formed urea linkage by the reaction of amine (of chitosan) and NCO of (PDMS-NCO). As expected, signal for peak at 2.8 ppm increased when the PDMS amount was increased (see Appendix B). Also, a peak at 3.3 ppm for -H₂C-NCO in PDMS-NCO completely disappeared.

Appendix C depicts representative integrated NMR for the Chitosan-g-PDMS, which was used to determine the PDMS grafting density onto chitosan. Peak areas at 0.1 ppm (owing to CH₃ groups of the PDMS) and the peak area at 3.5-4.0 ppm corresponding to the chitosan CH₂-OH peak were used to quantify the PDMS grafting density in the chitosan-g-PDMS. For example, two methyl groups of PDMS at 0.1 ppm and CH₂-OH (of chitosan peak) at 3.9 ppm have peak areas of 66.8 and 7.4, respectively. Considering the molecular weights of the chitosan D-glucosamine unit and PDMS as 161.2 g/mol and 2,000 g/mol, respectively; we estimated that~ 1 out of 10 amines of the chitosan is grafted with PDMS for the P2C-p graft copolymer.

Chitosan-g-PDMS samples with different PDMS contents were subjected to dynamic light scattering (DLS) characterization to determine their hydrodynamic diameters (D_h). The D_h of chitosan-g-PDMS are shown in Table 5.2. Results showed that chitosan was fully soluble in the medium and therefore no micelles were formed. Meanwhile, aggregated micelles formed after the

addition of PDMS-NCO into the chitosan solution. In addition, the D_h of the micelles grew as the ratio of PDMS increased with respect to chitosan. The formation of micelles was due to the presence of the water-insoluble PDMS chains that were grafted onto the water-soluble chitosan backbone.

Table 5. 2 Hydrodynamic diameters (*D*_h) of chitosan-*g*-PDMS micelles

	С-р	Р0.125С-р	Р0.25С-р	Р0.5С-р	Р1С-р	Р2С-р
D _h (nm)	0	(5.92 ± 0.51) $\times10^{2}$,	(2.25±0.14) ×10 ⁴	(4.83±0.36) ×10 ⁴	$(5.27\pm0.25) \times 10^4$

Water-based solutions of chitosan-g-PDMS were used to coat paper substrates. The thicknesses and basis weights of the coated paper substrates are summarized in Table 5.3. Results showed that the obtained coated-paper essentially had a homogenous coating surface with a small standard deviation for ten replicates. The thicknesses of the coated paper were relatively consistent at $\sim 236~\mu m$. Meanwhile, the coating content in the paper samples ranged between 3.26 and 4.19 g/m² as determined by basis weight analysis.

Table 5. 3 Basis weight, thickness, and coating load of uncoated and coated paper

Sample no.	Material thickness (μm)	Basis weight (g/m²)	Coating loading (g/m²)
U-p	219.8 ± 3.0	147.5 ± 0.2	-
С-р	235.3 ± 3.7	151.1 ± 0.8	3.63 ± 1.0
P0.125C-p	237.7 ± 3.1	151.0 ± 1.5	3.52 ± 1.7
P0.25C-p	236.6 ± 3.0	151.5 ± 1.6	4.04 ± 1.8
P0.5C-p	237.1 ± 3.2	151.2 ± 1.4	3.73 ± 1.6
P1C-p	232.9 ± 3.8	150.8 ± 1.6	3.26 ± 1.8
Р2С-р	235.6 ± 3.2	151.7 ± 2.4	4.19 ± 2.6

ATR-FT-IR analysis was used to confirm the presence of PDMS in the chitosan-*g*-PDMS-coated paper. As shown in **Figure 5.4**, characteristic PDMS peaks at 1257 and 800 cm⁻¹ which respectively corresponded to Si–CH₃ stretching and Si-O-Si bending vibrations were visible in the spectrum of P1C-p,³⁶ thus confirming the presence of chitosan-*g*-PDMS on the coated paper

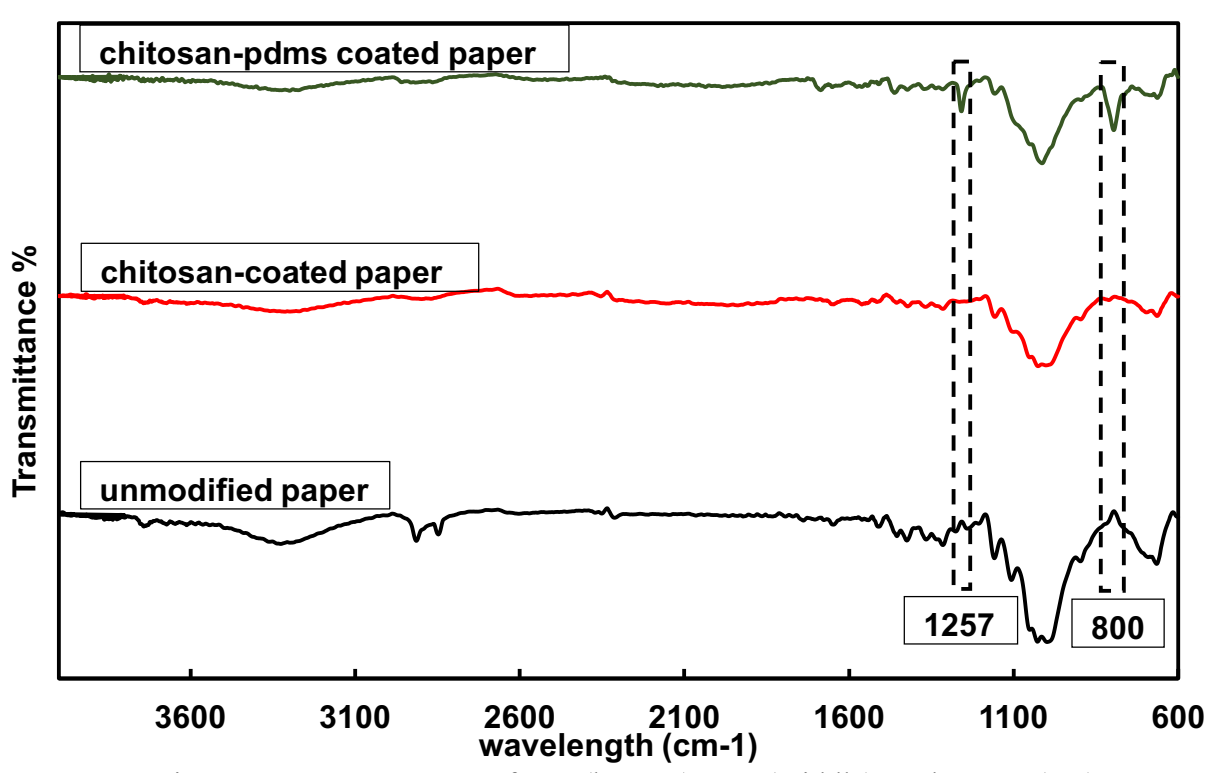


Figure 5. 4 FT-IR spectra of U-p (bottom), C-p (middle), and P1C-p (top).

The coated paper substrates were analyzed for their water resistance using both liquid water and water vapors as probes. Cobb 60 values were determined to evaluate the liquid water resistance, while for the water vapor barrier resistance WVTR measurements were performed (see **Figure 5.5**). The application of the chitosan coating onto paper substrates slightly increased the paper's barrier performance against both liquid water and water vapor in comparison with unmodified paper. For example, approximately 30% and 7.5% reductions in the WVTR and Cobb 60 values were respectively observed for the chitosan-coated paper in comparison with unmodified

paper. These reductions correspond to a reduced porosity in the paper after the application of chitosan coating as chitosan has excellent film-forming properties (see the SEM discussion below). Nevertheless, chitosan bears polar hydroxyl and amine groups that interact with water molecules, which causes the chitosan to swell. Consequently, the swollen film allows water vapors to pass through chitosan coated paper with relatively ease.³⁷ As expected, the chitosan-*g*-PDMS-coated paper offered improved barrier performance against water due to the grafting of the hydrophobic PDMS chains onto the chitosan backbone. For example, the Cobb 60 value decreased significantly to 9.89 g/m² for the P2C-p samples, a decrease of 63.37% from that of unmodified paper. In addition, a significant improvement in the WVTR of 48% in comparison with that of unmodified paper was achieved for sample P0.5C-p, which only contained 50 wt% of PDMS with respect to chitosan.

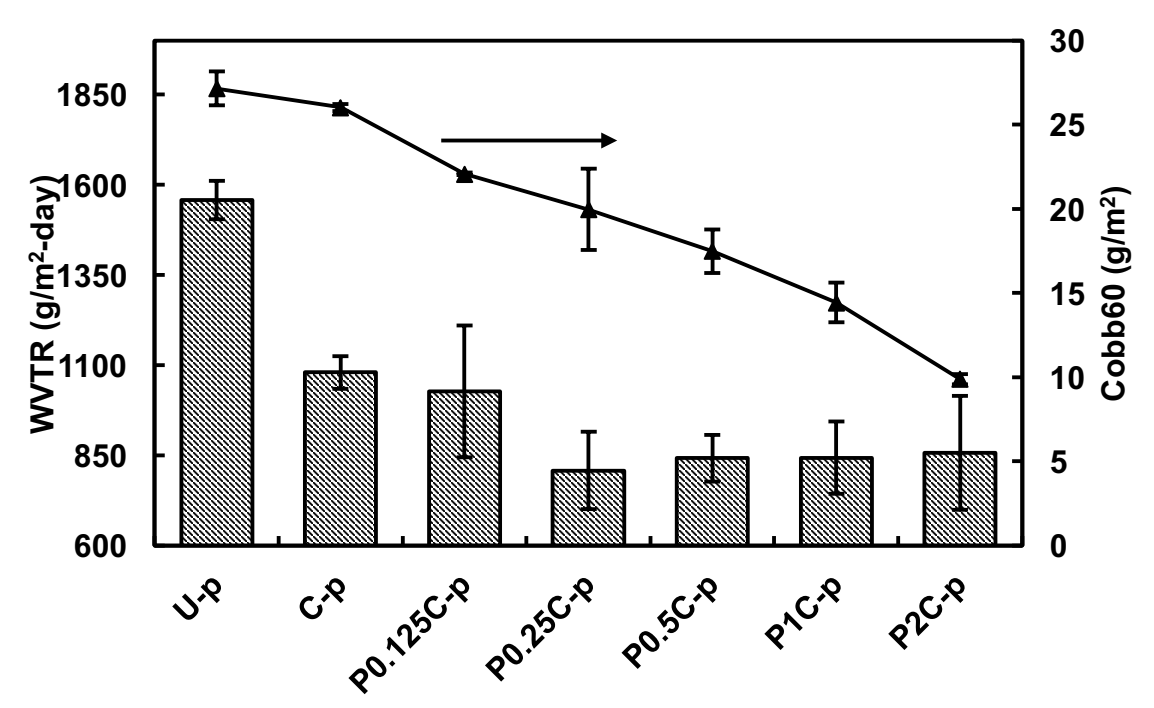


Figure 5. 5 WVTR (g/m²-day) and Cobb 60 values (g/m²) of uncoated paper and coated paper samples. U-p represents uncoated paper and C-p represents chitosan-coated paper. Notations PnC-p (where P denotes PDMS, n denotes the weight of the PDMS with respect to the weight of chitosan in the chitosan-g-PDMS, C represents chitosan, p denotes paper) represent paper coated with chitosan-g-PDMS at different PDMS content in the graft copolymer.

The wettabilities of the coated samples were also evaluated via contact angle (CA) measurements. The CAs of DI water (WCAs) and castor oil (OCAs) after 30 s and 5 min, as well as their sliding angles, are shown in Figure 5.6. The WCA of U-p was initially $103.5 \pm 0.5^{\circ}$ due to the natural roughness of the cellulose substrate, but this value quickly decreased to $81.4 \pm 2.9^{\circ}$ after 5 min due to the diffusion of water into the paper substrate, indicating that the U-p sample lacked water-resistance. The chitosan coating rendered minor water resistance to the paper substrate and a WCA of $100.0 \pm 1.9^{\circ}$ was observed, which decreased by 10° after 5 min. However, when chitosan-g-PDMS was applied as the coating, the water droplets remained on the surface to exhibit stable and higher WCAs. The WCAs initially became larger as the ratio of PDMS in the chitosan-g-PDMS copolymer increased. The maximum WCA among the coated samples was $120.5 \pm 1.0^{\circ}$ for paper samples coated with P0.5C-p. It is noteworthy that paper coated with much higher PDMS content in the graft copolymers showed a slight decrease in their WCAs, which was likely due to the smoother surface caused by the liquid-like nature of the PDMS chains on the surface. Smooth surfaces exhibit smaller contact angles relative to their rough counterparts because the contact angle is strongly dependent on the surface texture, ³⁸ as has been validated by SEM characterization and will be discussed later in this article. The corresponding sliding angles for various uncoated and coated the paper samples were recorded and are shown in Figure 5.6 (a). The sliding angles tests showed that water droplets readily slid off the paper samples coated with chitosan-g-PDMS without leaving any marks or trails. Meanwhile, water droplets wet the surfaces of unmodified and the chitosan-coated paper, and sliding water droplets left marks on these surfaces due to their hydrophilic nature.

To determine the oil resistance of the coated paper substrates, OCA and sliding angles, as well as the "kit rating" values of various samples were determined as shown in **Figures 5.6 (b)**

and 5.7, respectively. Higher OCAs and lower sliding angles were obtained for chitosan-g-PDMS-coated paper samples relative to the uncoated and chitosan-coated paper. For example, the OCA for P0.5C-p was $62.73 \pm 0.49^\circ$, which remained stable with the passage of time. Meanwhile, the initial OCA of $32.67 \pm 0.28^\circ$ observed on chitosan-coated paper decreased as oil began to stick and permeate into the chitosan-coated paper. Also, the sliding angles for the chitosan-g-PDMS were significantly improved. For example, P0.5C-p showed sliding angles of $12.33 \pm 0.58^\circ$, while the chitosan-coated paper had a sliding angle of $22.67 \pm 0.58^\circ$. It is noteworthy that the castor oil left a mark on the chitosan-coated paper. Thus, the chitosan-g-PDMS-coated paper only exhibited resistance against water and oil.

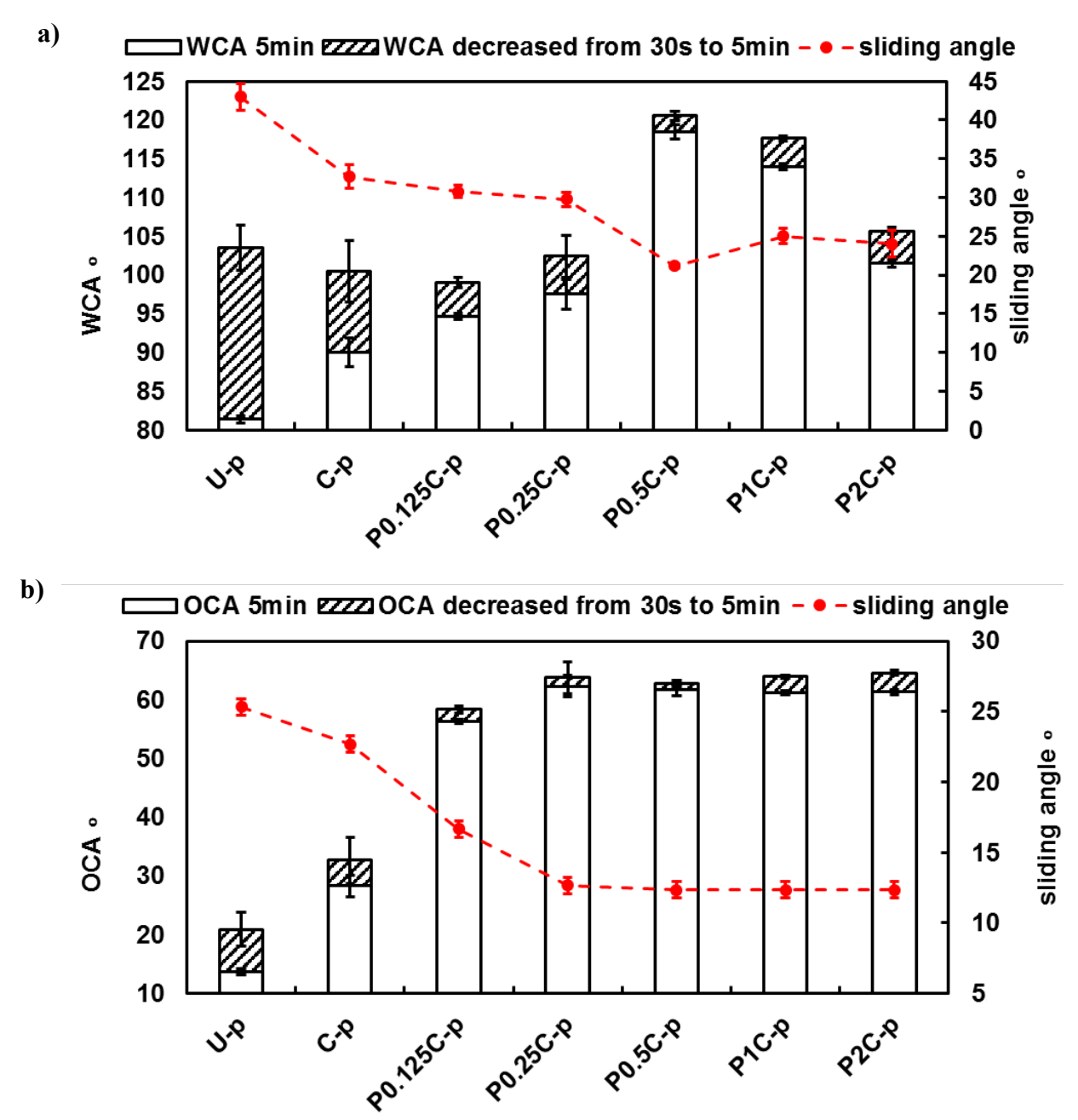


Figure 5. 6 Sliding angles and CAs (after 30 s and 5 min) of: a) water and b) castor oil. For the uncoated as well as the chitosan-coated paper, water slides on these surfaces but leaves a mark behind.

The "kit ratings" were also determined for the various coated substrates to determine the oil-resistance. A kit rating of "12" represents the maximum oil resistance while a rating of "0" indicates a lack of such resistance. The kit rating for C-p was 7.6/12, which had increased to essentially the maximum 11.7/12 for the chitosan-g-PDMS-coated paper. This improvement strongly demonstrated the high oil-resistance of the chitosan-g-PDMS-coated substrates.

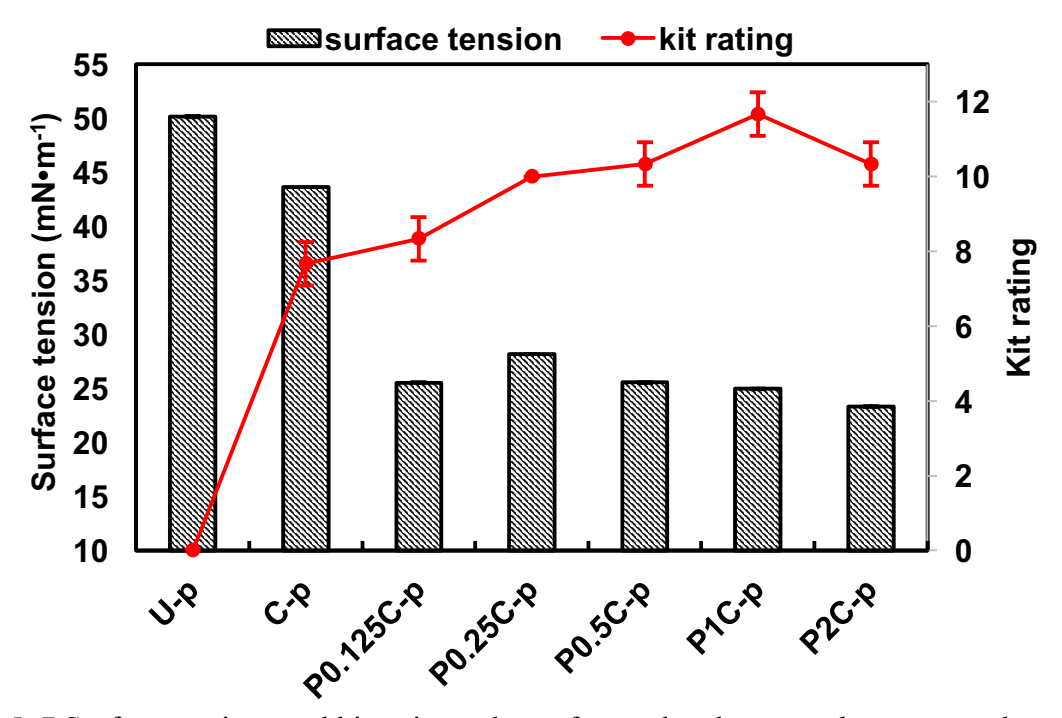


Figure 5. 7 Surface tensions and kit rating values of coated and uncoated paper samples. A kitrating of 12 corresponds to the maximum oil-resistance.

As the surface wettability of a substrate is strongly dependent on its surface energy; therefore, we determined the surface free energies of various coated paper samples as shown in **Figure 5.7**. The surface energy decreased dramatically for the chitosan-*g*-PDMS-coated paper compared to the uncoated and the chitosan-coated paper. For example, the surface energies decreased to 23 mN/m for the P2C-p-coated samples, which is consistent with the surface energy of PDMS (~ 22 mN/m). As cooking oils have surface energies greater than 31 mN/m,³⁹ which

exceeds that of the chitosan-*g*-PDMS coating (surface energy 23 mN/m),³⁶ thus the low surface energy of the coated paper imparted oil-resistance to the paper substrates.

To explore the effect of porosity on the water- and grease-resistance of the coated paper, the surface features of U-p, C-p, and P-C-p samples were explored via SEM (**Figure 5.8**). The rough texture arising from the cellulose fibers can be seen in the unmodified paper, whereas the chitosan-coated paper lacks the void spaces between these fibers thanks to the excellent film-forming properties of the chitosan. As expected, like chitosan-coated paper, pores and voids were also absent from the surface of the chitosan-g-PDMS-coated paper sample, again because the chitosan had filled the paper's pores.

TGA analysis of U-p, P1C-p, and chitosan-coated samples are shown in Appendix D. Results indicated that the decomposition of the paper substrate occurred between 200 and 400 °C (Appendix D, **Figure A-4a**), and the decomposition of chitosan films shows two regions of weight loss. First weight loss corresponding to the removal of acetic acid took place in the range of 130-190 °C, and the second weight loss corresponding to chitosan polymer degradation took place in the range of 220-400 °C as shown in **Figure A-4c** (Appendix D). Meanwhile, the peak between 440 and 560 °C for P1C in Figures 9c and 9d was due to the thermal decomposition of PDMS. TGA confirmed the good thermal stability of the coated paper. The coating loading was also calculated based on the differences in the percent (%) losses at each decomposition stage from Appendix D. Results revealed that the samples had a low coating loading of ~3 wt%, which was consistent with the results obtained from the basis weight approach using a microbalance.

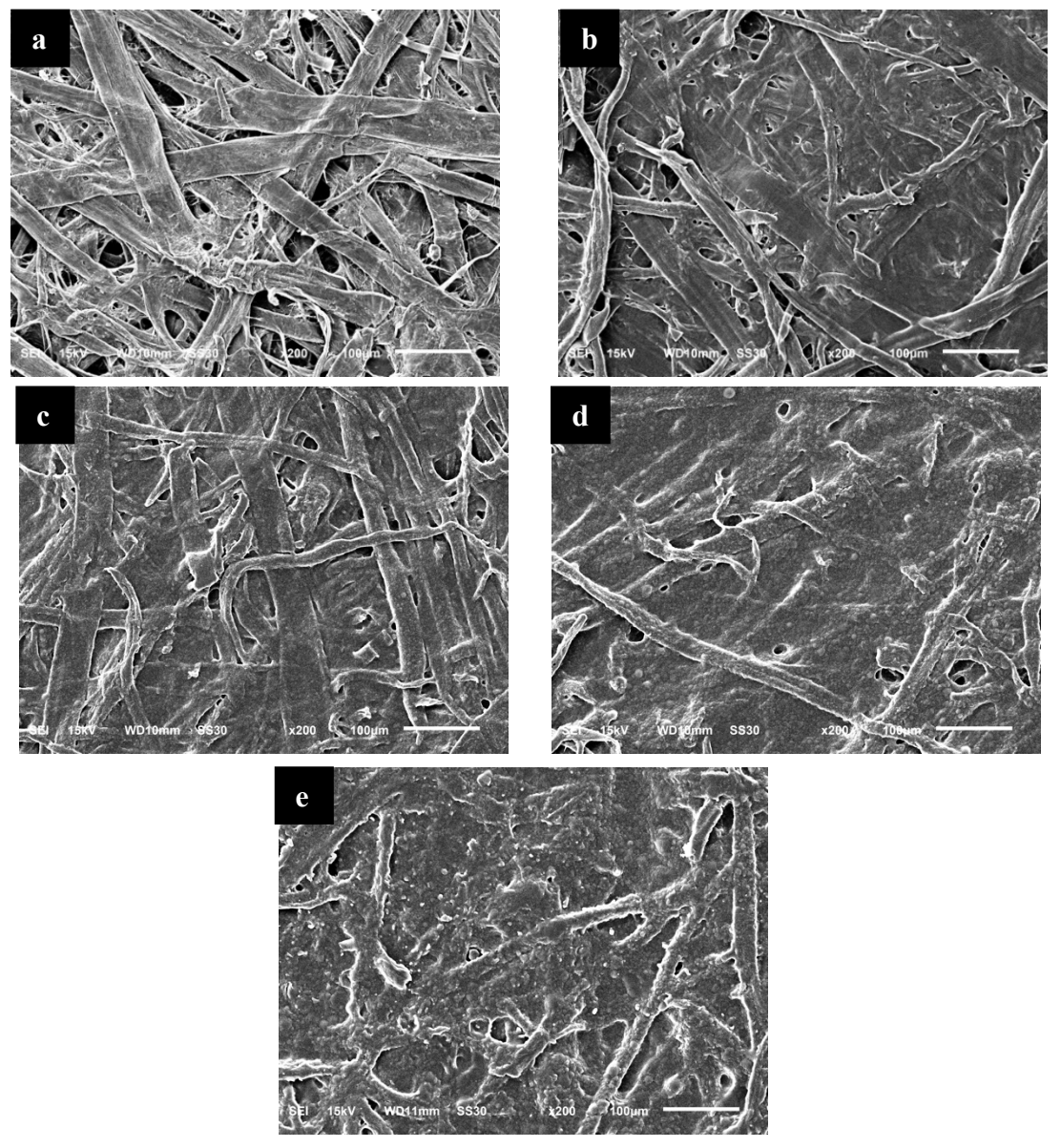


Figure 5. 8 SEM images (200×) of unmodified paper U-p (a), chitosan-coated paper C-p (b), and chitosan-g-PDMS-coated paper, including P0.5C-p (c), P1C-p (d), and P2C-p (e).

To explore the effect of the coating on the paper's mechanical properties, we measured the tensile strength (TAPPI T494), ring crush test (TAPPI T822), bending stiffness (TAPPI T489), and internal tearing resistance (TAPPI T414) of various paper samples as shown in **Figure 5.9**. Results indicated that the tensile strength, bending stiffness, and internal tearing resistance were slightly improved for the coated paper with respect to the uncoated paper. For example, the tensile strength in the cross-direction for the uncoated paper was 32 lbs/in, while the corresponding value

for the P0.25C-P sample was 36 lbs/in. The ring crush test (RCT) values remained essentially unchanged for the unmodified and chitosan-*g*-PDMS-coated paper. For example, U-p had an RCT value of 70 lbs, while the corresponding value for P0.25C-P was 69 lbs. Overall, the changes in the mechanical properties were minimal. Consequently, the coated paper is a promising candidate for practical applications as its desirable mechanical properties were retained.

The greatest challenge with water- and/or oil-resistant paper that is prepared from wax, latex, and synthetic polymers is the separation of paper pulp from the coating materials due the course of pulp recovery. For example, the presence of wax/latex/plastic impurities in the recycled pulp causes weakening of the mechanical properties and imparts the recycled paper with an uneven surface. Therefore, coated/laminated paper is typically sent to landfills (and also ends up in the ocean due to windstorms and floods), resulting in the waste of precious pulp and creating environmental pollution that threatens our ecosystems and human health. As our coating strategy does not involve any chemical modification of the paper itself, we thus anticipated that chitosang-PDMS could be readily separated from the pulp during the repulping process. With these considerations in mind, we evaluated the recyclability of the pulp from the coated paper (see Scheme 5.2). The ATR-FT-IR spectra of paper samples made from repulped fibers show that most of the PDMS was removed after the repulped paper had been washed (see Figure 5.10). Meanwhile, the use of acetic acid (0.1 %v/v acetic acid) to wash the pulp of the coated paper resulted in complete removal of the coating from the paper as demonstrated by the absence of signals at 1257 and 800 cm⁻¹. It is noteworthy that the chitosan-g-PDMS, which is separated from paper pulp can be recovered by neutralizing the chitosan and thus precipitating it from the water.

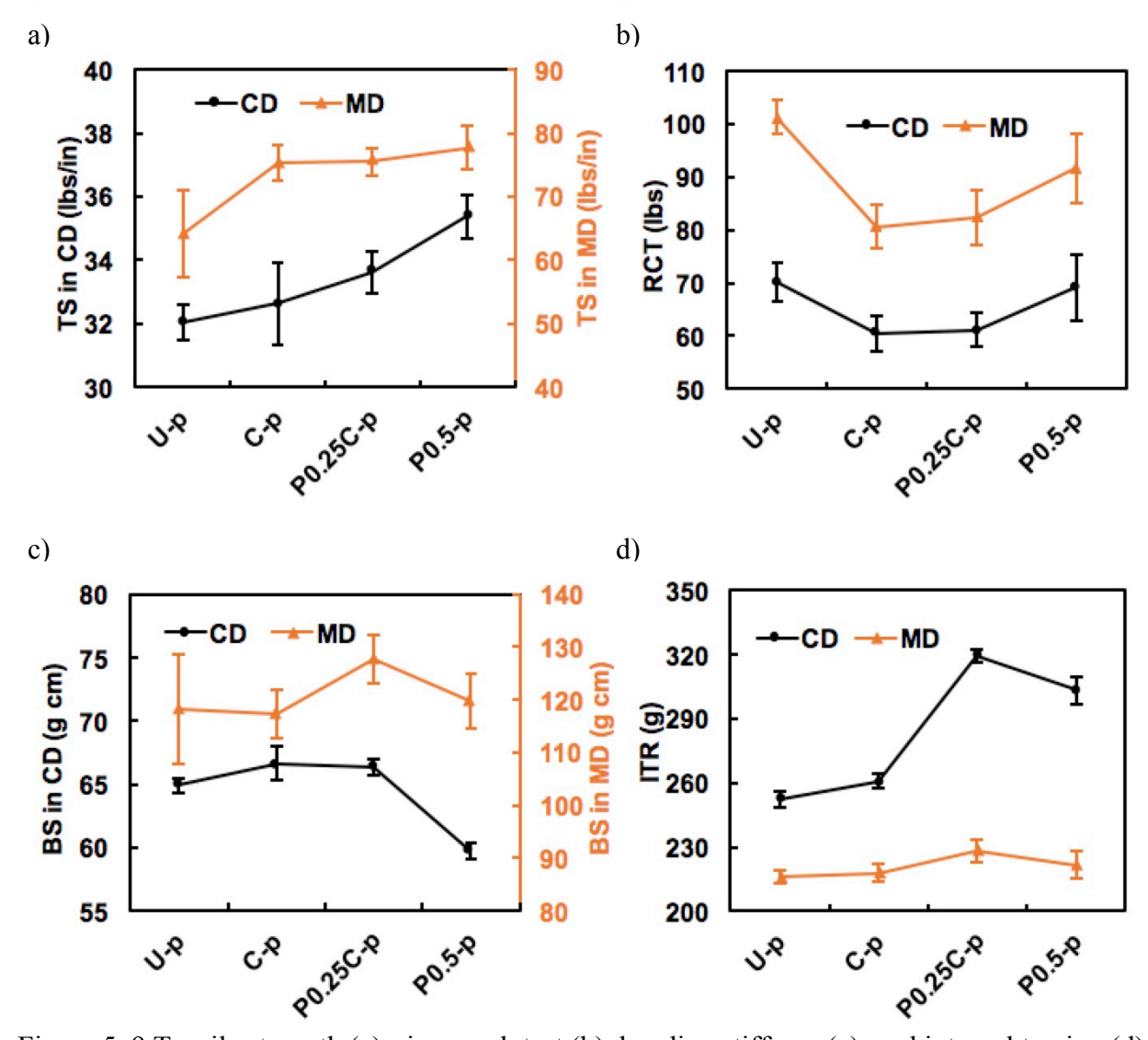


Figure 5. 9 Tensile strength (a), ring crush test (b), bending stiffness (c), and internal tearing (d) of uncoated paper (U-p), and coated paper (C-p, P0.25C-p, and P0.5C-p).



Scheme 5. 2 Illustration of the pulp recycling process for the coated paper.

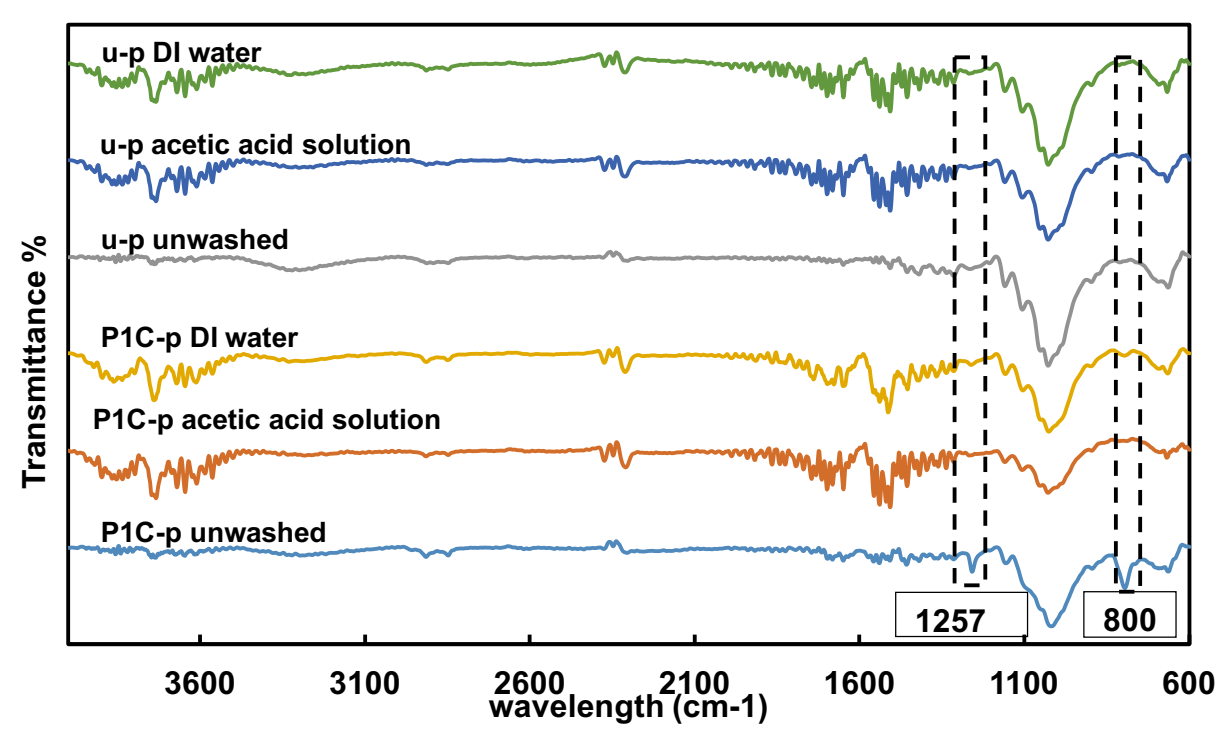


Figure 5. 10 FT-IR spectra of paper samples prepared from unwashed U-p as well as P1C-p fibers and fibers that had been washed with DI water and acetic acid solutions.

For the migration studies, first, the accuracy of NMR was determined for the PDMS quantification via developing a calibration curve as shown in Figure 5.11. This calibration curve denotes the relationship between the concentration of PDMS and the peak area at 0.0 ppm. The peak area at 0 ppm corresponds to the methyl peaks in PDMS. The calibration curve confirms that PDMS can be accurately quantified down to \sim 3 µg/mL. Then the concentration of PDMS in food simulants including 50% aqueous ethanol and Miglyol 812 after 10 days under 40 °C is shown in Figure 5.12. Results show that a higher concentration of PDMS was obtained in food simulant Miglyol 812 due to the nonpolar structure of PDMS, indicating that PDMS is easier to migrate to fat food substances. Interestingly, PDMS peaks were found for the blank control, which is considered as the siloxane from the environment. Migration never exceeded 46.19 µg/ml (7.16 mg/dm²) which is below the overall migration limit 60 mg/kg food (100 mg/dm²) by the Council of Europe's Resolution AP (2004) ⁴⁶.

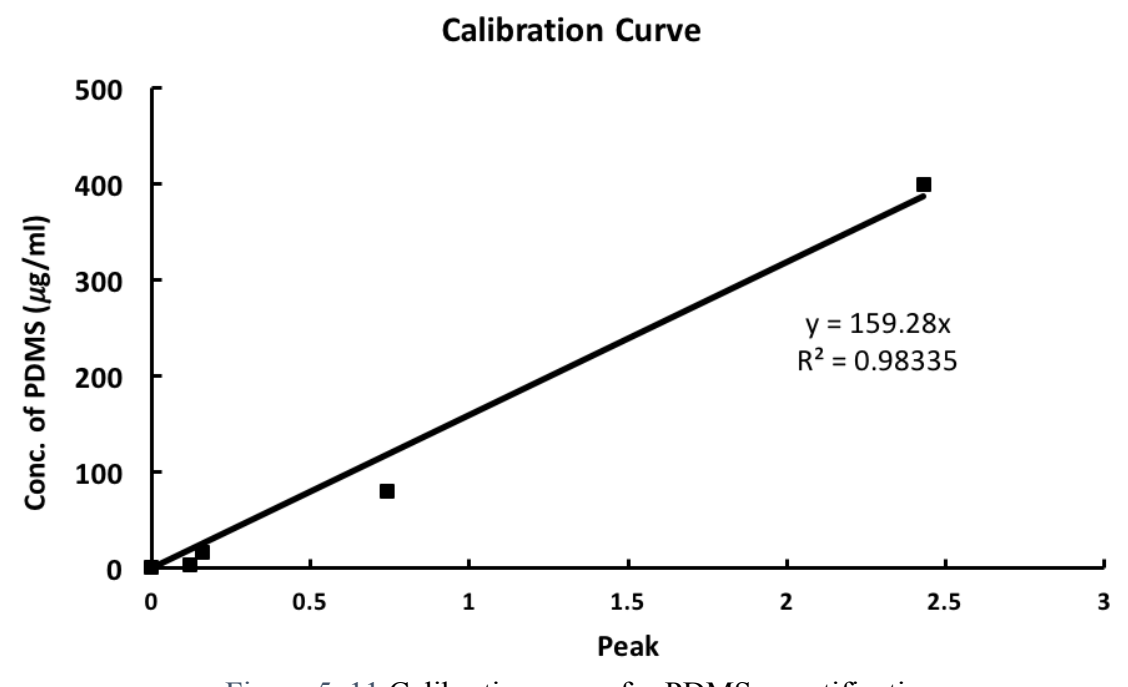


Figure 5. 11 Calibration curve for PDMS quantification

Table 5. 4 Analytical parameters of H1-NMR determination of PDMS in 50% aqueous ethanol and miglynol

Calibrated Range	μg/mL	3.2-400
Coefficient of determination r ²		0.9835
Recovery rate		
50% aqueous ethanol	%	90.29 ± 8.67
Miglyol 812	%	105.86 ± 6.59
LOD(S/N=3)		
50% aqueous ethanol	μ g/mL	4.01
Miglyol 812	μ g/mL	2.76
LOQ (S/N=9)		
50% aqueous ethanol	μ g/mL	12.03
Miglyol 812	μ g/mL	8.28

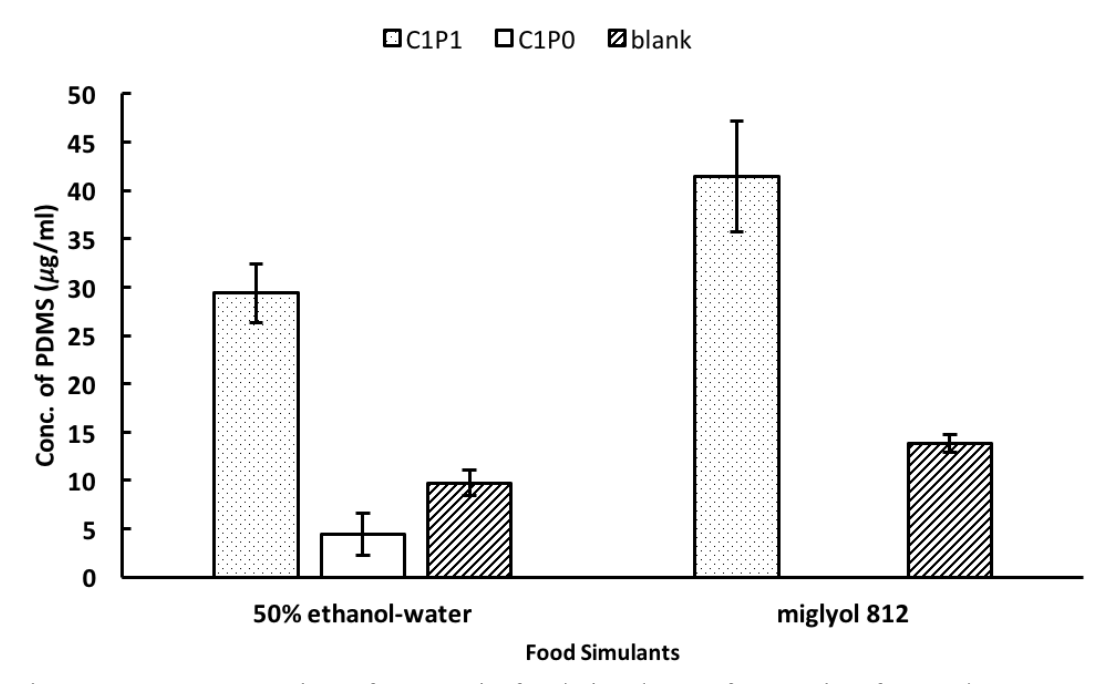


Figure 5. 12 Concertation of PDMS in food simulants after storing for 10 days at 4 °C.

Our coating materials are also environmentally friendly. For example, the biodegradability of chitosan and paper is well-known. In our case, samples P0.125C-p, P0.25C-p, P0.5C-p are biodegradable by the standard ASTM definition because their PDMS content is ≥ 1 wt%,

considering the 3 wt% total coating content that was used to fabricate these paper samples. Materials with 1 wt% of non-biodegradable component (in this case PDMS) contents no greater than 1 wt% are exempted from testing requirements for individual biodegradability.⁴⁴ Thus, our unique approach yields products that are not only recyclable but also biodegradable.

This coated paper has potential applications in both the packaging and non-packaging industry. The materials have been selected such that they are well-suited for food packaging. For example, PDMS copolymers in combination with other food safe additives such as polyoxyethylene (e.g., polyoxyethylene-*graft*-polydimethylsiloxanes) are considered to be safe for use in food contact applications.⁴⁵ In our case, we are using chitosan instead of polyoxyethylene, and chitosan is food safe and is, in fact, an edible polymer.

5.5 Conclusions

In summary, we have developed a unique approach for creating water- and oil-resistance paper that is fully recyclable. The coated paper has good water-resistance as confirmed by their WCA of $120.53 \pm 0.96^{\circ}$ and a Cobb 60 value of 9.89 ± 0.32 g/m². The coated paper also has good water vapor barrier properties, which were improved by 48.1% relative to uncoated paper. The coated paper has good oil-resistance as demonstrated by its OCA of 64.5° , and kit rating of 11.67/12. The desirable water- and oil-resistance can be attributed to the low surface energy of the coated paper and the masking of the pores by chitosan. SEM analysis confirmed that the voids and pores of the paper disappeared after coating treatment. The mechanical properties of the coated paper remained essentially matched or even exceeded that of the uncoated samples. The recyclability of the pulp from the coated paper was also confirmed via repulping and washing tests, which also validated this method as a closed-loop approach. The overall migration of siloxanes into 50% aqueous ethanol solution and Miglyol 812 never exceeded $46.19 \,\mu g/ml$ ($7.16 \,mg/dm^2$),

which is well below the overall migration limit 60 mg/kg food (100 mg/dm²) by the Council of Europe's Resolution AP (2004). This study offers significant contribution to the field of Green Chemistry by preventing pollution (e.g., the coated paper is repulpable), by offering safer chemicals for coating, by replacing existing harmful fluorinated chemicals, and utilizing renewable chitosan as feedstock. This Considering the facile coating approach and recyclability of the coated paper, this strategy has excellent applicability for real-world scenarios, thus providing benefits to the packaging and non-packaging sectors, as well as the environment.

APPENDICES

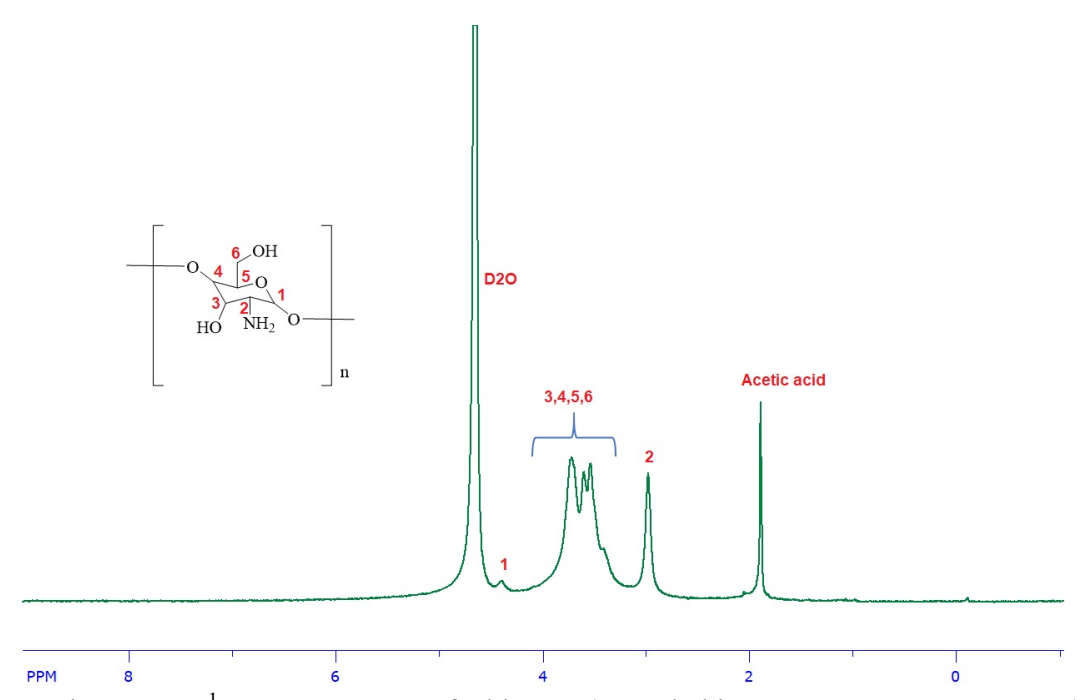


Figure A- 1 ¹H NMR spectra of Chitosan (recorded in D₂O at 2wt% CD₃COOD).

APPENDIX B: ¹H NMR spectra of Chitosan-g-PDMS, Chitosan and PDMS-NCO using D2O with 2wt% CD₃COOD

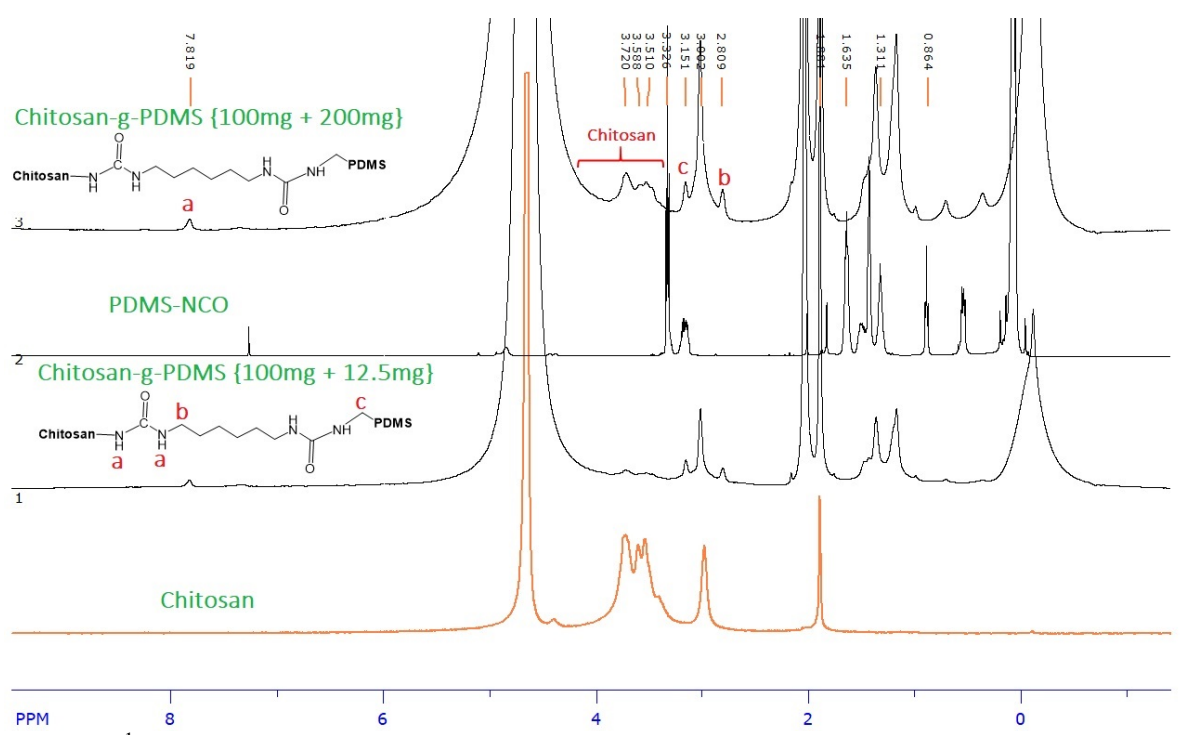


Figure A- 2 ¹H NMR spectra of Chitosan-g-PDMS, Chitosan and PDMS-NCO using D2O with 2wt% CD₃COOD.

APPENDIX C: ¹H NMR spectra of Chitosan-g-PDMS (after extraction) using D2O with 2wt% CD₃COOD.

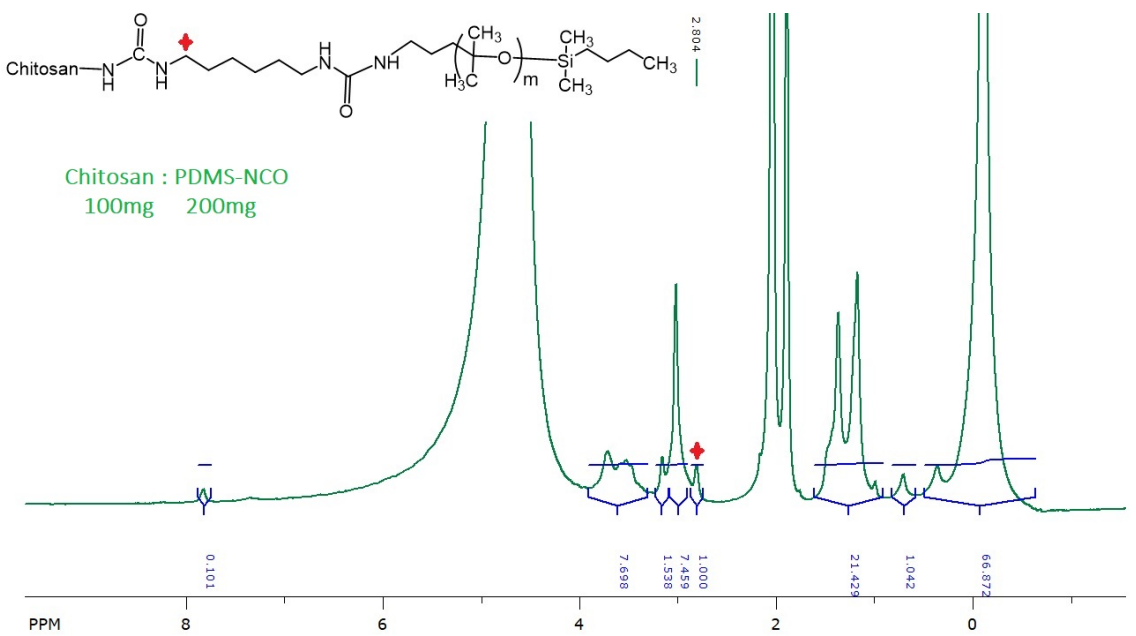


Figure A- 3 ¹H NMR spectra of Chitosan-g-PDMS (after extraction) using D2O with 2wt% CD₃COOD.

APPENDIX D: ¹H NMR spectra of Chitosan-g-PDMS (after extraction) using D2O with 2wt% CD₃COOD.

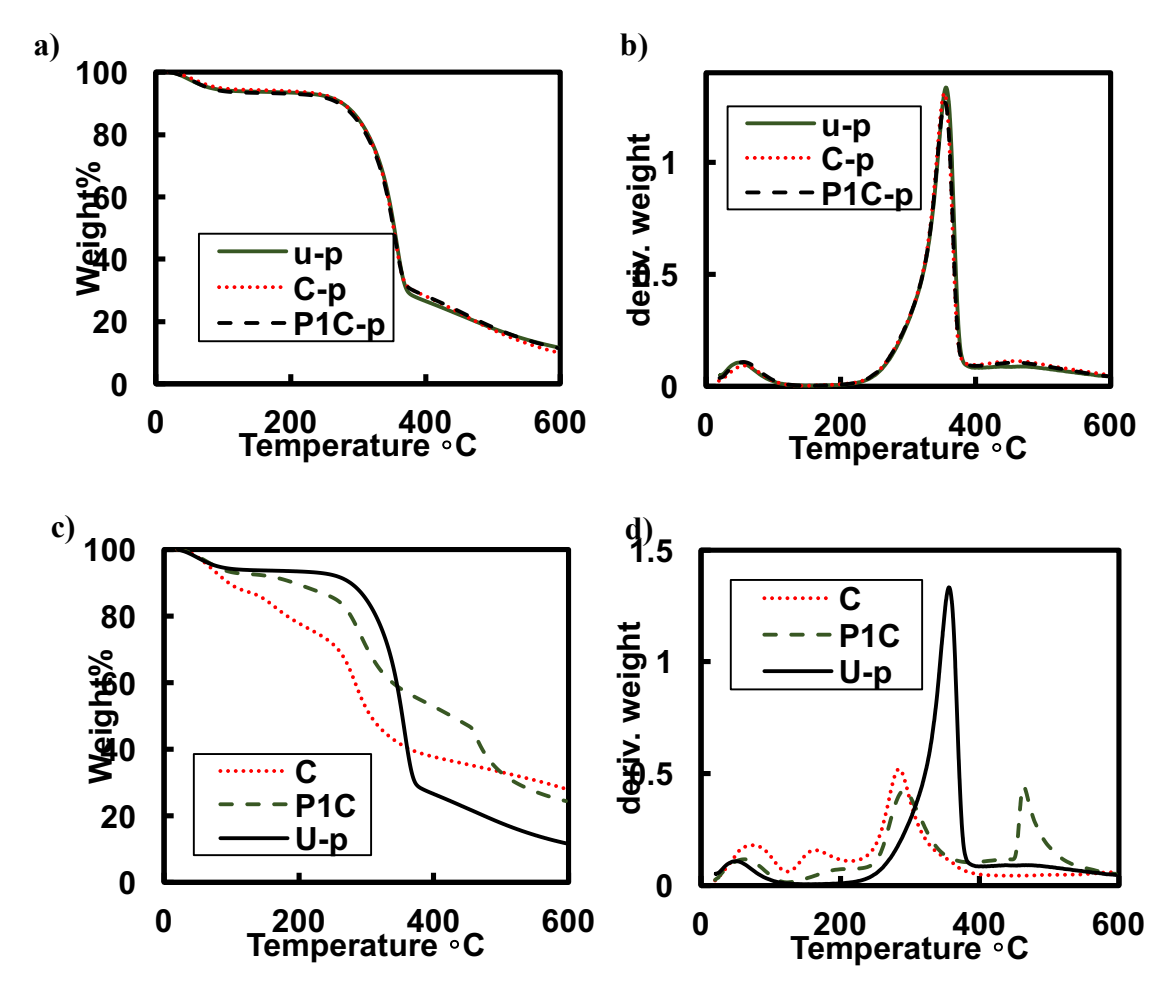


Figure A- 4 TGA (a) and DTG (b) plots of uncoated paper (U-p) and coated paper (C-p and P1C-p). Also shown are TGA (c) and DTG (d) plots of the chitosan coating (C), P1C coating (P1C), and unmodified paper (U-p)

REFERENCES

REFERENCES

- 1. V. Rastogi and P. Samyn, *Coatings*, 2015, **5**, 887-930.
- 2. C. Andersson, *Packag. Technol. Sci.*, 2008, **21**, 339-373.
- 3. J. Shen, P. Fatehi and Y. Ni, *Cellulose*, 2014, **21**, 3145-3160.
- 4. C. Dang, M. Xu, Y. Yin and J. Pu, *Bioresource*, 2017, **12**, 14.
- 5. *United States Pat.*, WO2005014283A1, 1987.
- 6. Municipal Solid Waste, https://archive.epa.gov/epawaste/nonhaz/municipal/web/html/index.html, (accessed 1-14, 2019).
- 7. R. Geyer, J. R. Jambeck and K. L. Law, *Sci. Adv.*, 2017, **3**, e1700782.
- 8. I. Wyman, R. Aurasto ensure further and S. Cheng, *Green Chem.*, 2017.
- 9. M. Rabnawaz, I. Wyman, R. Auras and S. Cheng, *Green Chem.*, 2017.
- 10. B. Shoot, EU Parliament Votes to Ban Single-Use Plastics, Including Plates, Cutlery, and Straws, http://fortune.com/2018/10/24/eu-ban-single-use-plastic-pollution/, (accessed 4-2, 2019).
- 11. D. I. Lee, in *Polymeric Dispersions: Principles and Applications*, ed. J. M. Asua, Springer Netherlands, Dordrecht, 1997, DOI: 10.1007/978-94-011-5512-0_32, pp. 497-513.
- 12. Y. Du, Y.-H. Zang and J. Du, *Ind. Eng. Chem. Res.*, 2011, **50**, 9781-9786.
- 13. A. Scott, Chem. Eng. News, 2019, **97**.
- 14. C. Ostiguy, B. Soucy, G. Lapointe, C. Woods, L. Ménard and M. Trottier, *Health Effects of Nanoparticles*, Institut de recherche Robert-Sauvé, Montréal 2008.
- 15. *United States Pat.*, US20080176015A1, 2007.
- 16. *United States Pat.*, AU2007212477B2, 2014.
- 17. European Pat., EP 2913361 A1, 2015.
- 18. J. A. Heredia-Guerrero, J. J. Benítez, P. Cataldi, U. C. Paul, M. Contardi, R. Cingolani, I. S. Bayer, A. Heredia and A. Athanassiou, *Ad. Sustain. Syst.*, 2017, **1**, 1600024.
- 19. C. Guillaume, J. Pinte, N. Gontard and E. Gastaldi, *Food Res. Int.*, 2010, **43**, 1395-1401.
- 20. J. Han, S. Salmieri, C. Le Tien and M. Lacroix, *J Agric. Food. Chem.*, 2010, **58**, 3125-3131.

- 21. M. Khanzadi, S. M. Jafari, H. Mirzaei, F. K. Chegini, Y. Maghsoudlou and D. Dehnad, *Carbohydr. Polym.*, 2015, **118**, 24-29.
- 22. J.-W. Rhim, J.-H. Lee and S.-I. Hong, *LWT Food Sci. Technol.*, 2006, **39**, 806-813.
- 23. V. Morillon, F. Debeaufort, G. Blond, M. Capelle and A. Voilley, *Crit. Rev. Food. Sci. Nutr.*, 2002, **42**, 67-89.
- 24. R. Sothornvit, Food Res. Int., 2009, 42, 307-311.
- 25. C. Tambe, D. Graiver and R. Narayan, *Prog. Org. Coat.*, 2016, **101**, 270-278.
- 26. X. Trier, K. Granby and J. H. Christensen, *Env. Sci. Pollut. Res.*, 2011, **18**, 1108-1120.
- 27. S. Vaswani, J. Koskinen and D. W. Hess, Surf. Coat. Technol., 2005, 195, 121-129.
- 28. A. K. Rosenmai, C. Taxvig, T. Svingen, X. Trier, B. Vugt-Lussenburg, M. Pedersen, L. Lesné, B. Jégou and A. Vinggaard, *Andrology*, 2016, **4**, 662-672.
- 29. X. Zhang, H. Wang, Z. Liu, Y. Zhu, S. Wu, C. Wang and Y. Zhu, *Appl. Surf. Sci.*, 2017, **396**, 1580-1588.
- 30. C. Xing, T. He, Y. Peng and R. Li, *J. Appl. Polym. Sci.*, 2018, **135**, 46358.
- 31. European Pat., EP1911801A2, 2017.
- 32. Y. Li, X. Men, X. Zhu, B. Ge, F. Chu and Z. Zhang, *J. Mater. Sci.*, 2015, **51**, 2411-2419.
- 33. E. H. I. J. Brandrup, Polymer Handbook, Wiley, New and York.
- 34. M. Rabnawaz, G. Liu and H. Hu, *Angew. Chem.*, 2015, **127**, 12913-12918.
- 35. Z. Li and M. Rabnawaz, *ACS Omega*, 2018, **3**, 11909-11916.
- 36. Z. Li and M. Rabnawaz, ACS Appl. Polym. Mater., 2018, DOI: 10.1021/acsapm.8b00106.
- 37. W. Zhang, H. Xiao and L. Qian, *Carbohydr. Polym.*, 2014, **101**, 401-406.
- 38. M. T. Khorasani, H. Mirzadeh and Z. Kermani, *Appl. Surf. Sci.*, 2005, **242**, 339-345.
- 39. S. N. Sahasrabudhe, V. Rodriguez-Martinez, M. O'Meara and B. E. Farkas, *Int. J. Food Prop.*, 2017, DOI: 10.1080/10942912.2017.1360905, 1-17.
- 40. G. Cardenas and S. P. Miranda, *J. Chil. Chem. Soc.*, 2004, **49**, 291-295.
- 41. H. Liu, Z. Wei, M. Hu, Y. Deng, Z. Tong and C. Wang, *RSC Adv.*, 2014, **4**, 29344-29351.
- 42. M. Rinaudo, *Prog. Polym. Sci.*, 2006, **31**, 603-632.

- 43. American Society for Testing and Materials, 2012, **D6400**.
- 44. Safe Drinking Water and Toxic Enforcement Act of 1986, http://leginfo.legislature.ca.gov/faces/codes_displayText.xhtml?lawCode=HSC&division=20.&title=&part=&chapter=6.6.&article, (accessed Jan -14, 2019).
- 45. *Code of Federal Regulatons*, 2012, **Title 21**.
- 46. R. Helling, A. Mieth, S. Altmann and T. J. Simat, Food Addit. Contam., 2009, 26, 395-407.

CHAPTER 6: RESPONSE SURFACE METHODOLOGY DESIGN FOR BIOBASED AND SUSTAINABLE COATINGS FOR WATER- AND OILRESISTANT PAPER

A version of this chapter is published as:

Li, Z.; Rabnawaz, M.; Khan, B. Response Surface Methodology Design for Biobased and Sustainable Coatings for Water- and Oil-Resistant Paper, ACS Applied Polymer Materials. **2020**, 2, 1378-1387. DOI: doi.org/10.1021/acsapm.9b01238

6.1 Abstract

Reported herein is the synthesis of biobased and sustainable chitosan-*graft*-castor oil (CHI-*g*-CO) copolymer that can be used for paper coating. CHI-*g*-CO was obtained via chemical grafting of castor oil-capped-isocyanate (CO-capped-NCO) onto a chitosan polymer backbone. The CHI-*g*-CO copolymer was then employed as a waterborne coating for Kraft unbleached paper to render the coated paper both water- and oil-resistant. The formulation of the CHI-*g*-CO-coated paper was optimized using the Response Surface Methodology. The oil- and water-resistance of the coated paper substrates were determined via kit rating measurements and Cobb60 value tests, respectively. Water and oil contact angles were also determined for the coated paper. In addition, the water vapor permeability and mechanical properties of the coated paper were evaluated. Scanning electron microscopy (SEM) was also used to evaluate the effect of the coating on the microstructures and the porosity of the paper. Considering the biobased nature of the coating materials (e.g., chitosan and castor oil), this fabrication strategy can offer an environmental-friendly, sustainable, and economical approach toward water- and oil-resistant paper.

Keywords: castor oil, water resistance, oil-resistant surfaces, paper, PFAS-free

6.2 Introduction

Paper is comprised of hydrophilic lignocellulose fibers that are derived from wood pulp and has been used for a broad range of applications since its invention. In comparison with conventional plastics, with the exception of some aliphatic polyesters, ¹⁻³ paper is biodegradable and is thus an excellent option for numerous applications from an environmental perspective. However, paper absorbs water and oil due to its hydrophilic lignocellulose-based composition and porous structure. Conventional methods that are used to improve the water-resistance of paper substrates involves paper lamination with synthetic polymers such as low-density polyethylene.⁴

Paper substrates are also commonly coated with wax in order to improve their water-resistance.⁵⁻⁶ However, the recyclability of laminated- and waxed-paper is limited due to the challenges encountered with the separation of laminates/coatings from the paper substrates, and hence these materials typically end up in landfills. According to the U.S. Environmental Protection Agency (EPA),⁷ the recycling rate for mixed paper containers/packaging was only 26.4% in 2015, which was significantly lower than the overall paper recycling rate in that year (68%).⁸

Latexes are polymer particles that are dispersed in water, which have been used as paper coatings. However, latexes are becoming a source of plastic pollution in marine environments (i.e., "microplastics") due to the persistence of these non-degradable polymer particles in the ocean, as they can enter into the human food chain through seafood. Another approach for fabricating water- and oil-resistant paper is the use of per- and poly(fluoroalkyl) substances (PFAS). The low surface energies of PFAS impart the coated paper with excellent water- and oil resistance, and hence these materials are used in food packaging. However, the persistence and toxic nature of PFAS has triggered new legislation aimed at eliminating the use of PFAS from the paper coatings. The paper coatings.

The chemical modification of paper substrates with hydrophobic materials is also commonly used to impart paper with water- and oil-repellency. The presence of hydroxyl groups in a paper substrate has been used for etherification, esterification, acetylation, quaternization, and metal chelation to improve the water-resistance. However, these modifications often involve harsh environmental conditions that prohibit their use for real-world applications. Also, the chemically modified paper is non-recyclable because of the permanent bonds that exist between the paper and the hydrophobic materials.

Biopolymers are considered as ideal candidates for sustainable paper coating applications owing to their biocompatible, non-toxic, biodegradable, and renewable nature. However, papers coated with biopolymers (e.g., proteins¹⁶⁻¹⁹ and polysaccharides²⁰⁻²²) generally lack the waterresistance that is required for real-world applications due to the hydrophilic nature of proteins and polysaccharides. To enhance the water-resistance of protein- or polysaccharide-coated paper, multi-layer/lamination, ²³⁻²⁵ additional hydrophobic treatments with lipids such as emulsion/blending, ²⁶ and chemical-grafting are often employed. ²⁷ Though multi-layer paper structures prepared by lamination or coating approaches offer excellent water resistance, however, their applications are limited because of their poor repulpability. ²⁴⁻²⁵ Studies show that paper substrates coated with an emulsion comprised of lipid/wax along with biopolymers such as polysaccharides and proteins had some improvement in their water-resistance.²⁵ Nevertheless, these materials the water resistance was modest only. In addition, numerous parameters including compatibility between hydrophobic and hydrophilic components, low stability of the emulsion (phase separation), and the use of surfactant should be carefully controlled during processing. Also, the use of surfactant makes these coatings less stable against water because surfactant is often very polar in nature as well as have migration concerns from the coatings to the product. Alternatively, biopolymers could be chemical modifications (e.g., etherification, esterification, acetylation, acetylation, quaternization) by utilizing reactive hydroxyl or amino functional groups. These modified materials are focused in areas of drug delivery, tissue engineering, biomedical, biosensor, and environmental application, and less explored as packaging materials for improving water- and oil-resistance purposes. ²⁷

Chitosan (CHI) is a biopolymer prepared via the deacetylation of chitin and is extracted from the exoskeletons of shellfish, the cell walls of fungi, and in various other organisms.²⁸ CHI

is an edible polymer and is also suitable for paper coating applications due to the presence of amines and hydroxyl groups that can form strong hydrogen bonds with the hydroxyl groups of the lignocellulose in paper. Furthermore, CHI has excellent film-forming properties along with flexibility that matches those of some synthetic polymers.²⁹⁻³⁰ Previous studies have proved that chitosan can improve the grease-resistance by filling the porous cellulosic structure of paper substrates. 29-30 The strong interaction between chitosan and paper allows for outstanding greaseresistance compared with other biopolymers. 21 31 27 Another advantage of using CHI instead of other biopolymers such as starch is the presence of amine groups, which react instantly with isocyanate groups in an aqueous medium. ³⁰In addition, the coating of paper substrates with CHI can significantly enhance the barrier properties against gases such as oxygen, nitrogen, and carbon dioxide³². However, CHI has poor water-resistance due to its hydrophilic nature.^{26, 32} Our group has recently demonstrated that the treatment of CHI-coated paper with polydimethylsiloxane (PDMS) enhanced the water- and oil-resistance of the paper.^{29-30, 33} PDMS was used because of its low surface energy and good water- and oil-resistance. However, PDMS is a relatively expensive and non-biodegradable material. This motivated us to find a sustainable replacement for the PDMS.

Plant oils are inexpensive, renewable, and abundantly available materials. Their long hydrophobic chains impart them with excellent water-resistance. Some plant oils such as castor oil (CO) bear reactive hydroxyl groups, which can be used for further modification. Also, CO is inexpensive and hence widely used in cosmetics, households, as well as the medical and pharmaceutical fields. To the best of our knowledge, there have been no previous studies on the development of sustainable, biobased coatings for water- and oil-resistant paper based on CHI and CO.

In this study, chitosan-*graft*-castor oil (CHI-g-CO) copolymers were synthesized and applied as coatings onto paper substrates. The oil- and water-resistance of the coated paper was then determined by kit rating and Cobb60 value tests. In addition, water and oil contact angles were recorded to evaluate the liquid-repellency of these materials. Furthermore, the mechanical properties and water vapor permeabilities of the coated paper were investigated. Considering the biobased and food safe nature of the coating materials (e.g., chitosan and castor oil), this fabrication strategy can offer an environmentally friendly route toward water- and oil-resistant paper.

6.3 Materials and Methods

6.3.1 Materials.

Castor oil (Sigma Aldrich,), chitosan (weight average molecular weight or Mw = 50,000-190,000 g/mol, 85%, Sigma Aldrich), isophorone diisocyanate (98%, Sigma Aldrich) were used as received. The materials were characterized via ¹H NMR spectroscopy prior to use. Unbleached Kraft paper was kindly provided by Michigan Packaging Co. (Mason, MI, USA) and was employed as a paper substrate.

6.3.2 Methods

Synthesis of Castor Oil-capped-Isophorone Isocyanate (CO-capped-NCO). In two separate Schlenk flasks, Castor oil (CO) and isophorone diisocyanate (IPDI) were purged with nitrogen for ~5 min. The IPDI was then transferred to the castor oil under a nitrogen atmosphere, and the resultant reaction mixture was stirred at 70 °C for 3 h. Careful stoichiometric control was employed to ensure that the desired quantity of isocyanate (NCO) groups was present in the CO-capped-NCO. The CO-capped-NCO was characterized by ¹H NMR and FTIR and spectroscopy (as well be explained later).

Synthesis of CHI-g-CO. A CHI stock solution (4.0 wt%) was prepared by dissolving 4.0 g of CHI in 94.0 g of deionized water containing 2.0 wt% of glacial acetic acid. The mixture was stirred at room temperature for 2 h to obtain a homogeneous and clear aqueous CHI solution. Meanwhile, a desirable amount of CO-capped-NCO was dissolved in acetone and the solution was then added dropwise under stirring to the CHI solution. Following the addition of the CO-capped-NCO solution, the reaction mixture was stirred for 30 min and then purged with air to remove residual acetone. The reaction mixture was subsequently stirred for an additional 10 h to obtain the graft copolymer chitosan-graft-castor oil (CHI-g-CO).

Paper Coating with CHI-*g***-CO.** A waterborne CHI-*g*-CO solution was applied onto one side of a Kraft paper substrate using a rod-coating machine (K303, RK PrintCoat Instruments Ltd., UK), and dried under ambient conditions for 24 h. Unless indicated otherwise, the obtained coated paper was preconditioned at 23 °C and at 50% relative humidity (RH) prior to further testing.

Experimental Design and Statistical Study. Response surface methodology (RSM) was employed to design the experiment and obtain the optimum formulation using JMP Statistical Software (Version 14.3, SAS Institute Inc., NC, USA). Two independent variables including the concentration of CHI (denoted as CHI Conc., denoted as X_1) and the ratio (on a dry basis) of CO-capped-NCO to CHI (abbreviated as the CO-to-CHI ratio, denoted as X_2) and) were applied for central composite design (CCD) at five-levels within predetermined ranges as shown in Table 6.1. CCD was chosen because it combines center points, axial points as well as a two-level fractional factorial, which is an ideal option for second-order RSM model. The range of each independent variable has been decided based on preliminary experiments. The CHI Conc. were varied within range approx. 0.5-3.5%, due to the fact that when the CHI Conc. went beyond 3.5%, the solution would be too viscous for preparing copolymer. The CO-to-CHI ranged between 0-2, beyond which

phase separation was an issue. Four responses, including the coating load, coating thickness, water-resistance, and oil-resistance were studied. The relationship between the independent variables and responses was modeled using the least-squares-fit method to fit a second-order (quadratic) polynomial regression equation as is shown in Equation 6.1.⁴⁵

Table 6. 1 Levels and codes of the independent variables

Independent variables	Levels				
	-1.41	-1	0	-1	+1.41
CHI Conc. $\%$ (X_1)	0.50	0.94	2.00	3.06	3.50
CO-to-CHI Ratio (X ₂)	0	0.29	1	1.71	2.00

$$Y = b_0 + b_1 \frac{X_1 - 2}{1.5} + b_2(X_2 - 1) + b_{11} \left(\frac{X_1 - 2}{1.5}\right)^2 + b_{22}(X_2 - 1)^2 + b_{12} \left(\frac{X_1 - 2}{1.5}\right)(X_2 - 1)$$
(Equation 6.1)

where Y is the response, X_1 and X_2 are independent variables, while b_0 , b_1 , b_2 , b_{11} , b_{22} and b_{12} are regression coefficients. The optimum formulations and responses were determined based on the desirability function by converting responses into a scale-free value (known as desirability) with higher desirability (up to 1), indicating an optimized formulation. P values were provided based on the analysis of variance (ANOVA) for evaluation of the statically significant importance of each coefficient. The coefficient of determination (R^2) was applied to evaluate the accuracy of the polynomial models. All of the other characterizations and tests including TGA, FTIR, SEM, CAs, WVTR were performed on coated paper samples that had been prepared from the obtained optimum formulation.

6.3.3 Characterization

¹H NMR and ATR-FTIR Analysis. The CO-capped-NCO was characterized via ¹H NMR spectroscopy with a 500 MHz NMR spectrometer (Agilent, Santa Clara, CA, USA) using CDCl₃ as the solvent. Similarly, CO-capped-NCO was also characterized by an ATR-FTIR spectrometer (Model: Prestige 21, Shimadzu Co., Columbia, MD). In addition, paper samples obtained at various stages of the coating treatment were characterized via ATR-FTIR spectroscopy. For the ATR-FTIR analysis, 64 scans with a resolution of 4 cm⁻¹ over a spectral range from 4000 to 400 cm⁻¹ were recorded for each sample, followed by 15-point smoothing treatment using LabSolutions IR Software (Shimadzu Co., Columbia, MD).

Thermogravimetric Analysis (TGA). TGA and derivative thermogravimetric analyses (DTG) were conducted to investigate the coating content and thermal stability of the coating materials as well as the coated paper. Samples were heated from 23 to 600 °C at a heating rate of 10 °C/min under a nitrogen atmosphere (flow rate = 40 mL/min) using a thermogravimetric analyzer (Model: Q-50, TA Instruments, New Castle, DE). The weight loss (%), as well as the derivative of weight losses, were recorded and plotted during these measurements.

Scanning Electron Microscopy (SEM). The SEM analysis of coated and uncoated paper samples was performed using an SEM system (Model: 6610, JEOL LTD., Japan) at an accelerating voltage of 15 kV after the application of a 15-nm gold coating layer. The basis weight was determined via the gravimetric method by weighing the sample with dimensions of 10×10 cm². The basis weight was calculated using Equation 6.2 and expressed in grammage (g/m²). The coating loading value was calculated based on the difference between the basis weights before and after the application of the coating.

Basis weight =
$$\frac{\text{weight } (g)}{\text{area } (m^2)}$$
 (Equation 6.2)

Contact Angles (CAs) and Surface Tension. An automated Goniometer (Model: 590-U1, Ramé-Hart Instrument Co., NJ, USA) was employed for contact angle determination by applying 5-μL liquid droplets (water or castor oil) onto the surfaces of uncoated paper and coated paper samples.²⁷ The surface energies of uncoated paper, as well as those of the best performing coated paper, were determined with the use of DROPimage Advanced software based on the values for the surface tensions and contact angles of water and diiodomethane.

Water-resistance (Cobb60) Tests. Water absorption was determined using the Cobb60 test according to standard tests ISO535 and TAPPI 441 protocols. A paper sample with an area of 100 cm² was exposed to DI water with a depth of 1 cm for 60 s, and the quantity of water absorbed by the paper material was then calculated based on the weight of the paper material before and after the test. The water absorption was expressed as a Cobb60 value (g/m²), which refers to the mass in grams of water that was absorbed per square meter of paper material.

Water Vapor Transmission Rate (WVTR). The WVTR of uncoated paper and coated paper that was prepared with the optimum formulation was determined using a Permatran-W (Model: 3/34, Mocon Inc., MN, USA) at 50% RH and 23 °C. Two sets of samples that were preconditioned for 48 h at 50% RH and 0% RH, respectively, were tested to investigate the effect of moisture on their barrier properties. The WVTRs of four-layer coated samples (of the same coating solution) were also determined to study the effect of the coating thickness on the water vapor barrier properties.

Oil/grease Resistance (kit rating). The kit test is a standard test (TAPPI UM 557) used to determine the repellency of paper and board to grease, oil, and waxes. In this study, we employed standard kit tests to evaluate the oil resistance of the coated samples.³⁰ A series of numbered solutions (kit numbers 1-12) were sequentially applied onto a coated paper specimen and then

cleaned with a tissue after 15 s. The tested area was examined immediately with the naked eye and the specimen was considered to fail this test if any darkened spots were visible on this surface. The number of the most aggressive solution (highest number) which the specimen could support was reported as the "kit rating" for that specimen.

Mechanical Properties. The mechanical properties of CHI-g-CO-coated, CHI-coated, and uncoated paper samples were evaluated using a Universal Instron Testing machine (Model: 5565, Instron, MA, USA). Specimens with dimensions of 1×7 in prepared in machine direction were stretched at a rate of 0.5 in/min according to a TAPPI standard (T 494) protocol. These tests were repeated in triplicate.

6.4 Results and Discussion

To enhance the water-resistance of chitosan (CHI)-coated paper, hydrophobic castor oil (CO) was first chemically grafted onto CHI to obtain CHI-g-CO (see Scheme 6.1). To enable the grafting of CO onto CHI, CO was initially reacted with isophorone diisocyanate (IPDI, the ¹H NMR spectrum is shown in Appendix A) to obtain CO-capped-NCO with free NCO functional groups by using a molar excess of IPDI. For example, in one case, 0.022 mol of the OH moieties in CO was reacted with 0.022 mol of IPDI (there are 2 NCO groups per IPDI molecule). We chose IPDI for this purpose because it is on the *Generally Regarded As Safe (GRAS)* list of the FDA. ⁴⁹ Aside from stoichiometric control, it is also widely known that the two NCO groups present in an IPDI molecule have different reactivities, where the NCO group attached to the secondary carbon is more reactive than the NCO moiety that is attached to the primary carbon. ⁵⁰ This difference in the reactivity of NCO groups on IPDI, in addition to stoichiometric control, can be leveraged for the synthesis of CO-capped-NCO.

Scheme 6. 1 The synthetic route followed for the preparation of the CHI-*g*-CO copolymer in this study.

¹H NMR spectra of CO and of the CO-capped-NCO are shown in Figure 6.1. Labeled peaks for the CO are shown in Figure 6.1 (top). For CO-capped-NCO, the characteristic peaks at 3.75 ppm (labeled as 12' in Figure 6.1) correspond to the reaction product between the OH group of the CO and NCO moieties of the IDPI. The presence of other characteristic peaks such as those denoted as 19,18, and 25 validated the synthesis of the desired CO-capped-NCO.⁵¹

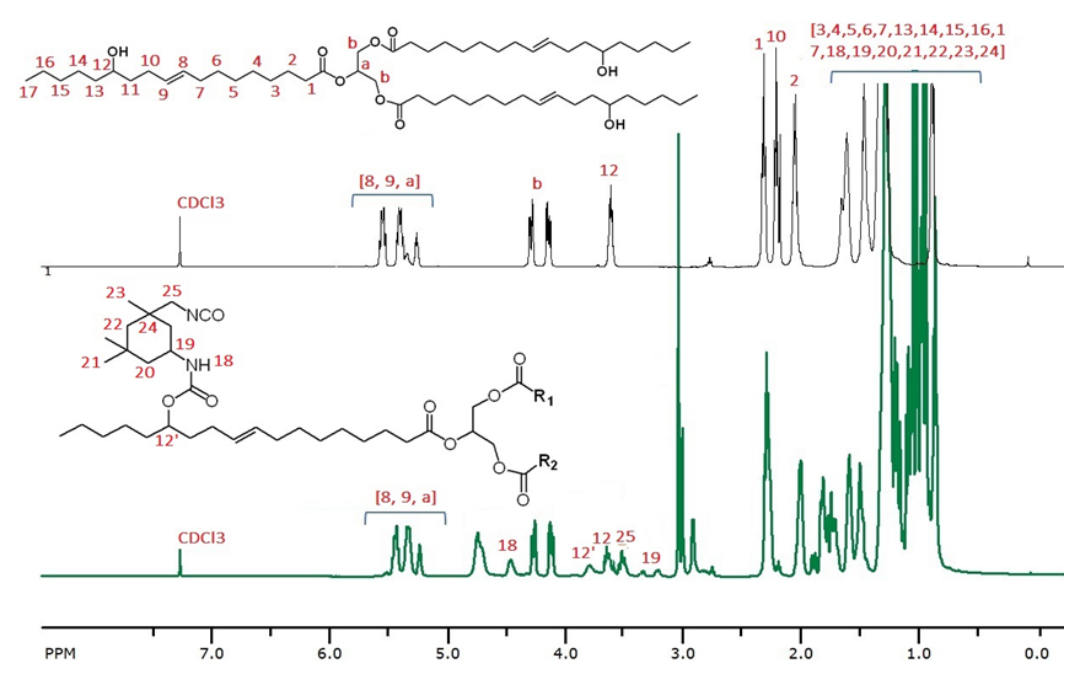


Figure 6. 1 ¹H NMR (recorded in CDCl₃ at 500 MHz) spectra of: (top) CO and (bottom) CO-capped-NCO.

ATR-FTIR spectroscopy was applied to identify the functional groups in the reactants and products to confirm the reaction between CO and IPDI (see Figure 6.2). The characteristic peak of IPDI is that corresponding to the isocyanate group (-NCO) at 2328 cm⁻¹ (Figure 6.2b). Meanwhile, the broadband observed between 3680-3100 cm⁻¹ in Figure 6.1c was attributed to the –OH group in the CO structure. In the spectrum of the product CO-capped-NCO (Figure 6.2a), the –OH peak (3680-3100 cm⁻¹) disappeared, and the –NCO peak (2328 cm⁻¹) became weakened. In addition, the typical peaks corresponding to urethane linkages existed in the product (CO-capped-NCO) at 1703 cm⁻¹ (-C=O), 1510 cm⁻¹ (N-H and C-N bending vibration), 1240 cm⁻¹ (C-O stretching vibration) and 1035 cm⁻¹ (C-O-C stretching vibration), thus demonstrating that the reaction between CO and IPDI had indeed occurred (see the Scheme 6.1 for synthetic route).⁵² The peak at 2328 cm⁻¹ confirmed the presence of residual –NCO in the CO-capped-NCO that could undergo reaction with CHI in the next step. The sharp peak at 2924 cm⁻¹ in Figure 6.2b was

attributed to the C-H stretching vibration of IPDI. Meanwhile, the peaks observed at 2918 and 2850 cm⁻¹ in Figure 6.2c were respectively due to the asymmetric and symmetric C-H stretching vibrations of –CH₂ groups in CO.

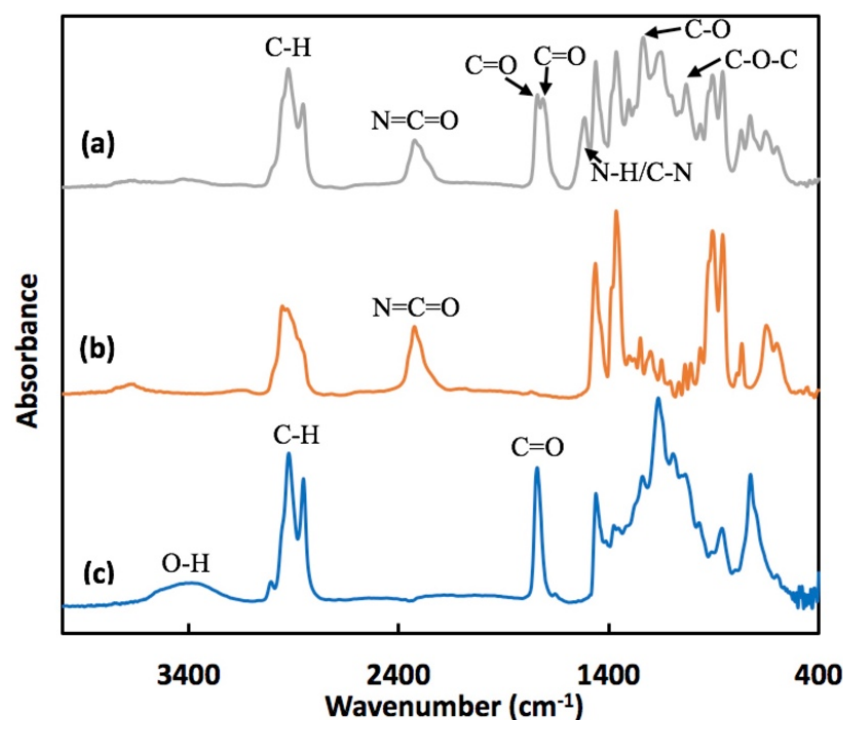


Figure 6. 2 ATR-FTIR spectra of: (a) CO-capped-NCO, (b) IPDI, and (c) Castor oil (CO)

Experimental design and formulation optimization of the CHI-g-CO was performed by using the Response Surface Methodology (RSM), where the kit rating, Cobb60 value, coating load, and thickness of the corresponding coated-paper samples were determined according to the CCD protocol (see Appendix B). The estimated coefficients of each response are shown in Appendix C. The coefficient of determination (R^2) of each response, including the kit rating, Cobb60 value, and coating load were 90%, 91%, and 90%, respectively, indicating that the models were acceptable. Meanwhile, the R^2 value for the thickness was only 76%, probably due to error associated with the measuring device and small differences among the samples. Figure 6.3 shows the 3D surface profiles with contours on the bottom of each profile. The results indicated that with

increases in the concentration of CHI (X_1) , the Cobb60 value, kit rating, thickness of the coated paper, and the coating loading increased significantly. These trends are in accordance with the Pvalues in Table 2S, thus indicating that the independent variable (X_1) was statistically significant for all four responses. In addition, the concentration of CHI (X_1) played an important role rather than the CO-to-CHI ratio (X_2) in imparting oil resistance (a higher kit rating) according to the results as demonstrated by the P-value of b_2 , which was 0.656. Higher concentrations of CHI could result in higher Cobb60 values due to the hydrophilic nature of this polymer, whereas the CO improved the water resistance by lowering the Cobb60 value due to the hydrophobic nature of CO as shown in Figure 6.3b. In addition, increasing the amount of CO and CHI in the coating solution yielded a higher coating loading as illustrated in Figure 6.3c. However, the thickness was less affected by the amount of CO in the coating solution with a P-value of 0.9556 (Table 2S). Based on these results, the optimum formulation was chosen as that having a CO-to-CHI ratio of 1 and a CHI concentration of 2 wt% with the desirability of 0.70 provided by the JMP software. The coating load is ~2.1 g/m² CO-to-CHI copolymer (1 to 1 ratio) on paper substrate. The predicted kit rating and Cobb60 values were 9.16 and 29.16 g/m², respectively.

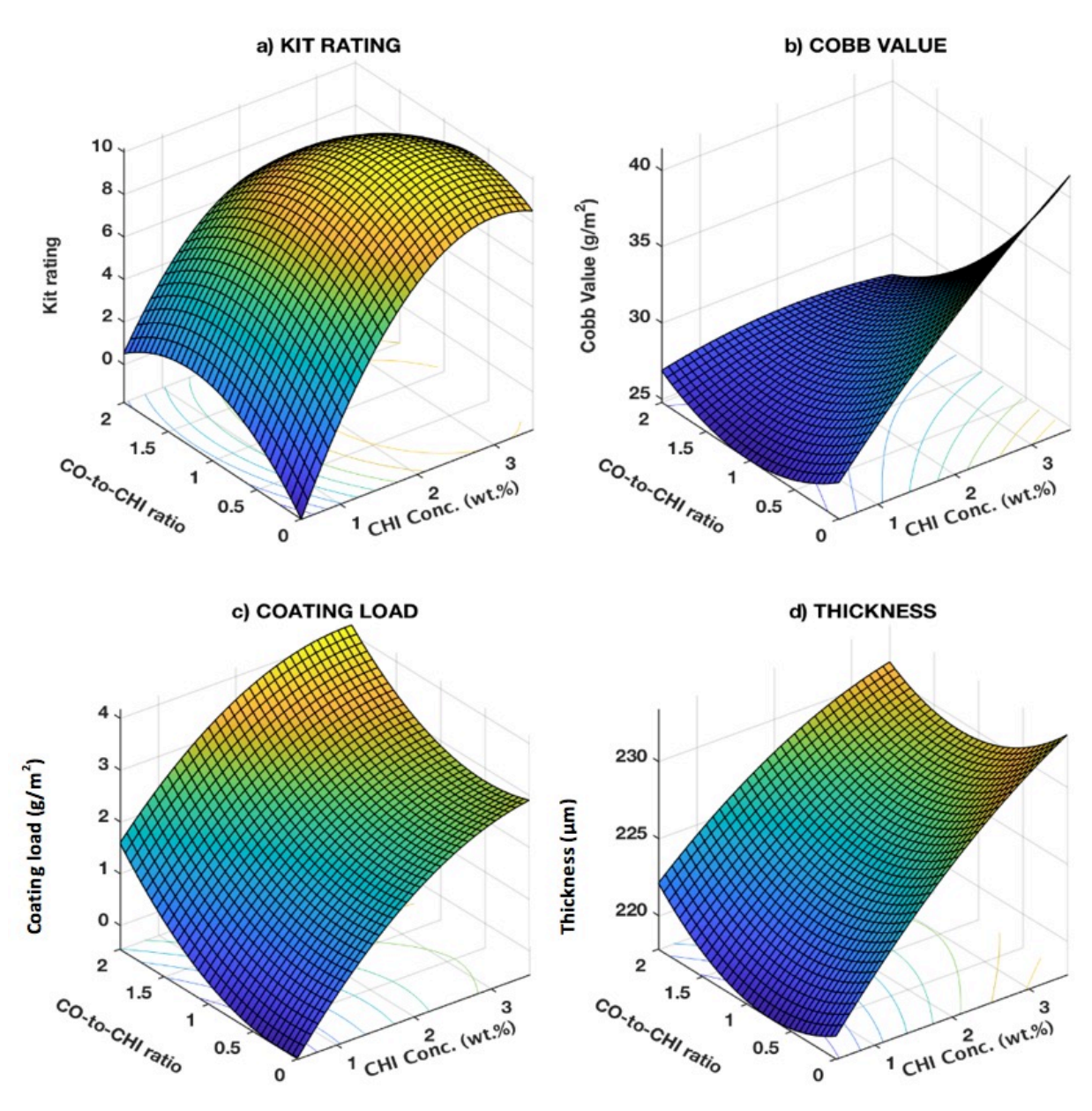


Figure 6. 3 Surface profiles for the (a) kit rating, (b) Cobb60 value, (c) coating load, and (d) thickness.

The optimal CHI to CO ratio suggested by RSM study was used to prepare CHI-*g*-CO. First, CHI was dissolved in acetic acid-water, followed dropwise addition of CO-capped-NCO (dissolved in acetone) under stirring. The reaction mixture was stirred at room temperature for at least 30 min to obtain the chitosan-*graft*-castor oil (CHI-*g*-CO). The amine group of the CHI

reacts with the NCO group of CO-capped-NCO. The efficient reaction of chitosan with isocyanates in acetic acid-water medium has been recently reported by our group.³⁰ The resultant waterborne CHI-*g*-CO solution was applied onto one side of a Kraft paper substrate using a rod-coating machine.

The surface compositions of coated- and uncoated-paper samples were characterized via ATR-FTIR spectroscopy (see **Figure 6.4**). A broad band between 3100 and 3600 cm⁻¹ revealed the presence of hydroxyl groups on the cellulose fibers.⁵³ Meanwhile, the peak observed at 1651 cm⁻¹ in Figure 6.4b corresponded to the N-H bending vibration of the –NH₂ moieties in CHI. The –NH₂ peak (at 1651 cm⁻¹) from the CHI structure and the -NCO peak (at 2328 cm⁻¹) from the CO-capped-NCO structure both disappeared from the spectrum of the CHI-g-CO coated paper, indicating that the reaction between –NCO and –NH₂ has occurred, as has been proven in a previous study.²⁹ The peaks at 2916 and 2848 cm⁻¹ were respectively attributed to the C-H stretching vibrations of the -CH₂ and -CH₃ moieties in CO.⁵⁴ Meanwhile, the peaks at 1460 cm⁻¹, 1228 cm⁻¹, and 1024 cm⁻¹ corresponded to the C-N, N-H (bending), C-O and C-O-C bonds in the CHI-g-CO structure. These peaks validated the presence of CHI-g-CO on the coated paper.

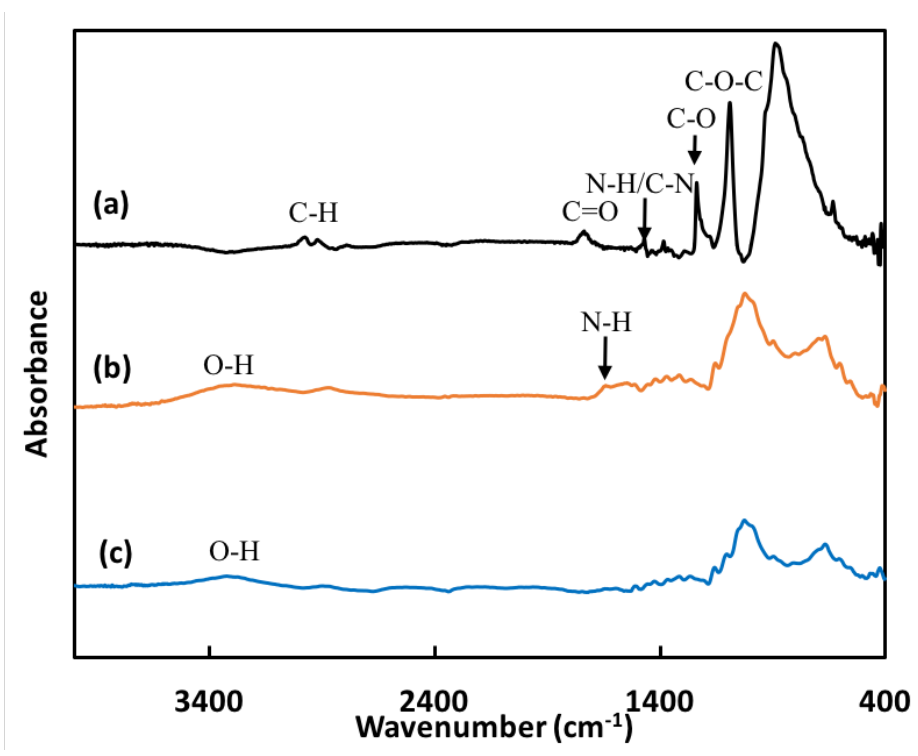


Figure 6. 4 FTIR spectra of: (a) CHI-g-CO-coated paper, (b) CHI-coated paper, and (c) uncoated paper.

TGA analysis was conducted to determine the thermal stability and the coating loading of the coated paper. TGA and DTG curves for the coated paper as well as the coating materials (without paper) are shown in Appendix D. The weight loss observed below 120 °C corresponds to the evaporation of the hydrogen-bonded water molecules. Only a small difference in the TGA (and DTG) traces between coated and uncoated paper was observed, indicating a low coating loading of ~ 2 wt%, which is consistent with the coating content determined by the gravimetric approach. The TGA analysis of coating materials (without paper) was performed to obtain the thermal profiles of these materials. In the DTG curve of CHI (see Figure A-7b), the weight loss occurred ~ 280 °C. For the CHI-g-CO sample, weight loss occurred between 230 and 510 °C, which can be attributed to the decomposition of CHI and CO. This behavior is also consistent with previous reports, where weight losses occurring between 300 to 410 °C and 410 to 510 °C

corresponded to the decomposition of monounsaturated fatty acids and saturated fatty acids, respectively.⁵⁵

SEM analysis was employed to investigate changes in the paper surface at various stages of the fabrication, as shown in Figure 6.5. It can be seen that the CHI- and CHI-*g*-CO-coated paper are non-porous while the uncoated paper is porous. The filling of the paper pores by CHI is due to the excellent film-forming properties of this polymer. The presence of some spherical structures on the surface of CHI-*g*-CO-coated paper is likely the microspheres formed due to inefficient mixing or phase separation of hydrophobic CO and hydrophilic CHI. One also cannot exclude the possibility of some crosslinking for the formation of microspheres. Further investigations are required to gain more in-depth insight into this behavior.

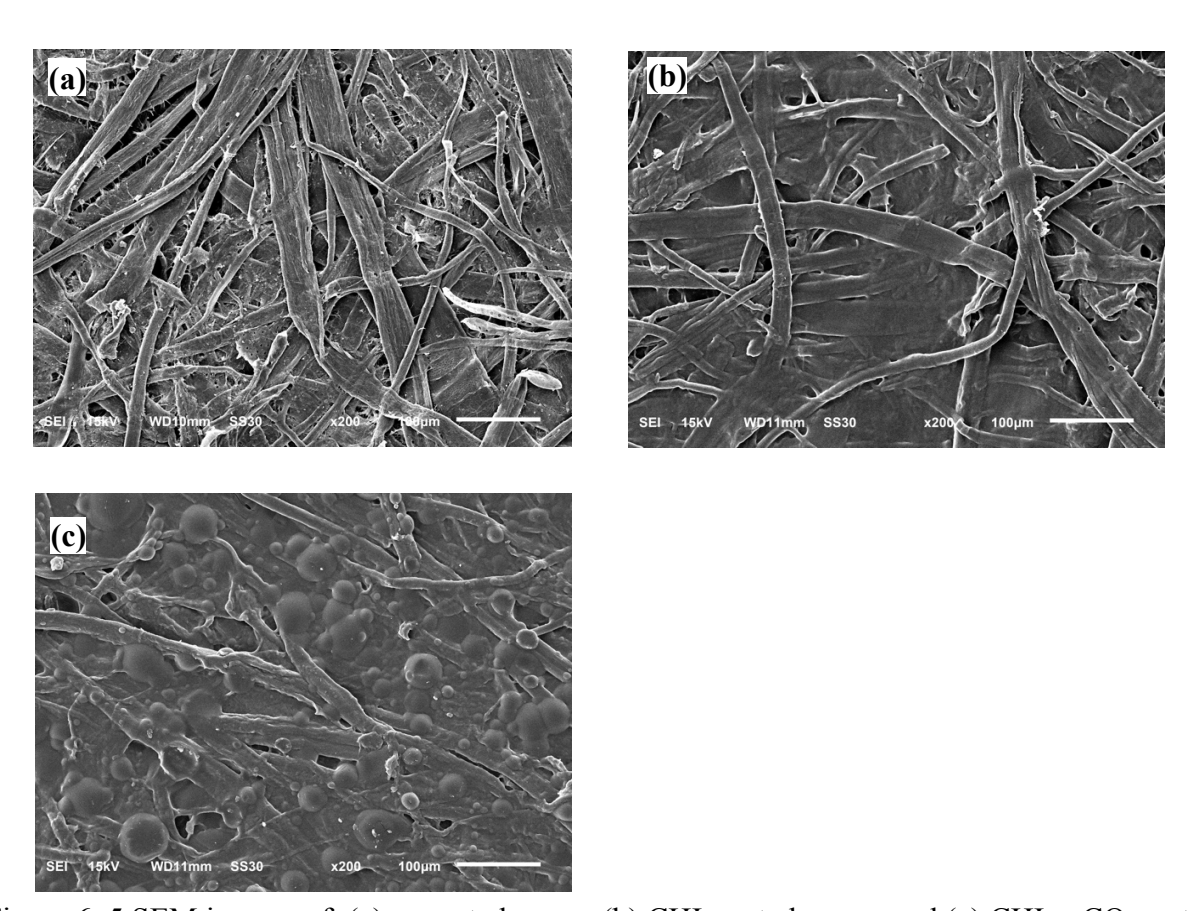


Figure 6. 5 SEM images of: (a) uncoated paper, (b) CHI-coated paper, and (c) CHI-g-CO-coated paper

Contact angles provide valuable information regarding the liquid-resistance (wettability) of a substrate. Contact angles are dependent on surface roughness as well as surface energy. In this study, water contact angles (WCAs) on CHI-g-CO-coated-, CHI-coated, and uncoated paper samples were monitored over a period of 25 min, as can be seen in Figure 6.6. The results indicated that the WCAs decreased only slightly with time on the CHI-g-CO-coated paper. For example, after 1400 s, the water contact angle decreased from 92.91° to 85.46° on the CHI-g-CO-coated paper. In contrast, sharp decreases in the WCAs were observed on the CHI-coated (from 84.17° to 54.38°) and uncoated paper (79.36° to 38.23°) samples during the 1400 s period.

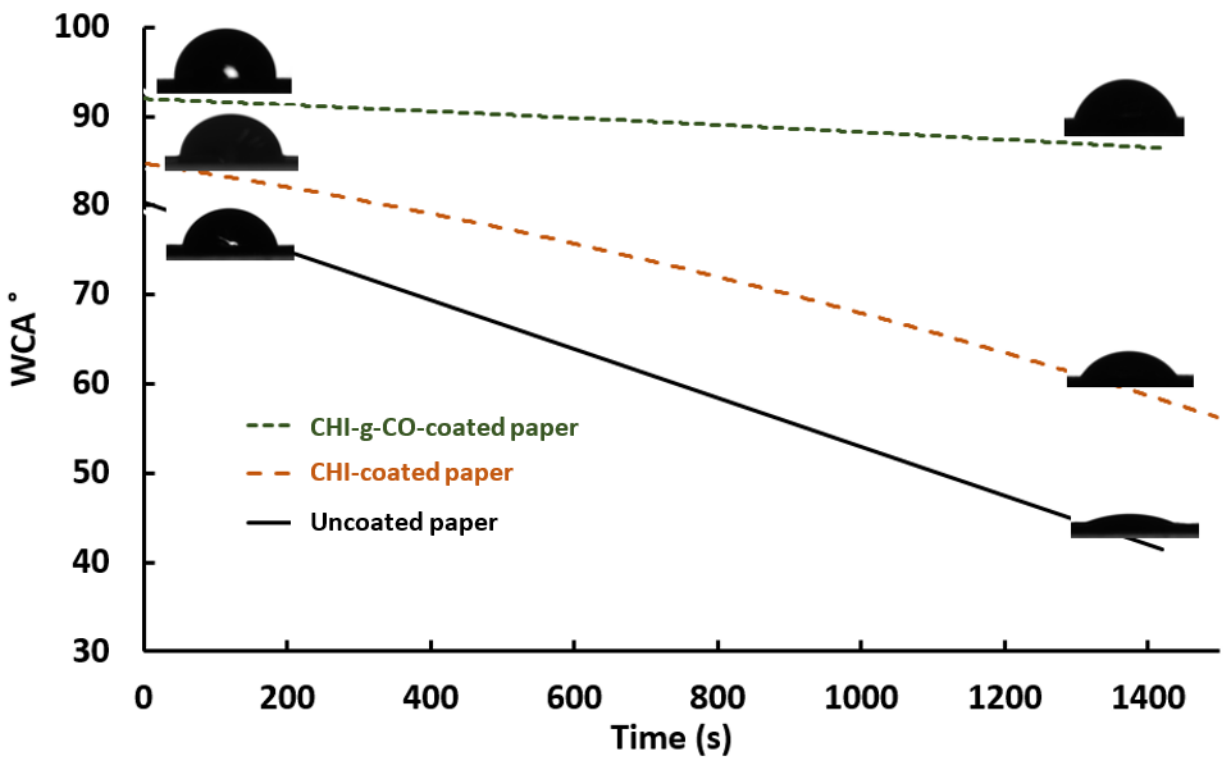
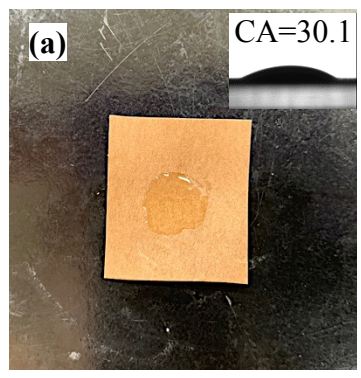


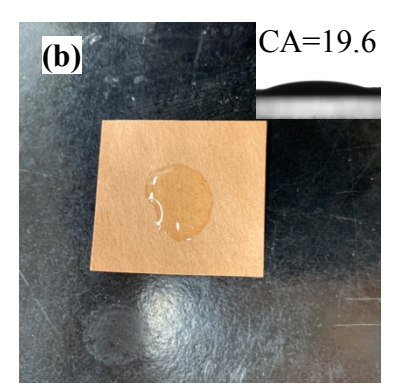
Figure 6. 6 WCAs on CHI-g-CO-coated, CHI-coated, and uncoated paper as a function of time. Images of the water droplet sitting on different paper samples were taken every 5 s until a duration of 1400 s was reached. A 5 μL droplet size was used in these tests.

The oil resistance of the coated and uncoated paper was also determined using castor oil as the test liquid. The oil contact angle (OCA) observed on the CHI-g-CO-coated paper was 30.12°,

which was ~35% higher than that observed on the CHI-coated-paper (19.61°). Figure 6.7 clearly shows the improved oil resistance of the CHI-g-CO-coated and CHI-coated-paper over that of the uncoated paper. One might see in Figure 6.7 that the OCA for uncoated and CHI-g-CO coated paper is similar. It is because the contact angle is affected by both the chemical composition as well as the morphology of the surface. As the uncoated paper substrate is very rough, that causes OCA to be higher than that of CHI coated paper. For the CHI-g-CO coated paper, an increase in the OCA corresponds to the hydrophobicity imparted by castor oil as well as roughness provided by the presence of some microspheres visible in the SEM images. In addition, the dark stains created on the uncoated paper by the castor oil droplet indicate oil diffusion into the porous structure of the paper substrates, thus reflecting weak oil resistance. While CHI-g-CO coated paper is oil resistant and does not allow the oil to diffuse into the paper as evident by the absence of dark spots (Figure 6.7a).

We also determined the surface energies of the CHI- and CHI-g-CO-coated paper, which were 43.82 and 40.87 mN•m⁻¹, respectively. Meanwhile, the predicted and experimental kit rating values for CHI-g-CO-coated paper were 9.16 and 9.16 ± 0.23 , respectively.





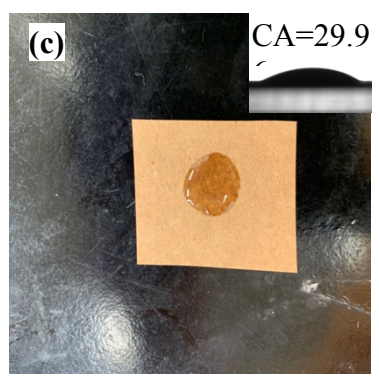


Figure 6. 7 Top-down images of the castor oil on: (a) CHI-g-CO-coated paper, (b) CHI-coated paper, and (c) uncoated paper (several drops were placed on the same spot). The inset images represent the OCAs of castor oil droplets on: (a) CHI-g-CO-coated paper, (b) CHI-coated paper, and (c) uncoated paper. For the OCA measurements, the CO droplet volume was 5 μL.

The water vapor transmission rates (WVTRs) for the coated paper, after preconditioning at 0% and 50% RH for 72 h, were determined, and the data is shown in **Figure 6.8**. As expected, the uncoated paper exhibited poor water barrier property with high WVTR values because of its porous and hydrophilic nature. In contrast, both the CHI- and CHI-g-CO-coated paper substrates showed improved water barrier performance primarily owing to the masking of papers' pores. In addition, the water barrier property of CHI-g-CO-coated paper is further improved due to the hydrophobic structure of CO. It is well-known that hydrophobic polymers, in general, have a high water vapor barrier because the solubility coefficient of water vapors in hydrophobic materials is lower relative to hydrophilic materials. Additionally, as the coating thickness increased in 4-layer CHI-g-CO-coated paper, the barrier properties were enhanced at both 50% and 0% RH. It is noteworthy that the water barrier performance of the CHI-coated and CHI-g-CO-coated paper was significantly influenced by the relative humidity of the environment. This decrease in the WVTR at an RH can be attributed to the moisture absorption and the subsequent swelling of the coating. ⁵⁷⁻

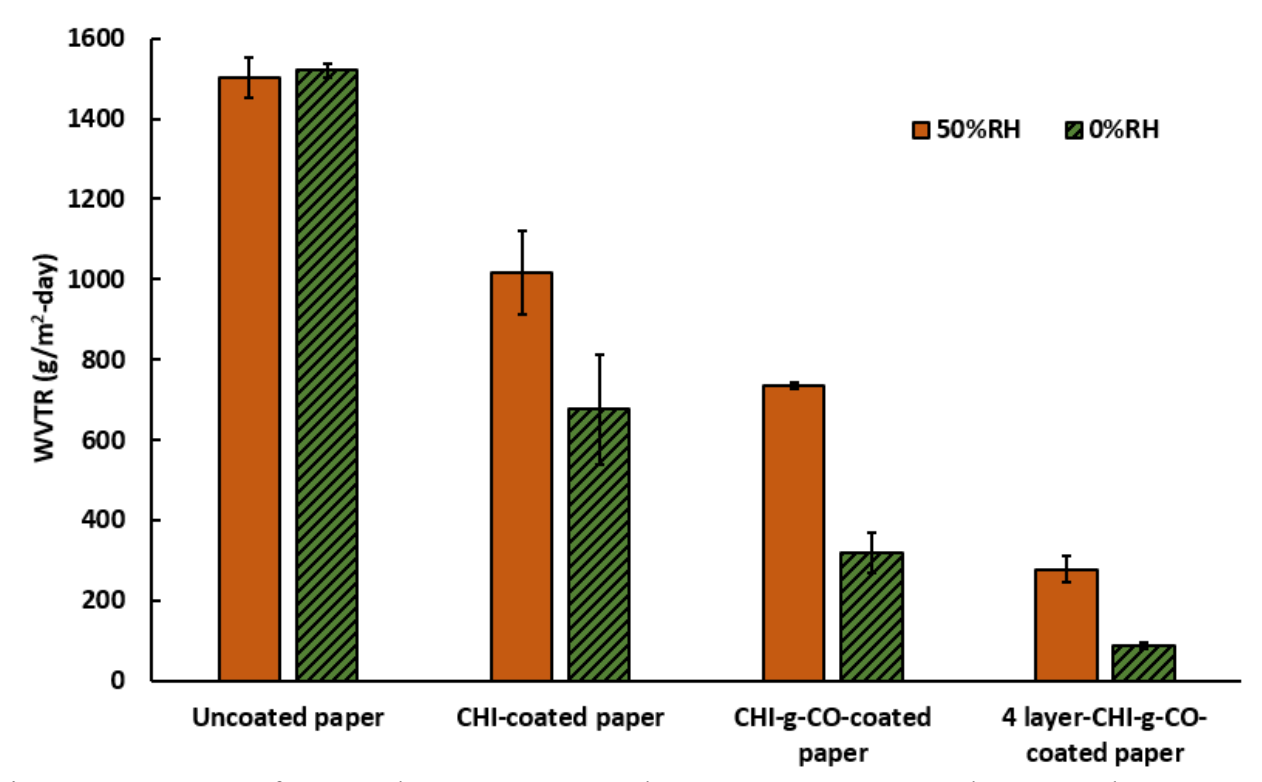


Figure 6. 8 WVTRs of uncoated-paper, CHI-coated paper, CHI-g-CO-coated paper, and paper coated by four layers of CHI-g-CO after these samples had been preconditioned at 50% RH and 0% RH for 72 h, WVTRs were *determined at 50% RH and 23 °C*.

The mechanical properties including the tensile strength, modulus of elasticity, and percentage elongation at break were evaluated to study the effect of the coating on the flexibility and brittleness of paper. The results for the CHI-g-CO coated-, CHI coated-, and uncoated paper are shown in Table 6.2. It is apparent that the CHI coating slightly decreased the tensile strength of the paper substrate (by less than 10%), possibly due to high moisture absorption, which is causing weakening of the interactions between paper's fibers. While the CHI-g-CO-coated paper exhibited a slight improvement in its tensile strength relative to the CHI-coated paper, as it is water-resistant than the CHI-coated paper. In addition, both the CHI-g-CO- and CHI-coated-paper

exhibited enhanced elongation percentages at their breaking points but also decreases in their moduli of elasticity.

Table 6. 2 Mechanical properties of CHI-g-CO-coated paper, CHI-coated paper, and uncoated paper.

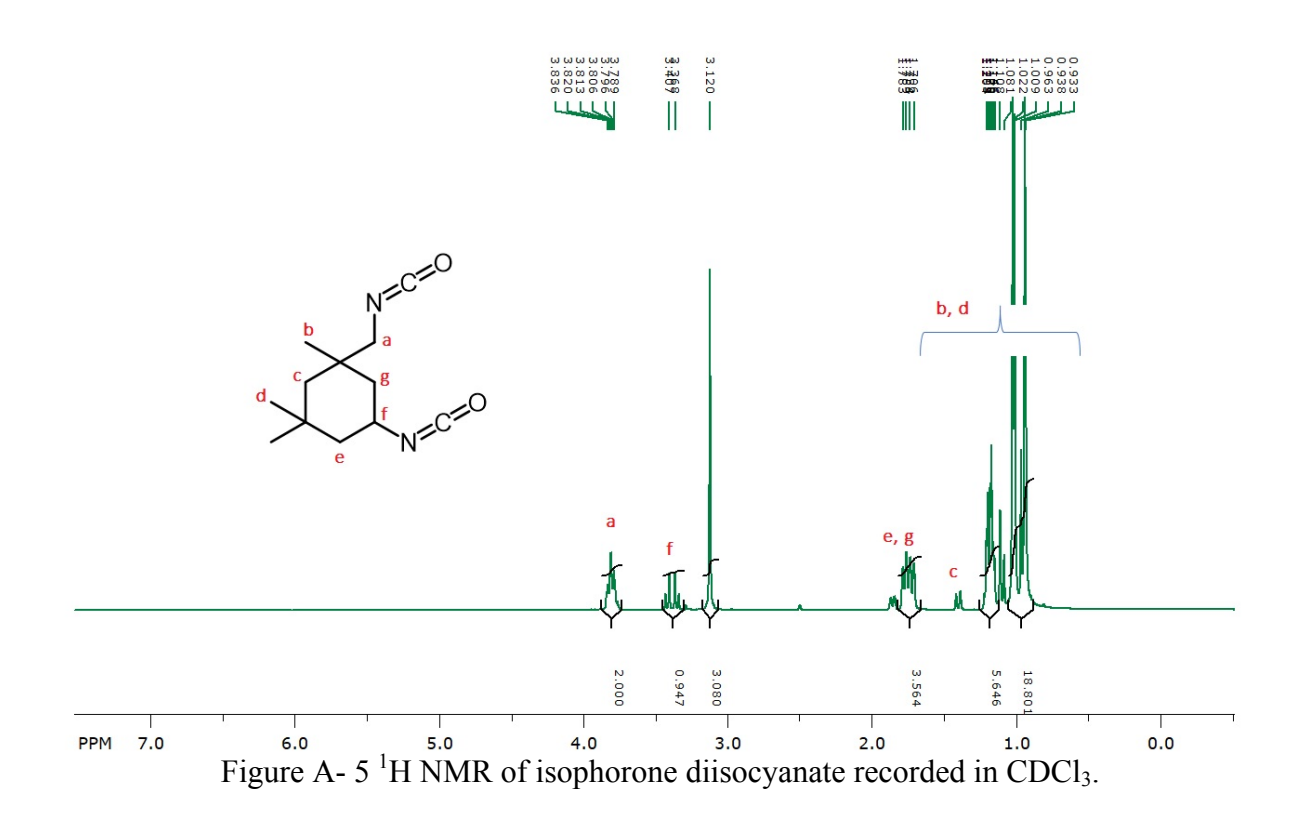
Mechanical Properties	CHI-g-CO-coated paper	CHI-coated paper	Uncoated paper	
Tensile Strength (N/m)	315.28 ± 0.76	298.84 ± 2.58	313.41 ± 12.29	
Modulus of Elasticity× 10 ⁹ (pa)	3.45 ± 0.04	2.97 ± 0.01	4.00 ± 0.03	
% Elongation at Break	2.26 ± 0.13	2.05 ± 0.23	1.71 ± 0.03	

6.5 Conclusions

A facile approach has been developed for the coating of paper using sustainable and biobased coating materials. CHI-g-CO was successfully synthesized and applied as a coating onto paper substrates. The optimized formulation with a CHI-to-CO ratio of 1:1 and a CHI concentration of 2 wt% was obtained according to the RSM study. The developed coated paper had good grease- and water-resistance, with a kit rating of 9 and Cobb60 value of 29.16 g/m^2 , which were in close agreement with the RSM predicted values. The obtained CHI-g-CO-coated paper showed modest barrier performance against water vapor with WVTR values of 734.67 \pm 6.66 and 318.01 \pm 50.27 g/m^2 -day at 50% and 0% RH, respectively. SEM analysis showed that the CHI-g-CO-coated paper was non-porous, and thus proved the improved water and oil-resistance is due to the non-porous nature of the coated paper. The presence of chitosan imparts oil resistance because of their very polar nature, while the CO which is chemically grafted to the CHI backbone enhances the hydrophobicity of the copolymer resulting in a high water-resistant

property. The tensile properties of the coated and uncoated paper did not change significantly. Due to the renewable and environmentally friendly nature of the coating materials, the method developed herein can address the problems created by the existing paper coatings practices and plastics.

APPENDICES



APPENDIX B: Central Composite Design of experimental and experimental responses

Table A- 1 Central Composite Design of experimental and experimental responses

Sample No.	Variables		Responses			
	X_1	X_2	$\overline{Y_1}$	Y_2	<i>Y</i> ₃	Y_4
	(CHI	(CO-to-	(Kit	(Cobb60	(Coating	(thickness
	Conc.)	CHI ratio)	rating)	g/m^2	load g/m ²)	μm)
1	0.50	1.00	1.33	25.41	0.96	216.1
2	0.94	1.71	3.33	26.54	2.28	222.8
3	0.94	0.29	4.00	26.65	1.59	223.4
4	2.00	1.00	9.00	29.41	2.15	221.3
5	2.00	1.00	9.33	29.02	2.01	228.8
6	2.00	2.00	8.00	27.76	3.91	229.1
7	2.00	0.00	6.33	37.11	1.31	226.0
8	3.06	0.29	9.67	34.86	3.62	230.4
9	3.06	1.71	6.00	27.83	3.92	227.2
10	3.50	1.00	10.00	33.43	4.30	231.0

APPENDIX C: Regression coefficients for the second-order polynomial model

Table A- 2 Regression coefficients for the second-order polynomial model

Term	Estimated	Std. Error	<i>P</i> −value, Prob.> <i>F</i>					
Kit rating								
b_0	9.16	1.03	0.0009^*					
b_1	3.64	0.73	0.0075^*					
b_2	-0.35	0.73	0.6560					
b_{12}	-1.50	1.46	0.3610					
b_{11}	-3.83	1.36	0.0481^{*}					
b_{22}	-2.33	1.36	0.1619					
Cobb60 value								
b_0	29.22	1.26	<0.0001*					
b_1	3.68	0.89	0.0146*					
b_2	-3.60	0.89	0.0158^*					
b_{12}	-3.46	1.79	0.1251					
b_{11}	-0.77	1.67	0.6677					
b_{22}	2.24	1.67	0.2513					
Coating weight								
b_0	2.08	0.38	0.0054^{*}					
b_1	1.48	0.27	0.0053^*					
b_2	0.82	0.27	0.0379^{*}					
b_{12}	-0.19	0.54	0.7430					
b_{11}	-0.66	0.50	0.2571					
b_{22}	0.64	0.50	0.2718					
Thickness								
b_0	225.05	2.46	<0.0001*					
b_1	5.74	1.74	0.0300^{*}					
b_2	0.10	1.74	0.9556					
b_{12}	-1.30	3.48	0.7279					
b_{11}	-1.30	3.26	0.7102					
b_{22}	2.70	3.26	0.4538					

^{*}Indicates that the coefficient was significant at a 95% confidential level (values of "Prob.>F" <0.05).

APPENDIX D: TGA and DTG of coating materials (CHI-*g*-CO and CHI) and coated and uncoated samples

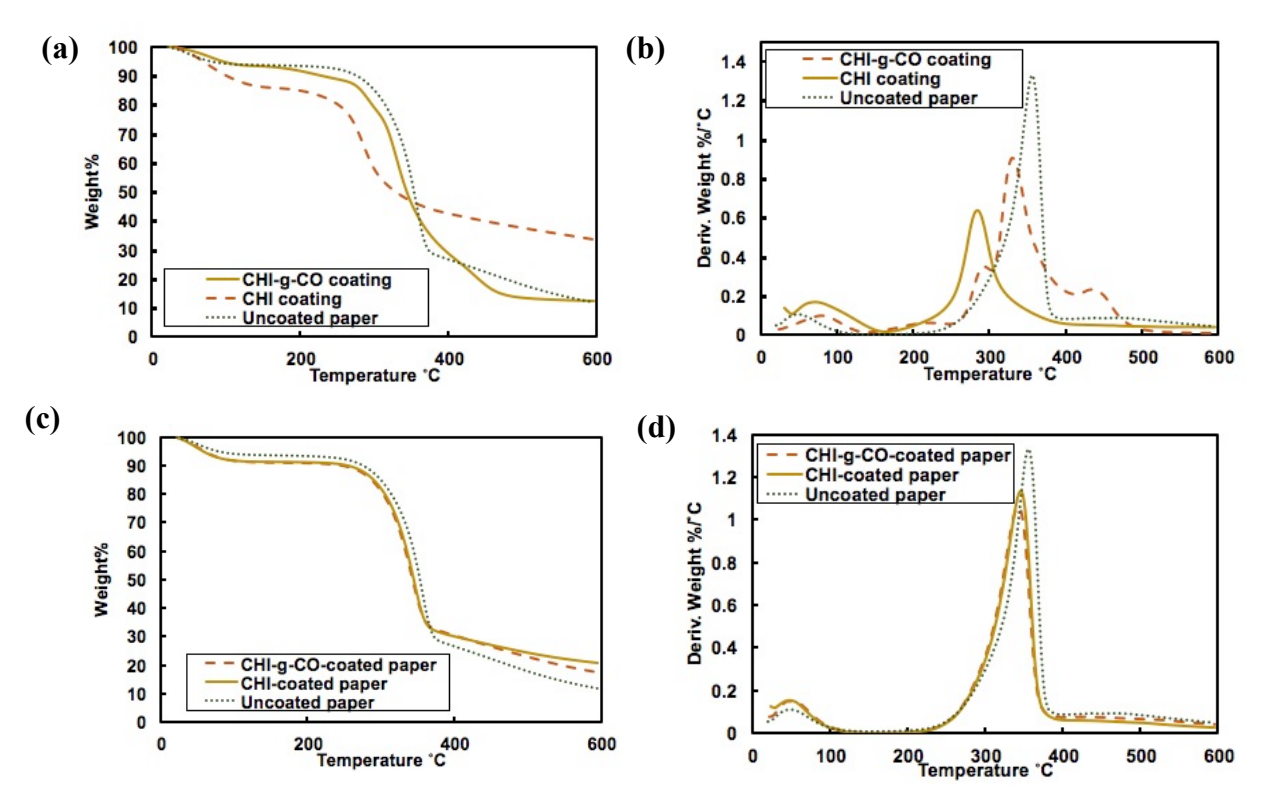


Figure A- 6 (a) TGA curves for coating materials (CHI-g-CO and CHI) as well as a paper substrate, (b) DTG curves for coating materials (CHI-g-CO and CHI) as well as the paper substrate, (c) TGA curves for coated paper (including uncoated paper) at various stages of fabrication, and (d) DTG curves for coated paper at various stages of fabrication.

REFERENCES

REFERENCES

- 1. Rabnawaz, M.; Wyman, I.; Auras, R.; Cheng, S., A Roadmap Towards Green Packaging: The Current Status and Future Outlook for Polyesters in the Packaging Industry. *Green Chem.* **2017**, *19* (20), 4737-4753.
- 2. Cheng, S.; Rabnawaz, M.; Khan, F.; Khan, B., Synthesis of High Molecular Weight Aromatic Polyesters via Integrated Alternating Ring-Opening Copolymerization and Chain Extension Methods. *J. Appl. Polym. Sci.* **2019**, *136* (11), 47200.
- 3. Cheng, S.; Khan, B.; Khan, F.; Rabnawaz, M., Synthesis of High Molecular Weight Polyester Using in Situ Drying Method and Assessment of Water Vapor and Oxygen Barrier Properties. *Polymers (Basel)* **2018**, *10* (10), 1113-1120.
- 4. Martin Jr, L. L. Paper Laminate and Method for Producing the Laminate and Paperboard Containers. Google Patents: US4806398A, 1989.
- 5. Oswald, R. G.; Harvey, W. T.; Johnson, H. L. Wax-coated Paper. Google Patents: US3231462A, 1966.
- 6. Knights, E. F. Wax Coated Paper of Improved Water Resistance. Google Patents: US3874905A, 1975.
- 7. Advancing Sustainable Materials Management: 2015 Fact Sheet; United States Environmetal Protection Agency: 2018-6, 2018.
- 8. Paper and Paperboard: Material-Specific Data. https://www.epa.gov/facts-and-figures-about-materials-waste-and-recycling/paper-and-paperboard-material-specific-data-PaperTableandGraph (accessed 2019-1-7).
- 9. Kotkamills Kotkamills' new plastic-free and easily recyclable consumer board AEGLE barrier light is now ready for world domination. <a href="https://www.google.com/url?sa=t&rct=j&q=&esrc=s&source=web&cd=1&cad=rja&uact=8&ved=2ahUKEwjSzfPT5bTcAhWJYJoKHWbXC44QFjAAegQIABAB&url=https%3A%2F%2Fwww.epressi.com%2Ftiedotteet%2Fpaperiteollisuus%2Fkotkamills-new-plastic-free-and-easily-recyclable-consumer-board-aegle-e2-84-a2-barrier-light-is-now-ready-for-world-domination.html&usg=AOvVaw0FUXLp9vfNaNJ7w I8nOiA (accessed 2019-8-3).
- 10. Du, Y.; Zang, Y.-H.; Du, J. Effects of Starch on Latex Migration and on Paper Coating Properties. *Ind. Eng. Chem. Res.* **2011,** *50* (16), 9781-9786.
- 11. Basic Information on PFAS. https://www.epa.gov/pfas/basic-information-pfas (accessed July 10).

- 12. Schaider, L. A.; Balan, S. A.; Blum, A.; Andrews, D. Q.; Strynar, M. J.; Dickinson, M. E.; Lunderberg, D. M.; Lang, J. R.; Peaslee, G. F. Fluorinated Compounds in U.S. Fast Food Packaging. *Environ. Sci. Technol. Lett.* **2017**, *4* (3), 105-111.
- 13. Rosenmai, A. K.; Taxvig, C.; Svingen, T.; Trier, X.; van Vugt-Lussenburg, B. M. A.; Pedersen, M.; Lesné, L.; Jégou, B.; Vinggaard, A. M. Fluorinated Alkyl Substances and Technical Mixtures Used in Food Paper-Packaging Exhibit Endocrine-Related Activity in Vitro. *Andrology* **2016**, *4* (4), 662-672.
- 14. Zhang, X.; Wang, H.; Liu, Z.; Zhu, Y.; Wu, S.; Wang, C.; Zhu, Y. Fabrication of Durable Fluorine-Free Superhydrophobic Polyethersulfone (PES) Composite Coating Enhanced by Assembled MMT-SiO₂ Nanoparticles. *Appl. Surf. Sci.* **2017**, *396*, 1580-1588.
- 15. Wang, J.; Wang, L.; Yu, H.; Zain Ul, A.; Chen, Y.; Chen, Q.; Zhou, W.; Zhang, H.; Chen, X., Recent Progress on Synthesis, Property and Application of Modified Chitosan: An overview. *Int. J. Biol. Macromol.* **2016**, *88*, 333-44.
- 16. Guillaume, C.; Pinte, J.; Gontard, N.; Gastaldi, E. Wheat Gluten-Coated Papers for Bio-Based Food Packaging: Structure, Surface and Transfer Properties. *Food Res. Int.* **2010**, *43* (5), 1395-1401.
- 17. Han, J.; Salmieri, S.; Le Tien, C.; Lacroix, M. Improvement of Water Barrier Property of Paperboard by Coating Application with Biodegradable Polymers. *J. Agric. Food Chem.* **2010**, 58 (5), 3125-3131.
- 18. Khanzadi, M.; Jafari, S. M.; Mirzaei, H.; Chegini, F. K.; Maghsoudlou, Y.; Dehnad, D. Physical and Mechanical Properties in Biodegradable Films of Whey Protein Concentrate-Pullulan by Application of Beeswax. *Carbohydr. Polym.* **2015**, *118*, 24-29.
- 19. Rhim, J.-W.; Lee, J.-H.; Hong, S.-I. Water Resistance and Mechanical Properties of Biopolymer (Alginate and Soy Protein) Coated Paperboards. *LWT Food Sci. Technol.* **2006**, *39* (7), 806-813.
- 20. Jost, V.; Kobsik, K.; Schmid, M.; Noller, K. Influence of Plasticiser on the Barrier, Mechanical and Grease Resistance Properties of Alginate Cast Films. *Carbohydr. Polym.* **2014**, *110*, 309-319.
- 21. Kopacic, S.; Walzl, A.; Zankel, A.; Leitner, E.; Bauer, W. Alginate and Chitosan as a Functional Barrier for Paper-Based Packaging Materials. *Coatings* **2018**, *8* (7), 235-249.
- 22. Yang, J.; Li, H.; Lan, T.; Peng, L.; Cui, R.; Yang, H. Preparation, Characterization, and Properties of Fluorine-Free Superhydrophobic Paper Based on Layer-by-Layer Assembly. *Carbohydr. Polym.* **2017**, *178*, 228-237.
- 23. Rivero, S.; García, M. A.; Pinotti, A. Composite and bi-layer films based on gelatin and chitosan. *J. Food Eng.* **2009**, *90* (4), 531-539.

- 24. Khwaldia, K.; Basta, A. H.; Aloui, H.; El-Saied, H. Chitosan-caseinate bilayer coatings for paper packaging materials. *Carbohydr. Polym.* **2014**, *99*, 508-516.
- 25. Khwaldia, K.; Arab-Tehrany, E.; Desobry, S. Biopolymer Coatings on Paper Packaging Materials. *Comprehensive Reviews in Food Sci. Food Saf.* **2009**, *9* (1), 82-91.
- 26. Zhang, W.; Xiao, H.; Qian, L. Enhanced Water Vapour Barrier and Grease Resistance of Paper Bilayer-Coated with Chitosan and Beeswax. *Carbohydr. Polym.* **2014**, *101*, 401-406.
- 27. Bordenave, N.; Grelier, S.; Coma, V. Hydrophobization and Antimicrobial Activity of Chitosan and Paper-Based Packaging Material. *Biomacromolecules* **2010**, *11* (1), 88-96.
- 28. Rinaudo, M., Chitin and Chitosan: Properties and Applications. *Prog. Polym. Sci.* **2006**, *31* (7), 603-632.
- 29. Li, Z.; Rabnawaz, M. Fabrication of Food-Safe Water-Resistant Paper Coatings Using a Melamine Primer and Polysiloxane Outer Layer. *ACS Omega* **2018**, *3* (9), 11909-11916.
- 30. Li, Z.; Rabnawaz, M.; Krishna, A.; Sirinakbumrung, N.; Khan, B.; Kamdem, D. P. A Closed-Loop and Sustainable Approach for the Fabrication of Plastic-Free Oil- and Water-Resistant Paper Products. *Green Chem.* **2019**, *21*, 5691-5700.
- 31. Reis, A. B.; Yoshida, C. M. P.; Reis, A. P. C.; Franco, T. T., Application of Chitosan Emulsion as A Coating on Kraft Paper. *Polym. International* **2011**, *60* (6), 963-969.
- 32. Kjellgren, H.; Gällstedt, M.; Engström, G.; Järnström, L. Barrier and Surface Properties of Chitosan-Coated Greaseproof Paper. *Carbohydr. Polym.* **2006**, *65* (4), 453-460.
- 33. Li, Z.; Rabnawaz, M. Oil- and Water-Resistant Coatings for Porous Cellulosic Substrates. *ACS Appl. Polym. Mater.* **2018**, *I*(1), 103-111.
- 34. Grozea, C. M.; Rabnawaz, M.; Liu, G.; Zhang, G., Coating of Silica Particles by Fluorinated Diblock Copolymers and Use of the Resultant Silica for Superamphiphobic Surfaces. *Polymer* **2015**, *64*, 153-162.
- 35. Rabnawaz, M.; Wang, Z.; Wang, Y.; Wyman, I.; Hu, H.; Liu, G., Synthesis of Poly(Dimethylsiloxane)-Block-Poly[3-(Triisopropyloxysilyl) Propyl Methacrylate] and its use in the Facile Coating of Hydrophilically Patterned Superhydrophobic Fabrics. *RSC Adv.* **2015**, *5* (49), 39505-39511.
- 36. Grozea, C. M.; Rabnawaz, M.; Liu, G.; Zhang, G., Coating of Silica Particles by Fluorinated Diblock Copolymers and Use of the Resultant Silica for Superamphiphobic Surfaces. *Polymer* **2015**, *64*, 153-162.
- 37. Wang, J.; Wang, L.; Yu, H.; Zain Ul, A.; Chen, Y.; Chen, Q.; Zhou, W.; Zhang, H.; Chen, X. Recent Progress on Synthesis, Property and Application of Modified Chitosan: An Overview. *Int. J. Biol. Macromol.* **2016**, *88*, 333-344.

- 38. Rabnawaz, M.; Liu, G.; Hu, H., Fluorine-Free Anti-Smudge Polyurethane Coatings. *Angew Chem Int. Ed. Engl.* **2015**, *54* (43), 12722-12727.
- 39. Khan, F.; Khan, A.; Tuhin, M. O.; Rabnawaz, M.; Li, Z.; Naveed, M., A Novel Dual-Layer Approach Towards Omniphobic Polyurethane Coatings. *RSC Adv.* **2019**, *9* (46), 26703-26711.
- 40. Khan, F.; Rabnawaz, M.; Li, Z.; Khan, A.; Naveed, M.; Tuhin, M. O.; Rahimb, F., Simple Design for Durable and Clear Self-Cleaning Coatings. *ACS Appl. Polym. Mater.* **2019**, *1* (10), 2659-2667.
- 41. Macoretta, D.; Rabnawaz, M.; Grozea, C. M.; Liu, G.; Wang, Y.; Crumblehulme, A.; Wyer, M., Clear Antismudge Unimolecular Coatings of Diblock Copolymers on Glass Plates. *ACS Appl. Mater. Interfaces* **2014**, *6* (23), 21435-21445.
- 42. Kunduru, K. R.; Basu, A.; Haim Zada, M.; Domb, A. J. Castor Oil-Based Biodegradable Polyesters. *Biomacromolecules* **2015**, *16* (9), 2572-2587.
- **43.** Mutlu, H.; Meier, M. A. R. Castor Oil as a Renewable Resource for the Chemical Industry. *European J. Lipid Sci. Technol.* **2010**, *112* (1), 10-30.
- 44. Ferreira, P.; Pereira, R.; Coelho, J. F.; Silva, A. F.; Gil, M. H. Modification of the Biopolymer Castor Oil with Free Isocyanate Groups to be Applied as Bioadhesive. *Int. J. Biol. Macromol.* **2007**, *40* (2), 144-152.
- 45. JMP, Modeling and Multivariate Methods. In *Fitting Standard Least Squares* [Online] 2012, 53-131.
- 46. Velickova, E.; Winkelhausen, E.; Kuzmanova, S.; Alves, V. D.; Moldão-Martins, M., Impact of Chitosan-Beeswax Edible Coatings on the Quality of Fresh Strawberries (Fragaria Ananassa Cv Camarosa) under Commercial Storage Conditions. *LWT Food Sci. Techn.* **2013**, *52* (2), 80-92.
- 47. Brereton, R. G., Introduction to Analysis of Variance. J. Chemom. 2019, 33 (1), e3018.
- 48. Ostertagová, E., Modelling using Polynomial Regression. *Procedia Eng.* **2012**, *48*, 500-506.
- 49. Indirective Food Additives: Polymers (21CFR177.1680), FDA, 2018.
- 50. Lucio, B.; de la Fuente, J. L. Rheokinetic Analysis on the Formation of Metallo-Polyurethanes Based on Hydroxyl-Terminated Polybutadiene. *Eur. Polym. J.* **2014**, *50*, 117-126.
- 51. Almenar, E.; Samsudin, H.; Auras, R.; Harte, B.; Rubino, M. Postharvest Shelf Life Extension of Blueberries Using a Biodegradable Package. *Food Chem.* **2008**, *110* (1), 120-127.
- 52. Chen, Y. C.; Tai, W., Castor Oil-Based Polyurethane Resin for Low-Density Composites with Bamboo Charcoal. *Polymers (Basel)* **2018**, *10* (10), 1100-1111.

- 53. Thakur, S.; Misra, M.; Mohanty, A. K. Sustainable Hydrophobic and Moisture-Resistant Coating Derived from Downstream Corn Oil. *ACS Sustain. Chem. Eng.* **2019**, *7* (9), 8766-8774.
- 54. Sultan, M.; Zia, K. M.; Bhatti, H. N.; Jamil, T.; Hussain, R.; Zuber, M., Modification of Cellulosic Fiber with Polyurethane Acrylate Copolymers. Part I: Physicochemical Properties. *Carbohydr. Polym.* **2012**, *87* (1), 397-404.
- 55. Babu Borugadda, V.; Goud, V. V. Comparative Studies of Thermal, Oxidative and Low Temperature Properties of Waste Cooking Oil and Castor Oil. *J. Renew. Sustain. Energy* **2013**, *5* (6), 63104.
- 56. Khare, P.; Jain, S. K., Influence of Rheology of Dispersion Media in the Preparation of Polymeric Microspheres through Emulsification Method. *AAPS Pharm. Sci. Tech.* **2009**, *10* (4), 1295-300.
- 57. Rogers, C. E. Permeation of Gases and Vapours in Polymers. In *Polymer Permeability*, Comyn, J. Ed. Springer Netherlands: Dordrecht, 1985, 11-73.
- 58. Wiles, J. L.; Vergano, P. J.; Barron, F. H.; Bunn, J. M.; Testin, R. F. Water Vapor Transmission Rates and Sorption Behavior of Chitosan Films. *J. Food Sci.* **2000**, *65* (7), 1175-1179.

CHAPTER 7: GENERAL CONCLUSIONS AND FUTURE WORK

7.1 General conclusions

The excessive use of conventional plastics has created environmental concerns such as landfilling and microplastic issues. In addition, the use of PFAS for water and grease resistant coatings have created various health concerns which have placed our communities at risk. Thus, there is an urgent need to develop PFAS- and plastic-free water and grease-resistant paper substrates as sustainable and environmentally friendly solutions to mitigate the problems created by PFAS and plastic usage. The major outcomes of this study are summarized below.

Chapter 3 describes a two-step dip-coating approach for the preparation of biodegradable water-resistant paper coating for food contact applications. Melamine, an FDA approved material for food contact applications, was applied as a primer due to the superior binding to cellulosic fiber and abundant amine groups. PDMS was then chemically grafted to melamine via urea linkages formed between PDMS-NCO and melamine, resulting in a firm bonding between PDMS and paper substrate. PDMS rendered excellent water-resistant properties to the paper substrate owing to its low surface energy, as evident from high WCA values (~125 ° at 1 wt%).

In Chapter 4, a two-step coating procedure was developed for water- and oil-resistant paper. Results validated that porous cellulosic substrates could be turned oil- and water-repellent by masking pores with chitosan and subsequent coating with PDMS as an outer layer. Excellent water- and oil-resistant properties with a kit rating value of 12/12 and WCA of 95.2° were obtained with a coating load of 8.6% of chitosan and 2.2% of PDMS. The outstanding oil resistance of the obtained coated materials was due to the non-porous surface of the coated paper, which has been confirmed by SEM analysis. The application of PDMS improved both oil- and water-resistant properties of the chitosan-coated paper.

In chapter 5, a unique and facile approach was developed for the fabrication of water- and oil-resistant paper products that are 100% recyclable. PDMS was chemically grafted to chitosan to form a chitosan-graft-PDMS copolymer, which was then applied as a coating solution for paper substrates as a single layer. The obtained coated paper showed excellent water resistance (WCA of $120.53 \pm 0.96^{\circ}$, and Cobb60 value of 9.89 ± 0.32 g/m²) as well as superior oil-repellency (kit rating value of 11.7/12). SEM analysis proved that pores and voids of the paper substrates disappeared after the coating application. T method is a closed-loop approach as the paper pulp of the coated paper can be recycled by repulping and washing treatment. This approach provides a significant contribution to sustainable packaging by offering recyclable and biodegradable PFAS free papers suitable for a wide range of applications. In addition, migration studies revealed the coating is potentially safe for food-contact application.

In Chapter 6, a sustainable and biobased copolymer Chitosan-*grafted*-CO was successfully synthesized by chemically grafting castor oil-isocyanate onto chitosan via urea linkages. The aqueous Chitosan-*grafted*-CO coating solution was applied as a coating onto paper substrates using a bar coating machine in one step. The chitosan imparted oil-resistant property due to the polar nature, and the castor oil enhanced the hydrophobicity of copolymer. The obtained coated paper showed good water- and oil-resistant properties with a kit rating value of 9/12 and a Cobb60 value of 29.16 g/m². This method can address the issues created by the existing plastics and paper coating practices due to the environmentally friendly and renewable nature of coating materials.

7.2 Future Work

This research has developed plastic- and PFAS-free closed-loop approaches toward oiland water-resistant paper-based materials. Characterization of the copolymers and coatings, as well as evaluation of water- and oil-resistant properties and safety have been performed, the formulation has been optimized using RSM. However, there are still more questions left behind which need to be addressed.

Formulation optimization for the Chitosan-grafted-CO coated paper is desirable to improve further the water-resistance performance. Thus, more studies are required to understand the effect of the ratio and concentration of different reactants on the water and oil resistance prorpties of the coated paper.

An overall migration study has been performed on this study using NMR analysis. However, a better understanding of the migration of chemicals from coated materials is crucial prior to moving forward with the option of using the coated paper for food contact applications. Quantification of released chemicals should be further studied using modern technologies such as gas chromatography, high-performance liquid chromatography, mass spectrometry, etc.